O presente trabalho beneficiou do apoio financeiro da Fundação para a Ciência e Tecnologia, Bolsa de Doutoramento SFRH/BD/75257/2010

Universidade do Minho
Escola de Ciências

Henrique Luis Silva de Noronha

Study of grapevine solute transporters involved in berry quality. A biochemical and molecular approach

maio de 2015

Study of grapevine solute transporters involved in berry quality. A biochemical and molecular approach
Henrique Luis Silva de Noronha
UMinho|2015

Universidade do Minho
Escola de Ciências

Henrique Luis Silva de Noronha

Study of grapevine solute transporters involved in berry quality. A biochemical and molecular approach

Tese de Doutoramento em Biologia de Plantas

Trabalho realizado sob a orientação do
Professor Doutor Hernâni Varanda Gerós
do
Professor Doutor Serge Delrot
e do
Doutor Carlos Conde

maio de 2015

STATEMENT OF INTEGRITY

I hereby declare having conducted my thesis with integrity. I confirm that I have not used plagiarism or any form of falsification of results in the process of the thesis elaboration. I further declare that I have fully acknowledged the Code of Ethical Conduct of the University of Minho.

University of Minho, _____

Full name:

_____

Signature:

_____

O presente trabalho beneficiou dos seguintes apoios financeiros:

Fundação para a Ciência e Tecnologia, Bolsa de Doutoramento SFRH/BD/75257/2010;

Fundação para a Ciência e Tecnologia - projeto PTDC/AGR-ALI/100636/2008 - "GrapeBerryFactory - Sugars, acids, phenolics and water on grape development and ripening";

Fundação para a Ciência e Tecnologia - projeto PTDC/AGR-AAM/099154/2008 - "AQUAVITIS - Compreender o transporte de água em *Vitis vinifera*: caracterização bioquímica de Aquaporinas através da sua expressão heteróloga em leveduras";

FEDER/COMPETE - Operational Competitiveness Programme – projeto Europeu "INNOVINE - Combining innovation in vineyard management and genetic diversity for a sustainable European viticulture" (FP7-KBBE-2012-6-311775)

To Rosa, Quito,
Berto and Cecília

Enquanto não alcançares a verdade, não poderás corrigi-la.
Porém, se a não corrigires, não a alcançarás.
Entretanto, não te resignes.
Livro dos Conselhos
História do Cerco de Lisboa
José Saramago

I believe smashing them is less a crime than making them. I am going to break two of your figurines first, and if you can demonstrate your knowledge of the Doctrine of Stoicism by holding back your tears, I'll stop.
Vera
Dogville
Lars von Trier

Acknowledgments

First and foremost, I want to deeply thank Professor Hernâni Gerós for his example, scientific qualities, and, most importantly, his friendship. I am truly honored to have gone through this years under his guidance.

I would like to deeply thank the supervision of Professor Serge Delrot, as well as his sharp and rigorous scientific analysis that allowed me to accomplish this work. Also, I would like to thank him for giving me the possibility to spend some time at his laboratory in Bordeaux, which was a very rewarding experience, both professionally and personally.

The supervision of Doctor Carlos Conde is deeply acknowledged, as well as the sharp and fruitful discussions, and the everlasting availability and companionship that undoubtedly allowed the success of this work.

I would like to thank Professor François Chaumont for his scientific contribution and companionship, and for allowing me to spend some time at his laboratory in Louvain-la-Neuve, which was a fantastic and fruitful experience. I want to acknowledge the help and kindeness shown to me from the AQP-team, particularly from Marie Berny, Arnaud Besserer, Gerd Patrick Bienert and Adrien Chevalier.

The scientific contribution, availability and kindness of Professor Graça Soveral is deeply acknowledged. Also, I would like to thank Ana Paula Martins for her sympathy and undeniable will to help me.

I would like to express my appreciation to Fatma Lecourieux and David Lecourieux for their sympathy and supervision during my stay at Bordeaux. I also want to thank Roberta Triolo, Maria Jose Clemente, Eloïse Brouard, Marc Hince, Diego Vergara, and Aurélie Lagarde for their companionship, and for making my stay at Bordeaux a memorable one.

I want to express my heartfelt gratitude to all the people from the Laboratório de Biologia Vegetal da Universidade do Minho. I would like to thank particularly to Professor Ana Cunha, Professor Alberto Dias, Franklin Gregory, Joana Silvestre, Vera Castro, Luis

Giraldo, Marslin Gregory, Rute Oliveira, António Freitas, Florência Alves, Weina Hou, Rupesh Kumar Rajput and Selva Kesavan.

I want to express my deepest appreciation to the members of the Vitis research group for sharing these past years with me. I can certainly say that besides colleagues we were friends, and I would like to mention Artur Conde, Viviana Martins, Richard Gonçalves, Natacha Fontes, António Teixeira, Diogo Araújo, Áurea Gomes, Diana Pimentel, Inês Carqueijeiro, Jorge Rodrigues and Paola Tessarin.

I would like to thank my comrades from Biologia Aplicada for all the moments spent together: João "rambo" Raimundo, Artur "shark" Conde, Richard Gonçalves, João "sono" Lopes, Rui Armada, Zé "brave" Pedro Faria, and Filipa Pereira. The unwillingness of dishes to wash themselves, the miraculous disappearance of madalenas, and many others, are memories that I hold dear.

Finally, I would like to express my unreserved appreciation to my parents, my brother and Cecília for their love and support.

Abstract

Due to its sessile nature, plants must take up mineral nutrients and water from the soil, and fix carbon in leaves from atmospheric CO_2. The resulting photoassimilates must be precisely delivered to each plant organ, including leaves, roots and fruits. The present dissertation explored key biochemical mechanisms involved in the transport and compartmentation of sugars and water in grapevine.

The fixation of carbon in chloroplasts, the synthesis of sugars in leaves and their transport to sink tissues are the most important biochemical steps in plant productivity, and have been investigated for several decades. Nonetheless, this is still a very relevant research topic because our knowledge is fragmented and the ongoing climate changes became an additional threat that may potentially affect plant productivity, in particular in grapevine. Plastids, which are characteristic of the plant kingdom, have pivotal roles in several important physiological processes. In grapevine, they are responsible for the accumulation of starch in woody tissues, roots, flowers and berries, and they are involved in the synthesis of secondary compounds. The first part of the present work was dedicated to the characterization of plastidial metabolism in grapevine, and focused on two plastidial glucose-6-phosphate/phosphate translocators (GPT), VvGPT1 and VvGPT2. It was found that three different splicing variants identified for *VvGPT2* (*VvGPT2α*, *VvGPT2β* and *VvGPT2*Ω) were more expressed in the leaves. Contrarily, *VvGPT1* was more expressed in mature berries, canes and flowers. Confocal microscopy revealed that VvGPT1 and VvGPT2Ω are localized in the plastidial envelope, and the transformation of *pgi1-1 Arabidopsis* mutant showed that these grapevine transporters mediate the uptake of glucose-6-phosphate into the plastid. In grape cell suspensions, ABA, light and galactinol, together with sucrose and fructose, increased the transcript abundance of *VvGPT1*. Furthermore, elicitation with MeJA dramatically increased the expression of *VvGPT1* and *VvPAL1*, suggesting a role for GPTs in the production of secondary compounds in grapevine. Given its importance, this research line deserves further attention, particularly regarding the biochemical mechanisms underlying starch accumulation in grapevine amyloplasts during the winter, and its remobilization during spring to allow a fast vegetative growth.

Besides sugar, water content is also an important parameter for berry quality, which is particularly intermingled with sugar status during berry development. Their content in the fruit is tightly regulated by the activity of sugar and water transporters (aquaporins –

AQPs) in response to the environment. Berry and wine quality are directly affected by the berry water content at harvest. The second part of the present dissertation was devoted to the characterization of two AQPs in grapevine, VvSIP1 (Small Basic Intrinsic Protein 1) and VvXIP1 (Uncharacterized –X- Intrinsic Protein 1). Results showed that *VvSIP1* was expressed in leaves and berries from field-grown vines, and in leaves and stems from *in vitro* plantlets, but not in roots. When expressed in tobacco mesophyll cells and in the yeast *Saccharomyces cerevisiae*, fluorescent-tagged VvSIP1 was localized at the ER. Stopped-flow spectroscopy showed that VvSIP1-enriched ER membrane vesicles from yeast exhibited higher water permeability and lower E_a for water transport than control vesicles, indicating the involvement of protein mediated water diffusion. This aquaporin was able to transport water but not glycerol, urea, sorbitol, glucose and inositol. VvSIP1-His-tag was solubilized and purified to homogeneity from yeast ER membranes and the reconstitution of the purified protein in phosphatidylethanolamine liposomes confirmed its water channel activity.

XIPs are a new group of MIP proteins recently identified, so their precise physiological role has remained elusive. In our study, VvXIP1-RFP protein co-localized with ZmTIP2;1-YFP in the tonoplast of transiently transformed *Nicotiana bethamiana* leaves. Sopped-flow spectrometry performed with microsomal vesicles from yeast expressing *pVV214-VvXIP1* showed that VvXIP1 is unable to transport water but transports glycerol. Plate growth assays showed that this AQP is also able to transport copper, boron and H_2O_2. Transcriptional analysis showed a much higher steady-state expression of *VvXIP1* in leaves than in berries, canes or flowers from field grown grapevine. Furthermore, *VvXIP1* transcripts were downregulated in leaves from plants treated with the copper-based fungicide Bordeaux mixture, and in vines under severe water deficit. In agreement, *VvXIP1* was downregulated by ABA and salt stress in *in vitro* cultured grape cells. Much work is still needed to fully elucidate the physiological role of SIPs and XIPs in grapevine in particular towards the confirmation of their involvement in intracellular compartmentation of specific solutes like heavy metals. Thus, this avenue of research is still wide open.

Resumo

Devido à sua natureza séssil, as plantas obtêm do solo os nutrientes minerais e a água e fixam o carbono nas folhas a partir do CO_2 atmosférico. A água e os solutos orgânicos e inorgânicos são distribuídos com precisão pelos diferentes tecidos da planta, incluindo as folhas, as raízes e os frutos. O presente trabalho de doutoramento visou o estudo de mecanismos bioquímicos envolvidos no transporte e compartimentação de açúcares e de água nos tecidos/células de videira (*Vitis vinifera* L.)

A fixação de carbono, a síntese de açúcares nas folhas e o seu transporte para os tecidos heterotróficos constituem os passos bioquímicos mais relevantes envolvidos na produtividade das plantas. Embora estes aspetos fisiológicos tenham sido alvo de investigação ao longo das últimas décadas o nosso conhecimento é ainda fragmentado, e as modificações climatéricas em curso representam uma limitação adicional à produtividade das plantas, em particular da videira. Os plastídios, que são organelos característicos do reino vegetal, desempenham papéis fundamentais em diversos mecanismos fisiológicos. Na videira, os plastídios são responsáveis pela acumulação de amido nos tecidos lenhosos, raízes, flores e frutos, e estão ainda envolvidos na síntese de compostos secundários.

A primeira parte do presente trabalho foi dedicada à caracterização do metabolismo plastidial na videira, tendo-se focado em dois antiportadores plastidiais de glucose-6-fosfato com fosfato (GPT), *VvGPT1* e *VvGPT2*. Os resultados demonstraram que três variantes de *splicing* alternativo do gene *VvGPT2* (*VvGPT2α*, *VvGPT2β* e *VvGPT2*Ω), são mais expressos nas folhas do que noutros órgãos. Pelo contrário, o gene *VvGPT1* demonstrou uma expressão mais elevada em bagos maduros, varas e flores do que nas folhas. Estudos de microscopia confocal demonstraram que as proteínas VvGPT1 e VvGPT2Ω localizam-se na membrana plastidial, e estudos de transformação estável do mutante de *Arabidopsis pgi1-1* confirmaram o seu papel na incorporação de glucose-6-fosfato. Estudos desenvolvidos com células em suspensão sugeriram que alguns fatores ambientais, como a luz e sinais hormonais ou endógenos, como o ABA ou os níveis de açúcar (incluindo o galactinol, a sacarose e a frutose), conduzem a um aumento do número de transcritos do *VvGPT1*. Adicionalmente, a eliciação com MeJA conduziu a um aumento acentuado da expressão dos genes *VvGPT1 e VvPAL1*, sugerindo que os GPTs desempenham um papel importante na produção de compostos secundários na videira. Dada a sua importância, esta linha de investigação merece estudos mais aprofundados no futuro, em particular no que diz respeito aos mecanismos bioquímicos de remobilização do amido armazenado durante o inverno nos amiloplastos, permitindo o rápido crescimento dos gomos caulinares na primavera.

A água constitui um parâmetro fundamental para a qualidade do bago de uva e os seus níveis encontram-se particularmente relacionados com a concentração dos açúcares

durante o desenvolvimento e amadurecimento do fruto. Tem sido demonstrado que a atividade de transportadores membranares de açúcares e de água (aquaporinas – AQPs) regula com precisão a concentração destes compostos em resposta às condições ambientais. Em bagos maduros, o conteúdo em água afeta diretamente a qualidade do fruto e do vinho. A segunda parte do presente trabalho de doutoramento foi dedicada à caracterização de duas AQPs de videira, VvSIP1 (*Small Basic Intrinsic Protein 1*) e VvXIP1 (*Uncharacterized – X - Intrinsic Protein 1*). Os resultados demonstraram que o gene *VvSIP1* foi expresso em folhas e bagos de videiras cultivadas em condições de campo, bem como em folhas e caules, mas não em raízes, de plântulas crescidas *in vitro*. Estudos de expressão transiente em células do mesófilo de tabaco e em *Saccharomyces cerevisiae* indicaram que a proteína de fusão VvSIP1-GFP localiza-se no retículo endoplasmático (RE). Ensaios de espectrometria de *stopped-flow* demonstraram que vesículas de membrana de RE purificadas de leveduras transformadas com a construção *VvSIP1-GFP* exibem uma maior taxa de permeabilidade à água e uma menor energia de ativação do que vesículas obtidas de leveduras controlo. Estes resultados sugeriram o envolvimento de um canal proteico no transporte de água. Ensaios de especificidade mostraram que a proteína VvSIP1 não transporta glicerol, ureia, sorbitol, inositol e glucose. A proteína quimérica VvSIP1-6his foi purificada a partir do RE de leveduras transformadas e a sua atividade transportadora reconstituída em lipossomas de fosfatidiletanolamina. Estes resultados permitiram demonstrar cabalmente que a proteína VvSIP1 é um canal transportador de água.

As aquaporinas XIP foram identificadas recentemente, pelo que o seu verdadeiro papel fisiológico é ainda pouco claro. Estudos de expressão transiente em folhas de tabaco mediada por *Agrobacterium*, demonstraram que a proteína de fusão VvXIP1-RFP colocaliza com a proteína ZmTIP2;1-YFP, sugerindo tratar-se de uma proteína da membrana vacuolar. Estudos de espectrometria de *stopped-flow* com vesículas de membrana de leveduras transformadas com o vector *pVV214-VvXIP1* demonstraram que a VvXIP1 é impermeável à água mas transporta glicerol. Experiências de crescimento em meio sólido mostraram ainda que esta AQP medeia o transporte de cobre, boro e H_2O_2. Em videiras cultivadas em condições de campo, estudos de PCR quantitativo em tempo real demonstraram que os níveis de transcritos do *VvXIP1* são mais abundantes em folhas do que nos frutos, varas e flores. Em folhas de videiras tratadas com o fungicida à base de cobre calda bordalesa, bem como de videiras submetidas a stresse hídrico severo, a expressão do *VvXIP1* é inibida. Em linha com estes resultados, a expressão do *VvXIP1* foi reprimida pelo ABA e por stresse salino em culturas celulares. A elucidação completa dos papéis fisiológicos das SIPs e das XIPs na videira requer ainda trabalho de investigação intenso, em particular com vista à confirmação do seu envolvimento na compartimentação intracelular de solutos específicos, como metais pesados, pelo que esta linha de investigação se mantém aberta.

Table of contents

Abbreviations and acronyms

2-NBDG - 2-[N-(7-nitrobenz-2-oxa-1,3-diazol-4-yl amino]-2-deoxy-D-glucose;

aa - Amino acid;

ABA - Abscisic acid;

ADP – Adenosine diphosphate;

AMY – α-amylase;

AQP – Aquaporin;

ATP - Adenosine triphosphate;

bp - Base pairs;

CoA – Coenzyme A;

cv. – Cultivar;

DAP – Dihydroxyacetone phosphate;

DMAPP – Dimethylallyl diphosphate;

DST – Disaccharide transporter;

E_a - Activation energy;

ER – Endoplasmic reticulum;

GAP – Glyceraldehyde -3-phosphate;

GFP - Green fluorescent protein;

GPT – Glucose-6-phosphate/phosphate translocator;

IPP – Isopentenyl diphosphate;

MeJA – Methyl jasmonate;

MEP – Methyl-D-erythritol 4-phosphate (plastidial pathway for isoprenoid synthesis);

MEX – Maltose transporter;

MFS – Major facilitator superfamily;

MIP – Membrane intrinsic protein;

MST – Monosaccharide transporter;

MVA – Mevalonate (cytosolic pathway for isoprenoid synthesis);

NIP – Nodulin 26-like intrinsic protein;

OPPP – Oxidative pentose phosphate pathway;

ORF – Open reading frame;

PAL – Phenylalanine ammonia-lyase;

PEG – Polyethylene glycol;

P_f – Permeability coefficient;

pGlcT – Plastidial glucose translocators;

PIP – Plasma membrane intrinsic protein;

PMSF – Phenylmethylsulfonyl fluoride;

PPT – Phosphoenolpyruvate/phosphate translocator;

pPT – Plastidial phosphate translocator;

RDI – Regulated deficit irrigation;

RFP – Red fluorescent protein;

SA – Salicylic acid;

SDI – Sustained deficit irrigation;

SIP – Small basic intrinsic protein;

SS – Starch synthase;

TIP – Tonoplast intrinsic protein;

TPT – Trioses-phosphate/phosphate translocator;

UDP - Uridine diphosphate;

XIP – Uncharacterized (X) intrinsic protein;

XPT – Xylulose-5-phosphate/phosphate translocator.

List of publications

Papers in International Journals with Peer-review

Noronha H, Conde C, Delrot S, Gerós H. 2015. Identification and functional characterization of grapevine transporters that mediate glucose-6-phosphate uptake into plastids. *Planta* (accepted for publication).

Noronha H, Agasse A, Martins AP, Berny MC, Gomes D, Zarrouk O, Thiebaud P, Delrot S, Soveral G, Chaumont F and Gerós H. 2014. The grape aquaporin VvSIP1 transports water across the ER membrane. *Journal of Experimental Botany* **65**, 981–993.

Teixeira A, Martins V, **Noronha H**, Eiras-Dias J, Gerós H. 2014. The first insight into the metabolite profiling of grapes from three Vitis vinifera L. cultivars of two controlled appellation (DOC) regions. International Journal of Molecular Sciences **15**, 4237-4254.

Carqueijeiro I, **Noronha H**, Duarte P, Gerós H and Sottomayor M. 2013. Vacuolar transport of the medicinal alkaloids from Catharantus roseus is mediated by a proton-driven antiport. *Plant Physiology* 162, 1486–1496.

Rodrigues J, Silva RD, **Noronha H**, Pedras A, Gerós H and Côrte-Real M. 2013. Flow cytometry as a novel tool for structural and functional characterization of isolated yeast vacuoles. *Microbiology* 159, 848–856.

Papers in National Journals

Conde A, Martins V, **Noronha H**, Conde C, Fontes N, Gerós H. 2011. Solute transport across plant cell membranes. *Canal BQ* 8, 20-34.

Communications in National and International Congresses

Araújo D, **Noronha H** and Gerós H. 2014. “The atypical nature of VvXIP in grapevine”. XVIII Congress of the Portuguese Biochemistry Society, Coimbra, Portugal, December 2014.

Noronha H, Martins AP, Soveral G, Chaumont F and Gerós H. "VvSIP1: cloning, expression, localization and functional studies of a grape intracellular aquaporin". XIII Congresso Luso-Espanhol de Fisiologia Vegetal. 24-28 Julho 2013. Lisboa, Portugal.

Noronha H, Delrot S and Gerós H. "Starch metabolism in the grape berry". XIII Congresso Luso-Espanhol de Fisiologia Vegetal. 24-28 Julho 2013. Lisboa, Portugal.

Teixeira A, Araújo D, **Noronha H**, Eiras Dias J and Gerós H. "Lipoxygenase in *Vitis Vinifera* culture cells and grape berry". XIII Congresso Luso-Espanhol de Fisiologia Vegetal. 24-28 Julho 2013. Lisboa, Portugal.

Carqueijeiro I, **Noronha H**, Duarte P, Gerós H and Sottomayor M. "Vacuolar transport of the alkaloid vindoline is mediated by a proton antiport in the medicinal plant *Catharanthus roseus*" 2nd Annual Meeting of COST Action PlantEngine "Plant Natural Products - From Science to Bioproducts”. Cluj – Napoca, Romenia, 26-28 September 2012.

Pereira MR, **Noronha H**, Gerós H and Cunha A. "Biological activity of Photosystem II incorporated in sol-gel derived matrices" MPA 2012 – 6th Int. Meeting on Developments in Materials, Processes and Applications of Emerging Technologies, Alvor, Portugal, 2 July 2012 - 4 July 2012.

Noronha H, Teixeira A and Gerós H. "The effect of high temperature and salicylic acid on the DAHPS expression and activity in grape cells: a link between primary and secondary metabolism in stress-response" Microbiotec 2011, Braga, Portugal, December 2011.

Breia R, Conde A, Martins V, **Noronha H**, Teixeira A, Cunha A, Gerós H. "Da bioquímica à agro-indústria". iSci - Interface Ciência Universidade do Minho, Braga, Portugal, Novembro 2011.

Noronha H, Conde A, Gerós H. "VvHT1 regulation by high temperature" XVI National Congress of Biochemistry, Porto, Portugal, December 2010.

Fontes N, Breia R, **Noronha H**, Delrot S, and Gerós H "Sugar import and accumulation into the vacuole of grape cells". XVI National Congress of Biochemistry, Açores, Portugal, Outubro 2008.

Chapter 1

Introduction

1. General introduction

Since pre-historic times humans have consumed plants, and the advent of agricultural communities is a hallmark of civilization. Agriculture led to the domestication of wild species and to the selection of the most valuable varieties for human consumption, which allowed early civilizations to thrive by obtaining greater amounts of sustenance and the establishment of the first socially organized societies (Maisels, 1993).

Due to its sessile nature, plants must absorb mineral nutrients and water from the soil, and fix carbon in leaves from atmospheric CO_2. Reduced carbon must then be distributed throughout the organism, from sources to sinks organs like roots and fruits. These processes are fundamental for plant development and productivity, but despite solute transport and compartmentation have been investigated in detail for several decades our knowledge is still limited.

The present review focuses on the mechanisms involved in the transport of solutes, mainly photoassimilates and water, throughout the plant. The role of plastids in photosynthetic and heterotrophic tissues is also highlighted, and particular attention is given to the mechanisms involved in starch synthesis and degradation in sink tissues, and also to plastid transporters. In this regard, the role of glucose-6-phosphate (glucose-6-Pi) and glucose-6-Pi transporters (GPT) in sink plastids will be detailed.

In plants, water is the source of reducing power in photosynthesis, thus playing a pivotal role in the life on earth. In grapevine, besides sugars, water content is an essential constituent of the ripe berry, and therefore of the wine. In this context, the biological role of aquaporins and their diversity in plants will be addressed in this review.

The second part of the present review is dedicated to grapevine, the biological model used in the present dissertation. Grape berries are sophisticated biochemical factories with major economic importance that import and accumulate water and sugars, along with minerals, but synthesize amino acids, organic acids, as well as flavor and aroma compounds. Important biochemical mechanisms that define grape berry quality are related to sugar and water transport as well as to plastidial metabolism and will be addressed in the context of grapevine response to environmental stress.

Finally, at the end of this chapter the main objectives of the present dissertation are detailed.

1.1 Long distance sugar transport and sugar loading and unloading

Membrane proteins play pivotal roles in mediating solute transport with a major impact in plant development and productivity. Photosynthetically produced sugars (mainly sucrose) are transported from source leaves to supply energy and carbon to heterotrophic sink tissues (Kühn and Grof, 2010). To reach sink tissues, sucrose is transported through the phloem, and symplastic and apoplastic pathways are responsible for its loading into this vascular tissue. In symplastic loading, sucrose moves from mesophyll cells to the SE-CCC (sieve element-companion cell complex) through small pores between adjacent cells called plasmodesmata, with diffusion and possibly some bulk flow representing the main driving force of this mechanism (Fig. 1.1). Apoplastic loading requires the export of sucrose from the mesophyll cells to the apoplast (cell wall space) and its uptake into the SE-CCC by sucrose/H^+ symporters. Up until recently, sugar efflux to the apoplast remained obscure until a new family of proteins named SWEET, with a role on sucrose efflux, was identified (Fig. 1.1; Chen *et al*., 2012). According to Munch's mass flow hypothesis, sucrose, as the major osmotically active constituent in the phloem, provides the driving force for translocating all other compounds in the phloem sap from source to sink tissues (Lalonde *et al*., 2004).

In sink organs, sucrose can be released apoplastically or symplastically, with the unloading pathway depending on the species, organ or tissue, and developmental stage (Turgeon and Wolf, 2009). In sinks connected through plasmodesmata, sucrose and other sap compounds may be directly incorporated into the cells, whereas in symplastically isolated organs sucrose is transported to the apoplast thanks to sucrose transporters (Chen *et al*., 2012). Sucrose can be transported directly from the apoplast through disaccharide transporters (sucrose/H^+ symporters) or be hydrolyzed by cell wall-bound invertases, and the resulting glucose and fructose incorporated by monosaccharide transporters (Fig. 1.1).

1.1.1 Sucrose transporter family

Plant sucrose transporters (SUT) are members of the glycoside-pentoside-hexuronide (GPH):cation symporter family, which belongs to the major facilitator superfamily (MFS). These proteins have 12 transmembrane helices that form a single pore for sucrose, and both the N- and C-termini, as well as 5 loops, are localized in the cytosol (Lalonde *et al*., 2004). The first sucrose transporter characterized from plants was the *SoSUT1* from spinach, which was successfully expressed in a yeast mutant lacking sugar transport (Riesmeier *et al*., 1992), So far, all plant sucrose transporters described are sucrose/H^+ symporters, with the exception of the sucrose facilitators from *Pisum sativum* and *Phaseolus vulgaris*, which function as bi-directional sucrose carriers (Zhou *et al*., 2007; Kühn and Grof, 2010).

1.1.2 Monosaccharide transporters family

Monosaccharide transporters (MST), which are found in all domains of life, are part of the GPH:cation symporter family of the MFS. These highly conserved proteins have 12 transmembrane-spanning helices separated by cytoplasmic and extracellular loops, and cytosolic N- and C-terminal domains (Lalonde *et al*., 2004).

AtSTP1 (*Arabidopsis thaliana Sugar Transporter Protein 1*) was the first higher plant MST to be characterized when hexose transporters (*hxt*) null-mutant yeasts were functionally complemented (Sauer *et al*., 1990). Since then, MST from several plant species have been identified and all proteins characterized so far were shown to operate as energy-dependent H^+-symporters (Büttner and Sauer, 2000).

1.1.3 The SWEET family

Before the identification of the SWEET transporter family, the efflux of sugars from mesophyll cells into the apoplastic space remained one of the most puzzling mysteries in plant physiology (Chen *et al*., 2010). Studies of sugar transport in plants tissues with radioactive substrates typically show multi-phase kinetics and generally two components are identified: a linear low-affinity high-capacity component and a saturable high-affinity, low-capacity component (Delrot and Bonnemain, 1981; Maynard and Lucas, 1982;

Chaudhuri *et al*., 2008). Studies performed in our group (Conde *et al*., 2007a), showed that cultured cells from *Olea europaea* display a linear non-saturating glucose uptake system up to concentrations of 100 mM glucose that was inhibited by mercury, which is normally used to inhibit channels, and by cytosolic acidosis. Contrarily, the protein kinase inhibitor staurosporine stimulated this diffusional uptake.

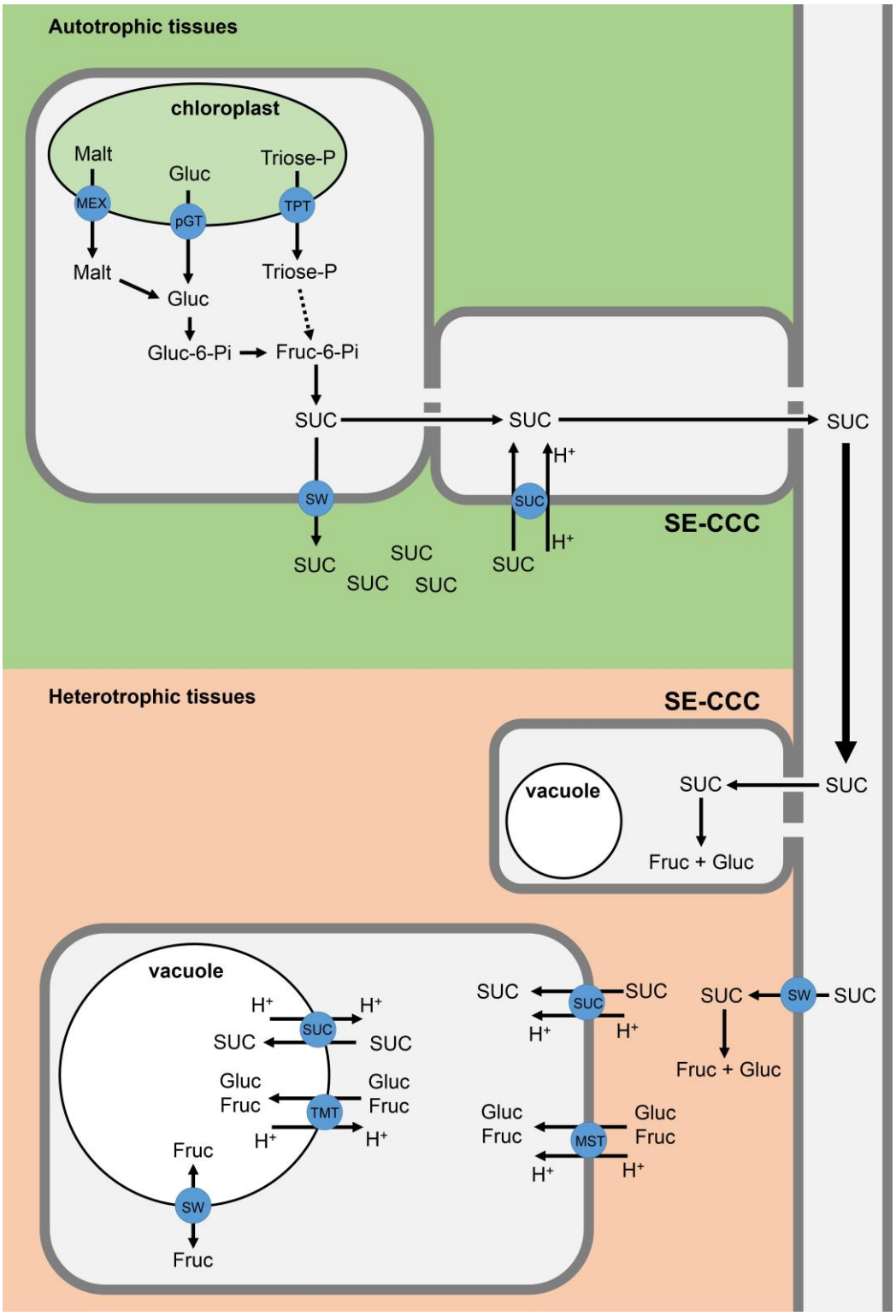

Figure 1.1 Long distance transport of photoassimilates. During the day carbon fixed in the chloroplast is transported to the cytosol in the form of trioses-phosphate by the TPT and during the night in the form of glucose and maltose by the pGT and MEX, respectivelly. In the cytosol, glucose is the precursor of sucrose synthesis that can be loaded into the phloem by symplastic or apoplastic pathways. In the apoplastic pathway, sucrose is transported into SE-CCC and loaded into the phloem by diffusion through plasmodesmata. In the apoplastic pathway, sucrose is transported into the extracellular space by a SWEET (SW) transporter, and loaded into the SE-CCC by the action of SUC transporters. In heterotrophic tissues, phloem unloading may occur through a symplastic, via plasmodesmata, and apoplastic pathways. The apoplastic unloading requires sucrose transport from the phloem into the apoplast, a process possibly mediated by SWEETs. In the apoplast, sucrose can be incorporated directly into sink cells by SUC transporters or by MST, following sucrose hydrolysis by cell wall bound invertases. In sugar accumulating fruits, large amounts of carbohydrates may be stored in the central vacuole by the action of SWEETS, SUC and MSTs.. Fruc, fructose; Fruc-6-P, fructose-6-phosphate; Gluc, glucose; Gluc, glucose; Gluc-6-P, glucose-6-phosphate; Malt, maltose; MEX, maltose translocator; MST, monosaccharide transporter; pGT, plastidial glucose translocator; SE-CCC, sieve element-companion cell complex; SUC, sucrose/H^+ symporter; SUC, sucrose; SW, SWEET transporter; TMT, tonoplast monosaccharide transporter; TPT, triose-phosphate/phosphate translocator; Triose-P, triose-phosphate. Adapted from Lalonde *et al*., 2004 and Chen *et al*., 2010.

These evidences led to the conclusion that a channel-like structure whose transport capacity may be regulated by intracellular protonation and phosphorylation could account for the diffusional component of glucose uptake. Following these observations in cultured cells, the involvement of a channel-like protein was proposed for sugar uptake in *Arabidopsis* root tips, where glucose and sucrose accumulation was shown to be insensitive to extracellular pH and protonophores (Chaudhuri *et al*., 2008). More recently, the same group (Chen *et al*., 2010) used a new and elegant screening system, based on the simultaneous expression of a highly sensible glucose-sensor and uncharacterized *Arabidopsis* membrane proteins, to identify AtSWEET1 as the first plant sugar efflux carrier. This transporter belongs to the SWEET superfamily, which diverges substantially from the MFS, and includes members from a wide variety of organisms acting as low-affinity uniporters. SWEETs are small proteins, with less than 300 aa and 7 transmembrane helices, which form a pore that mediates both sugar influx and efflux in a pH-independent manner (Chen *et al*., 2010). These findings paved the way to another study by Chen and co-workers, in which they showed that AtSWEET11 and 12 are sucrose uniporters localized in the plasma

membrane of the phloem tubes (Fig 1.1; Chen *et al*., 2012). Also, mutant plants carrying insertions in *AtSWEET11* and *12* showed alterations in phloem loading, which led to the conclusion that these proteins are essential for long distance sugar transport.

More recently, it was shown that AtSWEET17 is a tonoplast sugar exporter fundamental for the control of fructose content in the leaves and roots of *Arabidopsis* (Chardon *et al*., 2013; Guo *et al*., 2013), and that AtSWEET9 has a central role in flowers, where it is involved in the efflux of sucrose required for nectary secretion (Lin *et al*., 2014).

1.2. Plastidial metabolism

Plastids are organelles found virtually in all plants with fundamental roles in the photosynthesis, in the assimilation of carbon, sulfur, and nitrogen. Furthermore, they are the place of lipid synthesis, starch, protein and oil storage, fruit and flower coloration, gravity sensing, stomatal function, and environmental perception. They can also be found in algae cells, several taxa of marine mollusks and in one phylum of parasitic protists (Wise, 2007).

Like mitochondria, plastids have an endosymbiotic origin that can be traced back to the engulfment of an ancestral cyanobacteria by a primitive protist around 1.5 million years ago (Flügge, 1999; Fischer, 2011). Higher plants have different types of plastids, comprising undifferentiated proplastids, colorless etioplasts, chloroplasts, chromoplasts, starch-storing amyloplasts, and lipid-storing elaioplasts (Fischer, 2011).

1.2.1 Chloroplasts are the source of carbon assimilation

In leaves, chloroplasts are the place of carbon assimilation, via the Calvin-Benson cycle, which is then used as the main precursor for all biosynthetic reactions in plants (Weber, 2007). Carbon assimilated during photosynthesis is used for the production of transient starch in the chloroplast, and for the export of trioses-phosphate to the cytosol, feeding the biosynthesis of sucrose. This transport is mediated by the TPT (Triose-phosphate/phosphate translocator) that exchanges GAP (glyceraldehyde -3-phosphate) and DAP (dihydroxyacetone-phosphate) with inorganic phosphate, ensuring that the chloroplast is replenished with Pi used in ATP synthesis (Linka and Weber, 2010; Fig. 1.2).

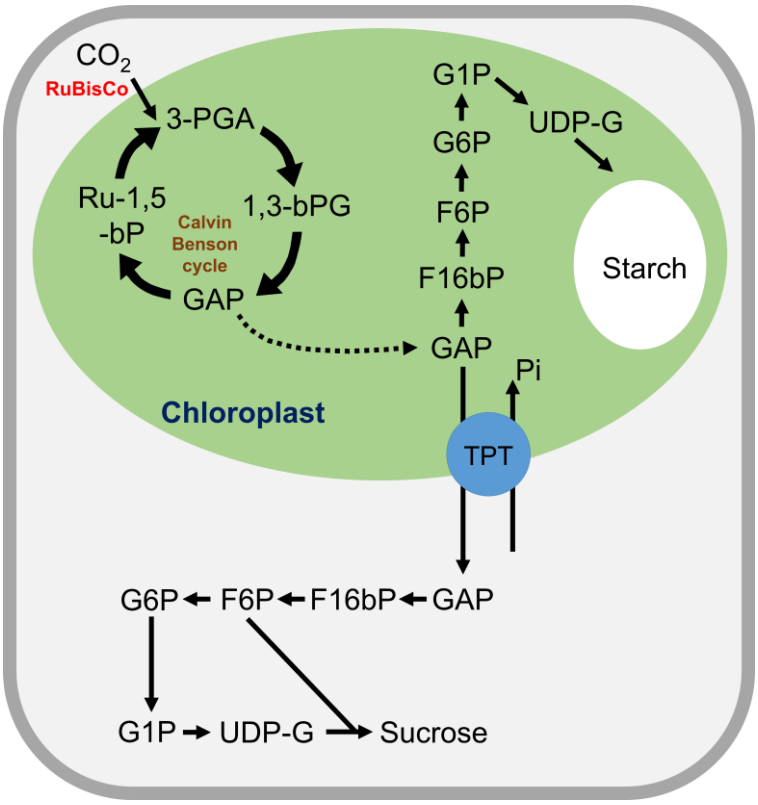

Figure 1.2 Carbon fixation in autotrophic tissues. Plants obtain carbon from atmospheric CO_2 that is introduced in the Calvin-Benson cycle by RuBisCo. Trioses-phosphate (GAP) produced in this cycle are used to synthesize transient starch in the chloroplast, and sucrose in the cytosol, after translocation through the TPT. 1,3-bPG, 1,3-bisphosphoglycerate; 3-PGA, 3-phosphoglyceric acid; F16bP, fructose 1,6-bisphosphate; F6P, fructose-6-phosphate; G1P, glucose-1-phosphate; G6P, glucose-6-phosphate; GAP, glyceraldehyde-3-phosphate; Pi, inorganic phosphate; Ru-1,5-bP, ribulose-1,5-bisphosphate; TPT, triose-phosphate/phosphate translocator; UDP-G, uridine-diphosphate-glucose.

During the dark period, transitory starch is mobilized to continuously supply sink organs with carbon, as well as to maintaining leaf metabolism. Due to its insoluble nature, starch must undergo a degradation step allowing the release of soluble carbohydrates. In the leaves, the hydrolytic pathway is thought to be the most relevant for the degradation of starch. This yields glucose and maltose that must be exported to the cytosol by specific transporters (Fig. 1.3; Weise *et al.*, 2004). The cloning of putative plastidial glucose translocators (pGlcT) was reported in spinach, potato, tobacco, *Arabidopsis* and maize (Weber *et al.*, 2000). The transport of maltose from the chloroplast to the cytosol was elucidated after the characterization of the MEX (Maltose Excess) protein as a maltose transporter (Niittylä *et al.*, 2004). This protein, which is unrelated to other known sugar

transporters, is the main route of carbon export from the chloroplast during the night (Fig. 1.3; Niittylä *et al*., 2004; Weber, 2004; Weise *et al*., 2004). Therefore, the generation of sucrose in the cytosol, which is used as the main carbohydrate for long distance transport, is intrinsically related with the activity of the TPT during the day and MEX during the night, and thus plastid transporters play a central role in the regulation of carbohydrate metabolism.

1.2.2 Role of the plastids in sink tissues

Although plastids play a fundamental role in source tissues, their importance in sinks should not be overlooked. The storage of starch in the amyloplasts of potato tissues or in the cereal endosperm, and the accumulation of carotenoids in the chromoplasts of flowers and fruits illustrates well the relevance of plastids in sink tissues.

Non-green plastids of heterotrophic tissues are carbohydrate-importing organelles. Due to the absence of 1,6-bisphosphatase activity, they are unable to generate hexose phosphates from C_3-compounds, and therefore must rely on the uptake from the cytosol of generated C_6 compounds (Flügge, 1999; Niewiadomski *et al*., 2005). This step is mediated by a GPT that imports glucose-6-Pi in exchange with inorganic phosphate or C_3-sugar phosphates (Hill and Smith, 1991; Neuhaus *et al*., 1993; Flügge and Weber, 1994; Schunemann and Borchert, 1994; Quick and Neuhaus, 1996; Niewiadomski *et al*., 2005). In the plastid, glucose-6-Pi may be used as a carbon source for starch synthesis, as a substrate for fatty acid and carotenoid biosynthesis, or as a starter molecule for the Oxidative Pentose Phosphate pathway and glycolysis (OPPP; Niewiadomski *et al*., 2005).

1.2.3 The role of plastids in starch accumulating tissues

Amyloplasts are the place of starch synthesis and storage in sink organs like the cereal grain, tubers, roots and trunk in woody perennials and green fruits. After its transport to the plastid stroma through GPT, glucose-6-Pi is converted into ADP-glucose, which is then incorporated into the starch grain by the action of starch synthases (Fig. 1.4). In the cereal endosperm, UDP-glucose synthesized in the cytosol is the main precursor of starch synthesis after its incorporation in the amyloplast through the brittle-1 translocator (Shannon *et al*., 1998).

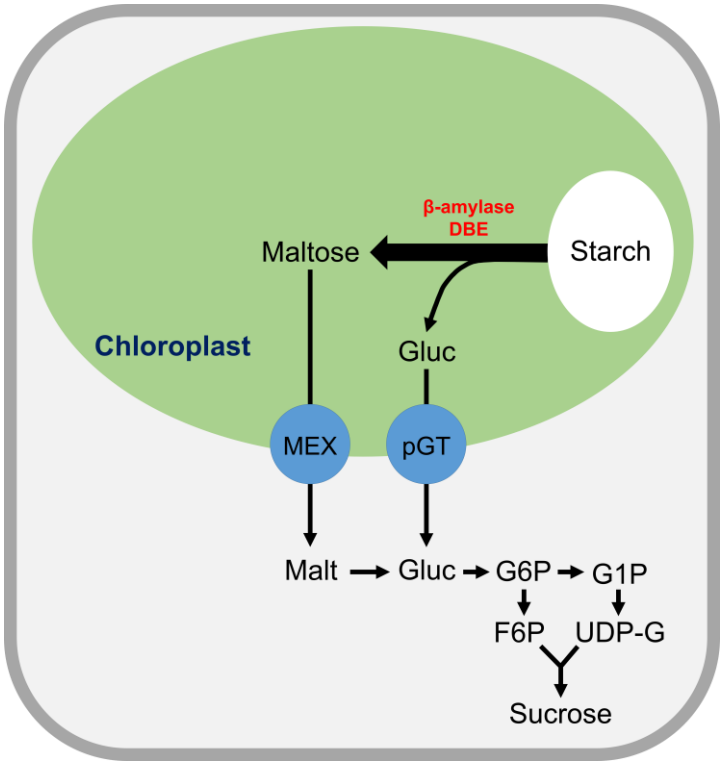

Figure 1.3 Remobilization of leaf transient starch during the night sustains cellular metabolism and continuously feed sink tissues with sugars. The carbon accumulated in the chloroplast during the light period is remobilized following the action of the hydrolytic enzymes β-amylase and DBE that yields glucose and, mainly, maltose. These sugars are transported into the cytosol by the MEX and pGT transporters and used for sucrose synthesis. DBE, debranching enzyme; F6P, fructose-6-phosphate; G1P, glucose-1-phosphate; G6P, glucose-6-phosphate; Gluc, glucose; Malt, maltose; MEX, maltose translocator; pGT, plastidial glucose translocator; UDP-G, uridine-diphosphate-glucose.

Also, green fruits contain photosynthetically active starch-containing chloroplasts, which are generally converted into non-photosynthetically plastids during the ripening phase (Bouvier and Camara, 2007).

1.2.4. Plastids are involved in secondary metabolism

The plastids found in fruits have central roles in isoprenoids biosynthesis, acyllipid metabolism, and shikimate pathway (Fig 1.5; Bouvier and Camara, 2007; Flügge *et al*., 2011). In plants, all isoprenoid compounds are produced from two universal 5-carbon precursors: isopentenyl diphosphate (IPP) and dimethylallyl diphosphate (DMAPP), by two distinct biosynthetic pathways. The first, the mevalonate pathway (MVA), takes place

in the cytosol where IPP and DMAPP are synthesized from mevalonic acid, and its final products are sesquiterpenes and polyterpenes (Lichtenthaler, 1999; Cordoba *et al*., 2009). The second one, known as the methyl-D-erythritol 4-phosphate (MEP) pathway, uses pyruvate and glyceraldehyde-3-phosphate for IPP and DMAPP synthesis and exclusively takes place within the plastids (Lichtenthaler, 1999).

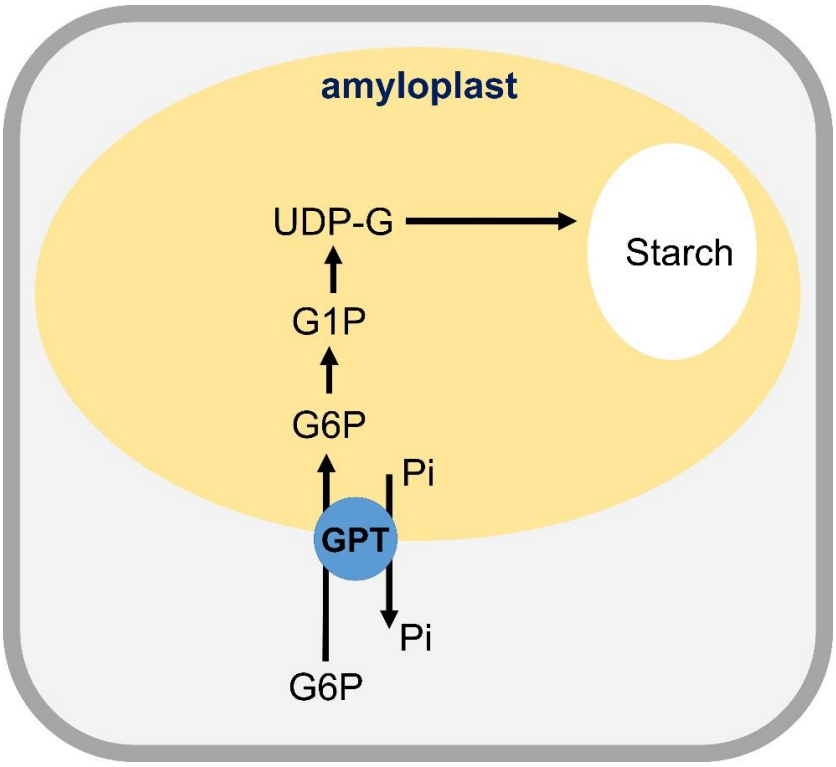

Figure 1.4 Starch synthesis in storage tissues. In heterotrophic tissues, sucrose imported from the phloem is hydrolyzed to glucose and fructose by invertases and phosphorylated by hexokinases. Glucose-6-Pi is transported into the amyloplast by GPT and used as a precursor for starch biosynthesis. G1P, glucose-1-phosphate; G6P, glucose-6-phosphate; GPT, glucose-6-phosphate/phosphate translocator; Pi, inorganic phosphate; UDP-G, uridine-diphosphate-glucose.

Carotenoids synthesized in the plastids as C_{40} isoprenoid derivatives are responsible for the yellow, orange and red colors of many fruits. In addition to their role promoting seed dispersal by herbivores, carotenoids are a fundamental quality parameter in several crops used in human diet. Besides carotenoids, several other important compounds are derived from the MEP pathway, like plastoquinone, tocopherols, gibberellins, phytol-PP involved in chlorophyll biosynthesis, strigolactones, and the phytohormone abscisic acid (ABA; Fig 1.5; Cordoba *et al*., 2009). In this pathway, both pyruvate and GAP can be obtained from glycolysis within plastids but, since plastids from some heterotrophic tissues

are unable to form pyruvate from 3-phosphoglyceric acid, they must incorporate cytosolic PEP by the action of PPT (phosphoenolpyruvate/phosphate translocator) (Fischer *et al*., 1997; Flügge *et al*., 2011). Interestingly, it was reported in *Arabidopsis* that a plastidial enolase is not expressed in photosynthetic tissues, but shows high transcript abundance in some heterotrophic organs, suggesting that these plastids have a complete glycolytic pathway capable of providing pyruvate and GAP (Prabhakar *et al*., 2009).

1.2.5. Plastids are involved in lipid metabolism

The *de novo* biosynthesis of fatty acids occurs exclusively within plastids. Although most of the commercial oils are obtained from seeds, a significant part is derived from fruits, mainly from the pericarp of oil palm and olives (Bouvier and Camara, 2007).

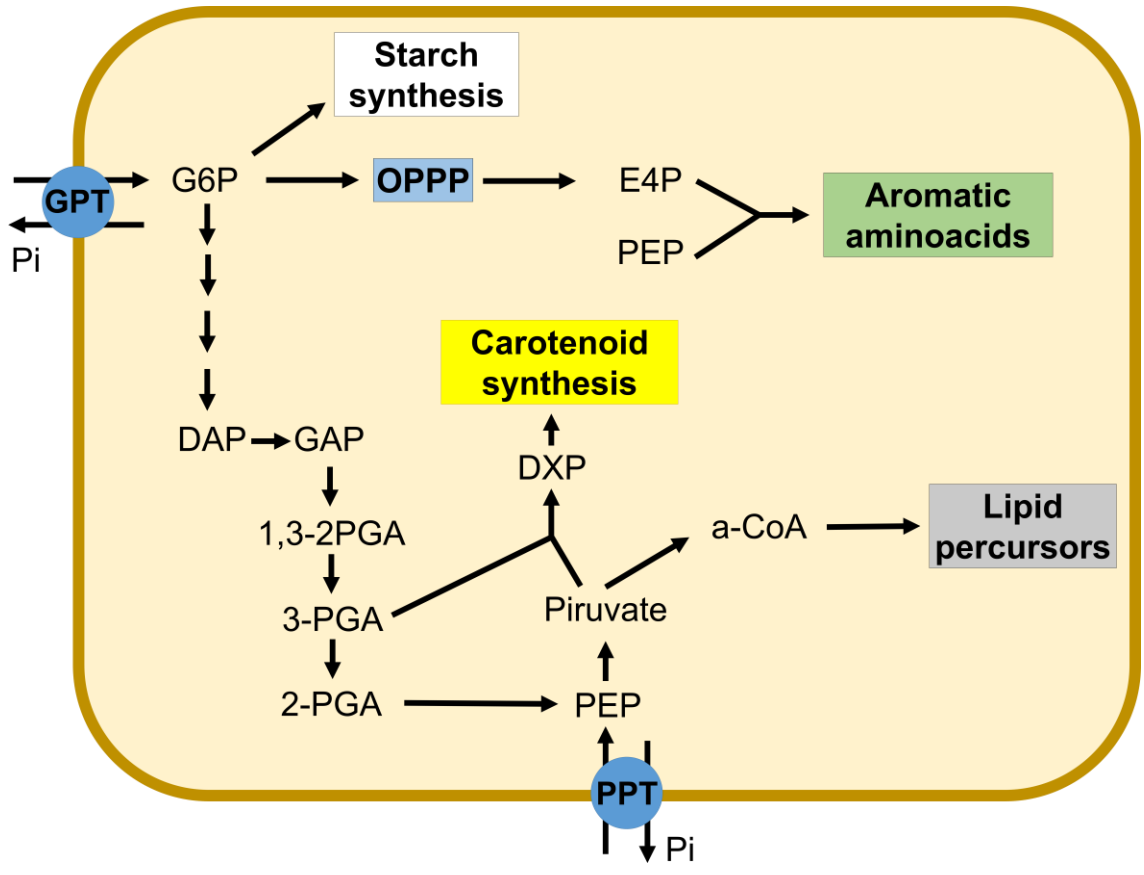

Figure 1.5 Simplified model of the potential role of plastids in the fruits. Plastids that have a complete glycolytic pathway may synthesize starch, carotenoids, aromatic amino acids, and lipid precursors. These processes are interconnected with the cytosolic metabolism by the action of several plastidial transporters. 1,3-2PGA, 1,3-bisphospho-D-glycerate; 2-PGA, 2-phosphoglyceric acid; 3-PGA, 3-phosphoglyceric acid; a-CoA, acetyl coenzyme A; DAP, dihydroxyacetone-3-

phosphate; DXP, 1-deoxy-D-xylulose 5-phosphate; E4P, erythrose-4-phosphate; G6P, glucose-6-phosphate; GAP, glyceraldehyde-3-phosphate; GPT, GPT, glucose-6-phosphate/phosphate translocator; OPPP, oxidative pentose-phosphate pathway; PEP, phosphoenolpyruvate; Pi, inorganic phosphate; PPT, phosphoenolpyruvate/phosphate translocator.

In fruit plastids, the *de novo* synthesis of fatty acids occurs from acetyl-CoA before undergoing further modification in the endoplasmic reticulum where triacylglycerol may accumulate (Salas *et al*., 2000). Two major mechanisms for the synthesis of acetyl-CoA in the plastid are described, the first one involving the degradation of C_6 sugars via glycolysis, which can yield acetyl-CoA by the action of a plastid-localized pyruvate dehydrogenase (Fig 1.5). In the second one, acetyl-CoA is produced in the mitochondria, by mitochondrial pyruvate dehydrogenase, and converted into acetic acid that is transported into the plastid and re-activated to acetyl-CoA (Salas *et al*., 2000; Conde *et al*., 2008).

1.3. Water transport in plants and aquaporins

Water is the most important resource for plant growth and metabolism, but also the most limiting factor in agriculture. The distribution of water throughout the plant is fundamental for several physiological processes (Chaumont and Tyerman, 2014). The most recognized event of water movement in plants is the evapotranspiration when water evaporates through the stomata. The gradient of water potential ($\Delta\Psi$) is the main driver of movement of water from the root xylem (high Ψ) to the leaf surface (low Ψ; Chaumont and Tyerman, 2014). This gradient creates a tension in the xylem vessels, thus drawing water from the soil to the root up to the leaves (Steudle, 2001). Three different known paths for water flow across plant roots to the central vessels are recognized: apoplastic, symplastic and transcellular (Fig. 1.6). In the apoplastic route water flows through the space between the cell walls; in the symplastic pathway, it moves from cell to cell through plasmodesmata; and in the transcellular pathway, it moves across plasma membranes through the action of aquaporins (AQP). It has been proposed that the transcellular pathways should be essential for the passage of water in selective cell layers such as the exodermis and endodermis, particularly in the latter due to the presence of apoplastic barriers like the Casparian strip and suberin lamellae (Steudle and Peterson, 1998; Chaumont and Tyerman, 2014), as observed in maize (Hachez *et al*., 2006), rice (Sakurai *et al*., 2008), and poplar (Laur and Hacke, 2013).

AQPs are found in most living organisms, and are involved in many different physiological processes (Gomes *et al*., 2009). Seminal work postulated the involvement of water channels activity in biological membranes based on the observation that the rate of water diffusion across an artificial lipid bilayer is relatively low when compared to the water permeability of the membrane The first aquaporin (CHIP28 latter renamed AQP1) was discovered by Peter Agre and collaborators in 1992 (Preston *et al*., 1992), although in a parallel work protein mediated water transport in erythrocytes was shown (Benga *et al*., 1986).

The first plant water channel was identified by Maurel *et al*. (1993) and named AtTIP1;1. Since then, several plant AQPs have been identified, cloned, and functionally characterized (Gomes *et al*., 2009). Today, it is widely accepted that AQP-mediated water transport in plants plays key physiological roles in cell elongation, seed germination, and osmoregulation (Maurel, 2007; Chaumont and Tyerman, 2014). Comparatively to other organisms, plants have a remarkable large number of aquaporins ubiquitously expressed, with more than 30 members in rice (*Oryza sativa*; Sakurai *et al*., 2005), maize (*Zea mays*; Chaumont *et al*., 2001), *Arabidopsis* (Johanson *et al*., 2001), tomato (*Solanum lycopersicum*; Reuscher *et al*., 2013), poplar (*Populus trichocarpa*; Gupta and Sankararamakrishnan, 2009), cotton (*Gossypium hirsutum*; Park *et al*., 2010), and soybean (*Glycine max*; Zhang *et al*., 2013).

Aquaporins belong to the MIP family (Major Intrinsic Protein) together with two other sub-families, the glycerol-facilitators and the aquaglyceroporins (Gomes *et al*., 2009). They are small membrane proteins (21 to 34 kD) consisting of six membrane-spanning α-helices connected by five loops (A to E) and with N- and C-termini facing the cytosol. Two loops, B and E, are hydrophobic α-helices that dip halfway into the membrane from opposite sides. Together with the membrane-spanning helices, these loops form a pore with two filter regions responsible for the aquaporin specificity (Fig. 1.7A). The first filter region is formed by two NPA (Asp-Pro-Ala) motifs from loops B and E that meet at the center of the pore creating the first size exclusion zone. The second one, the ar/R filter (aromatic/arginine), is formed by four amino acids and is also a size exclusion barrier involved in substrate specificity (Hub and de Groot, 2008; Azad *et al*., 2012). A particularly interesting feature of AQPs is their capacity to assemble as homo- and/or hetero-tetramers

in the membrane, with each monomer acting as independent water channel (Fig. 1.7B; Murata *et al*., 2000; Fetter *et al*., 2004; Chaumont and Tyerman, 2014).

Considering their sequence homology and subcellular localization, AQPs have been grouped in five subfamilies: the plasma membrane intrinsic proteins (PIPs), the tonoplast intrinsic proteins (TIPs), the Nodulin26-like intrinsic proteins (NIPs), firstly found in the legume symbiosome, the small basic intrinsic proteins (SIPs), and the X (from "uncharacterized") intrinsic proteins (XIPs) (Gomes *et al*., 2009; Chaumont and Tyerman, 2014). This particularly high number of AQPs and their relative ubiquity and diversity in plant tissues may emerge from the continuous need of water absorption, flux and subsequent evaporation during plant growth and development, as well as from their involvement in the transport of several other solutes besides water (Bienert *et al*., 2007, 2011; Gomes *et al*., 2009). Indeed, several plant AQPs have been shown to mediate the transport of small uncharged solutes, including glycerol, urea, ammonia, carbon dioxide, hydrogen peroxide, and the metalloids boric acid, silicic acid, and arsenite, which may account for an important role in plant metabolism, nutrition, and signaling processes (Chaumont and Tyerman, 2014). The movement of water and other solutes through AQPs or aquaglyceroporins is a passive mechanism driven by the concentration gradient of the transported molecule.

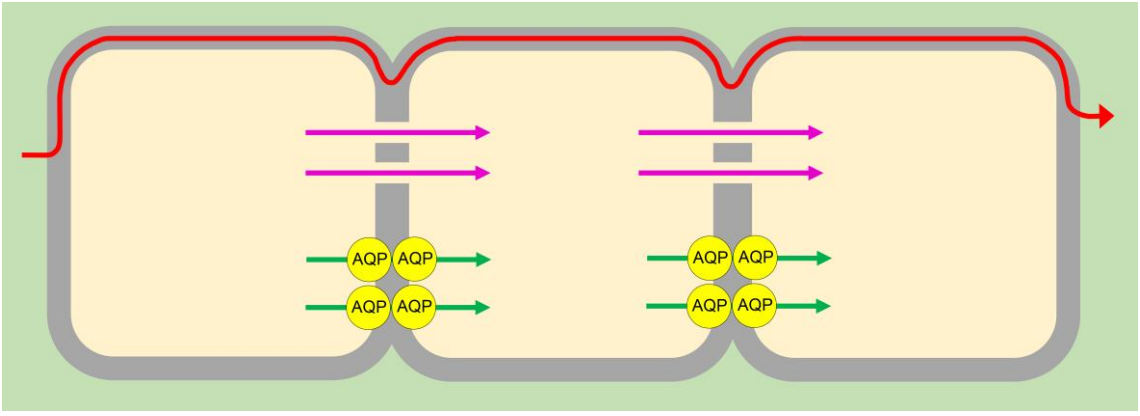

Figure 1.6 Different pathways for water movement across plant tissues, excluding long-distance transport. In the apoplastic pathway (red), water moves through the apoplast (grey, cell walls). In the symplastic pathway (pink), water moves through plasmodesmata that bridge the cytoplasm (light brown) of adjacent cells. In the transcellular pathway (green), water moves across the plasma membranes of the adjacent cells through AQP (aquaporins, yellow). Adapted from Steudle and Peterson (1998).

1.4. Solute transporters in grapevine environment-interactions and berry quality

Wine is an emblematic product of the Mediterranean culture. Grapevine (*Vitis vinifera* sp.) is native from the geographical region between the Black Sea and Persia, and might have been introduced in the Iberian Peninsula by the Phoenicians in the last millennium BC (Terral *et al*., 2010). Portugal has a long-standing tradition in grape-growing, with a production of 828700 tons of grapes in 2013 (19th biggest world producer, FAO). Douro is the oldest controlled appellation (DOC) region in the world and is well-known for its premium wines, including Port wine.

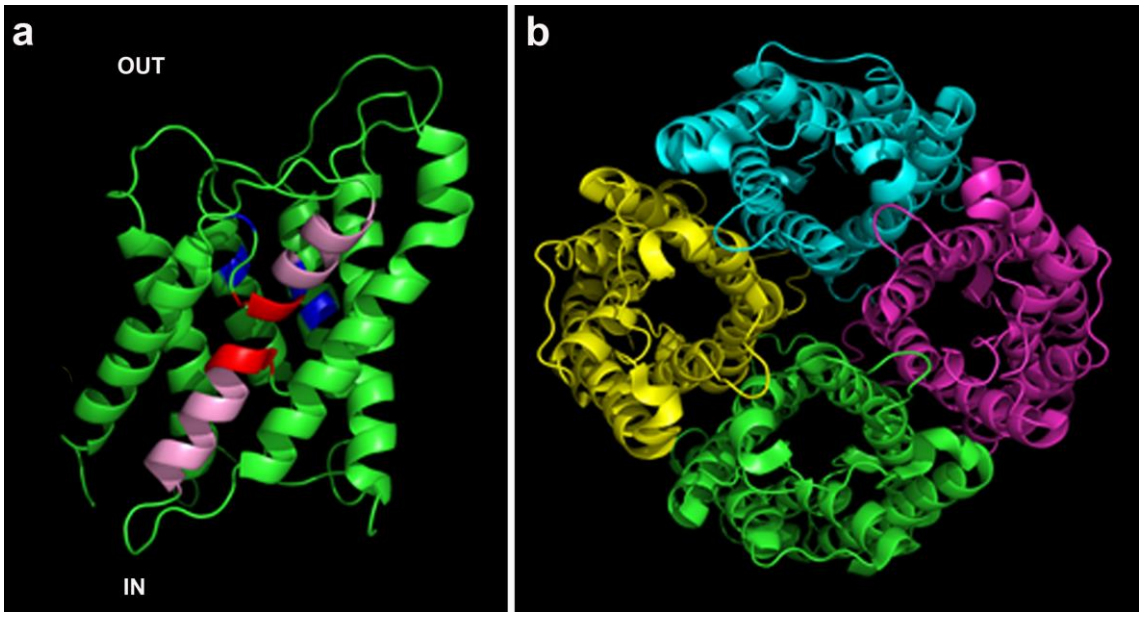

Figure 1.7 3-D representation of AQP1 (De Groot *et al*., 2001) depicting the NPA filter (red), the Ar/R filter (blue) and the characteristic loops B and E that form α-helixes that dip into the membrane (pink). In (B) the tetrameric assembly of AQP5 (Horsefield *et al*., 2008) is shown. Protein simulation was downloaded from the Protein Data Bank (AQP1, 1H6I; AQP5, 3D9S) and visualized using the PyMOL software.

The most important characteristic of grape berries, for both wine production and consumption as fresh fruit, is their ability to accumulate enormous amounts of sugars (Conde *et al*., 2007b). These sugars, mainly glucose and fructose, are produced in autotrophic tissues and translocated via the phloem in the form of sucrose, and are accumulated in the vacuole of grape berry tissues, mainly in the mesocarp (Agasse *et al*., 2007; Fontes *et al*., 2011). In addition, a close relationship between sugar and anthocyanin

contents in berries has been reported, suggesting that sugar accumulation is central for the synthesis of secondary metabolites (Pirie and Mullins, 1977; Hunter *et al*., 1991; Larronde *et al*., 1998). Thus, unlocking the mechanisms and regulation of solute transporters is of the utmost scientific and agronomical importance, ultimately aiming at the improvement of berry quality through the optimization of agricultural practices.

1.4.1 Grapevine sugar transporters

Similarly to other dicots, the sucrose transporter family of grapevine is a small multigenic family of four members (Afoufa-Bastien *et al*., 2010; Lecourieux *et al*., 2014). Three sucrose transporter cDNAs were cloned from Shiraz and Cabernet Sauvignon berries (*VvSUC11* or *VvSUT1*, *VvSUC12*; and *VvSUC27*) and characterized as H^+-dependent sucrose transporters by heterologous expression in *Saccharomyces cerevisiae* (Ageorges *et al*., 2000; Manning *et al*., 2001; Lecourieux *et al*., 2014). As reported above, sucrose transporters are fundamental in phloem loading from the apoplast, and also in maintaining sucrose in the conducting bundle until it reaches the sites of unloading (Lecourieux *et al*., 2014). This role was highlighted in maize, where the *sut1* (*Sucrose Transporter 1*) null-mutant showed leaves with reduced sucrose export leading to the accumulation of carbohydrates, chlorosis and early senescence, causing a reduced growth and delayed flowering (Slewinski *et al*., 2009).

In grapevine, a shift from symplastic to apoplastic unloading of the phloem was reported at, or just prior to, the onset of ripening (Zhang *et al*., 2006). The blocking of the plasmodesmata correlated well with the increase in the expression and activity of cell wall invertases, which also coincided with a rise in apoplastic sugar concentration and osmotic pressure (Zhang *et al*., 2006). It was also observed that the expression of several grapevine *MSTs* increased after veraison (Afoufa-Bastien *et al*., 2010), hence pointing to a fundamental role of MSTs in the accumulation of the high amounts of sugars observed in the grape berry.

A bioinformatics approach allowed the identification of 59 putative hexose transporter homologues in grapevine (Jaillon *et al*., 2007; Afoufa-Bastien *et al*., 2010; Lecourieux *et al*., 2014). Six full-length cDNAs encoding *MSTs* named *VvHT1–VvHT6* (*Vitis vinifera hexose transporter*) were cloned from several cultivars including Pinot noir,

Ugni blanc, Chardonnay, Cabernet Sauvignon, and Syrah (Fillion *et al*., 1999; Vignault *et al*., 2005; Hayes *et al*., 2007). Despite the high number of putative *MSTs* identified in grapevine, no other transporter, besides *VvHT1-VvHT6* were cloned from berry tissues (Afoufa-Bastien *et al*., 2010; Lecourieux *et al*., 2014). The plasma membrane localization of VvHT1, VvHT4 and VvHT5 was demonstrated by immunofluorescence, immunolabeling, and GFP fusion proteins (Vignault *et al*., 2005; Hayes *et al*., 2007), but VvHT2 and VvHT6 (also known as VvTMT2, *Vitis vinifera* tonoplast monosaccharide transporter) seem to be localized at the tonoplast (Lecourieux *et al*., 2014). More recently, a polyol transporter termed *VvPLT1* (*Vitis vinifera* polyol transporter 1) was cloned from mesocarp tissues, and the VvPLT1-GFP fusion protein is localized at the plasma membrane (Conde *et al*., 2015).

To tackle the effects of biotic and abiotic stresses, plants have developed complex strategies involving a wide range of biochemical and physiological processes, which include the fine regulation of sugar transporters. Thus, it has been reported that powdery and downy mildew infections affect the expression of *VvHT5* in grapevine leaves (Hayes *et al*., 2010). Also, infection with the Grapevine leaf-roll-associated virus-3 (GLRaV-3) decreases the accumulation of sugars and anthocyanins in berries paralleled with a decreased expression of *VvHT1* and one of its transcription regulators, *VvMSA* (Cakir *et al*., 2003; Vega *et al*., 2011). Besides biotic stress, several other factors, like water deficit, alter the expression of *MSTs* in grapevine. This is the case for *VvPLT1*, whose expression is higher in mature berries subjected to water-deficit stress and correlates well with the observed increased amounts of polyols in pulp tissues (Conde *et al*., 2015). These results suggest that grapevine MSTs may be involved in the modification of the berry composition in response to environmental stress.

Seventeen *SWEETs* were identified in grapevine and divided into five sub-classes (Chong *et al*., 2014). All genes were differently expressed in vegetative and reproductive organs, with *VvSWEET3* and *VvSWEET5a* highly expressed in flowers, and *VvSWEET4* and *VvSWEET15* in berries. The expression of the glucose uniporter *VvSWEET4* was substantially increased after the inoculation of leaves with the necrophitic fungus *Botrytis cinerea* (Chong *et al*., 2014). In agreement, *Arabidopsis* null-mutants for the homolog *AtSWEET4* and *AtSWEET5* genes showed an increased resistance against *Botrytis cinerea*

infection, suggesting that plant *SWEETs* can be recruited by pathogens to their benefit (Chen *et al*., 2010).

1.4.2 Grapevine plastidial metabolism

As stated above, a significant part of secondary metabolites or their intermediates are synthesized in plastids, but knowledge about their metabolism in grapevine is still very limited. Although anthocyanins are not synthesized in the plastid, the generation of aromatic amino acids in the shikimate pathway takes place exclusively within this organelle. Stress conditions stimulate the production of secondary metabolites in grapevine plastids (Chaves *et al*., 2010). In grape cell suspensions, the enzyme geranyl-diphosphate, that adds IPP to elongating chain during terpenoids biosynthesis is localized in the plastid (Soler *et al*., 1992) and IPP is compartmented into this organelle by a plastidial membrane protein (Soler *et al*., 1993). Furthermore, feeding experiments with detached leaves showed that monoterpenes are exclusively synthesized in the plastid *via* MEP pathway (Hampel *et al*., 2005), but sesquiterpenes may be generated in the plastid and cytosol (MVA pathway). A similar approach with detached berries confirmed that the exocarp is able to synthesize sesquiterpenes also via both pathways (May *et al*., 2013).

As a woody perennial plant, grapevine relies in the accumulation of carbon reserves in the woody tissues and roots, to sustain its characteristic rapid seasonal growth. The starch accumulated in amyloplasts during the previous season, mainly in the roots, trunk and canes, is rapidly remobilized to allow the growth in the spring (Zapata *et al*., 2004). The molecular mechanism of starch accumulation in grapevine plastids is further explored in Chapter 2 in the context of the characterization of plastidial glucose-6-Pi translocators *VvGPTs*.

1.4.3 Grapevine water relations and aquaporins

Water transport in grapevine is an important research topic because water is the most important constituent of the fruit and, thereby, of the wine. Grape berries normally contain 75–85% water, which is the main solvent of sugars, acids and phenolic compounds (Conde *et al*., 2007b). Therefore, the quality, via the concentration of sugars and flavor

compounds, and yield of the vintage are directly affected by berry water content at harvest (Tyerman *et al*., 2012).

Different resistances to soil water availability and leaf-to-air vapor pressure deficit are found among the numerous grapevine varieties (Costa *et al*., 2012). Grapevines are classified in two distinct groups regarding their control of stomatal opening/closure: isohydric (drought avoiders or "pessimistic"), and anisohydric ("optimistic"). So far, the contribution of aquaporins to the isohydric and anisohydric behaviours of the cultivars is still a matter of debate. Isohydric genotypes are characterized by a tight regulation of stomatal closure when exposed to water deficit. On the other hand, anisohydric cultivars typically show a less marked control of stomatal aperture under drought. Nevertheless, this classification cannot be strict because anisohydric cultivars may behave has isohydric, or vice-versa, depending on the experimental conditions (field vines vs. potted vines) and on the intensity of water deficit (Chaves *et al*., 2010). Thus, understanding the physiological and molecular bases of grapevine responses to water-deficit stress may allow the optimization of the irrigation protocols and the identification of water-stress resistant cultivars.

Up to 30 *AQPs* have been found in grapevine genome and grouped in the five subfamilies described above (Fouquet *et al*., 2008; Shelden *et al*., 2009; Leitão *et al*., 2012; Sabir *et al*., 2014). Data from macroarrays showed that the expression levels of some *PIPs* and *TIPs* depend on the grape berry developmental stage, and a global decrease in *AQP* expression was observed during fruit maturation (Fouquet *et al*., 2008). The water transport activity of nine grapevine AQPs upon its expression in *Xenopus laevis* oocytes was reported by Shelden *et al*. (2009). Interestingly, only VvPIP2 (VvPIP2;1, VvPIP2;2, VvPIP2;3 and VvPIP2;4) and VvTIP (VvTIP1;1 and VvTIP2;1), but not VvPIP1 (VvPIP1;2 and VvPIP1;4), showed water transport activity. This agrees with previous reports made for maize, where PIP1 needs to be co-expressed with PIP2 members to effectively function as a water channel (Fetter *et al*., 2004). The activity of VvPIP2;1 (Shelden *et al*., 2009) and VvTIP2;1 (Leitão *et al*., 2012) were down-regulated by cytosolic acidosis, a mechanism of AQP regulation previously described (Tournaire-Roux *et al*., 2003). In VvTIP2;1 the histidine at position 131 in loop D is fundamental for the gating (Leitão *et al*., 2012).

More recently, the specificity of three VvPIPs and three VvTIPs was reported (Sabir *et al*., 2014). VvPIP1;4, VvPIP2;1, VvPIP2;3, VvTIP1;1, and VvTIP2;2 could mediate H_2O_2 transport and VvTIP1;1 and VvTIP2;2 transported H_3BO_3, which confirms the broad specificity of grapevine AQPs (Bienert *et al*., 2007, 2011; Gomes *et al*., 2009; Chaumont and Tyerman, 2014).

It is generally assumed that aquaporins play a fundamental role in the maturation zone of the roots, where more suberization occurs and there is a blockage of the plasmodesmata. Interestingly, in fine roots of grapevine the highest *AQP* expression was observed in the root tip, dropping considerably in the maturation zone, which suggests that AQPs play a limited role in the control of water uptake in secondary growth zones (Gambetta *et al*., 2013).

In Chapters 3 and 4 the diversity and role of grapevine aquaporins are further explored, and special emphasis will be given to intracellular aquaporins, in particular SIPs and XIPs.

1.5 Research objectives

Our group generally focus its research on the elucidation of the biochemical mechanisms and transport steps involved in the accumulation of sugars, organic acids, phenolics and water in the grape berry, and how these processes are coordinated during ripening and influenced by environmental stresses. In the present thesis, we aimed to characterize specific grapevine sugar and water transporters involved in intracellular metabolism, to investigate their role at tissue- and whole-plant levels and evaluate their impact in grape berry development and composition. Studies were performed with cultured cells and plant organs, including berries. *In vitro* plantlets, potted and field-grown plants under well-defined experimental conditions were the source of biological material. The work was developed in the context of national (FCT) and international (EU: Innovine) research projects in progress in our laboratory in cooperation with several national and international research groups.

In Chapter 2, *GPT* members of grapevine were identified and two of them, *VvGPT1* and *VvGPT2*Ω, were cloned and characterized. Expression of *35S-VvGPT1-GFP* and *35S-*

*VvGPT2*Ω-*GFP* in tobacco leaf epidermal cells showed that the fusion proteins localized at the plastidial envelope. These genes showed different expression levels and regulation in plant organs. *VvGPT1* expression was higher in berries more exposed to the sun, thus subjected to higher temperatures. Results will be discussed in terms of the role of both glucose-6-Pi transporters in the accumulation of starch in storage tissues and in the secondary metabolism.

In Chapter 3, the localization, expression and functional characterization of a *SIP* aquaporin from grapevine is described. *VvSIP1* was expressed in leaves and berries from field-grown vines, and in leaves and stems from *in vitro* plantlets, but not in roots. When expressed in tobacco mesophyll cells and in *Saccharomyces cerevisiae*, fluorescent-tagged VvSIP1 was localized at the endoplasmic reticulum (ER). The capacity of VvSIP1 to transport water was accessed by stopped-flow spectroscopy in membrane vesicles from transformed yeasts. To provide further insights into gene function, the expression of *VvSIP1* in mature grapes was also studied when vines were cultivated in different field conditions. Results will be discussed with reference to the potential role of an ER aquaporin in cell and plant physiology.

Chapter 4 is devoted to the study of other atypical grapevine aquaporin, termed *Uncharacterized Intrinsic Protein 1* (*VvXIP1*). VvXIP1 showed unusual substrate specificity. Stopped-flow spectrometry in microsomal vesicles from yeast transformed with *pVV214-VvXIP1* revealed that VvXIP1 is unable to transport water but transports glycerol, copper, boron and H_2O_2. The response of *VvXIP1* to environmental stresses and hormonal signals was also evaluated in grapevine tissues and cultured cells. Results will be discussed in terms of the physiological role of such atypical tonoplast aquaporin. The observed capacity of VvXIP1 to transport copper was particularly intriguing.

Finally, in Chapter 5 the main conclusions of the present study are integrated with the state of the art, and results are discussed in terms of its implications for our understanding of grapevine - environment interactions at solute transport level. Moreover, the findings presented in the present thesis pave the way for future research avenues that are also discussed.

1.6 References

Afoufa-Bastien D, Medici A, Jeauffre J, Coutos-Thévenot P, Lemoine R, Atanassova R, Laloi M. 2010. The Vitis vinifera sugar transporter gene family: phylogenetic overview and macroarray expression profiling. *BMC Plant Biology* **10**, 245.

Agasse A, Vignault C, Kappel C, Conde C, Delrot S. 2007. Sugar transport & sugar sensing in grape. In: Roubelakis-Angelakis K, ed. Grapevine Molecular Physiology & Biotechnology. Springer, 105–139.

Ageorges A, Issaly N, Picaud S, Delrot S, Romieu C. 2000. Identification and functional expression in yeast of a grape berry sugar carrier. *Plant Physiology* **38**, 177–185.

Azad AK, Yoshikawa N, Ishikawa T, Sawa Y, Shibata H. 2012. Substitution of a single amino acid residue in the aromatic/arginine selectivity filter alters the transport profiles of tonoplast aquaporin homologs. *Biochimica et Biophysica Acta - Biomembranes* **1818**, 1–11.

Benga G, Popescu O, Pop VI, Holmes RP. 1986. *p*-(chloromercuri)benzenesulfonate binding by membrane proteins and the inhibition of water transport in human erythrocytes. *Biochemistry* **25**, 1535–1538.

Bienert GP, Bienert MD, Jahn TP, Boutry M, Chaumont F. 2011. *Solanaceae* XIPs are plasma membrane aquaporins that facilitate the transport of many uncharged substrates. *The Plant Journal* **66**, 306–317.

Bienert GP, Møller ALB, Kristiansen K a, Schulz A, Møller IM, Schjoerring JK, Jahn TP. 2007. Specific aquaporins facilitate the diffusion of hydrogen peroxide across membranes. *The Journal of Biological Chemistry* **282**, 1183–92.

Bouvier F, Camara B. 2007. The role of plastids in ripening fruits. In: Wise RR, Hoobe JK, eds. The structure and function of plastids. Springer, 419–432.

Büttner M, Sauer N. 2000. Monosaccharide transporters in plants: Structure, function and physiology. *Biochimica et Biophysica Acta - Biomembranes* **1465**, 263–274.

Cakir B, Agasse A, Gaillard C, Saumonneau A, Delrot S, Atanassova R. 2003. A grape ASR protein involved in sugar and abscisic acid signaling. *The Plant cell* **15**, 2165–2180.

Chardon F, Bedu M, Calenge F, *et al.* 2013. Leaf fructose content is controlled by the vacuolar transporter SWEET17 in *Arabidopsis*. *Current Biology* **23**, 697–702.

Chaudhuri B, Hörmann F, Lalonde S, Brady SM, Orlando DA., Benfey P, Frommer WB. 2008. Protonophore- and pH-insensitive glucose and sucrose accumulation detected by FRET nanosensors in *Arabidopsis* root tips. *The Plant Journal* **56**, 948–962.

Chaumont F, Barrieu F, Wojcik E, Chrispeels MJ, Jung R. 2001. Aquaporins constitute a large and highly divergent protein family in maize. *Plant Physiology* **125**, 1206–15.

Chaumont F, Tyerman SD. 2014. Aquaporins: highly regulated channels controlling plant water eelations. *Plant Physiology* **164**, 1600–1618.

Chaves MM, Zarrouk O, Francisco R, Costa JM, Santos T, Regalado a. P, Rodrigues ML, Lopes CM. 2010. Grapevine under deficit irrigation: hints from physiological and molecular data. *Annals of Botany* **105**, 661–676.

Chen L-Q, Hou B-H, Lalonde S, *et al.* 2010. Sugar transporters for intercellular exchange and nutrition of pathogens. *Nature* **468**, 527–32.

Chen L-Q, Qu X-Q, Hou B-H, Sosso D, Osorio S, Fernie a. R, Frommer WB. 2012. Sucrose efflux mediated by SWEET proteins as a key step for phloem transport. *Science* **335**, 207–211.

Chong J, Piron M-C, Meyer S, Merdinoglu D, Bertsch C, Mestre P. 2014. The SWEET family of sugar transporters in grapevine: VvSWEET4 is involved in the interaction with *Botrytis cinerea*. *Journal of Experimental Botany* **65**, 6589–6601.

Conde C, Delrot S, Gerós H. 2008. Physiological, biochemical and molecular changes occurring during olive development and ripening. *Journal of Plant Physiology* **165**, 1545–62.

Conde A, Regalado A, Rodrigues D, Costa JM, Blumwald E, Chaves MM, Gerós H. 2015. Polyols in grape berry: transport and metabolic adjustments as a physiological strategy for water stress tolerance in grapevine. *Journal of Experimental Botany* **66**, 889–906.

Conde C, Silva P, Agasse A, Tavares RM, Delrot S, Gerós H. 2007a. An Hg-sensitive channel mediates the diffusional component of glucose transport in olive cells. *Biochimica et Biophysica Acta* **1768**, 2801–11.

Conde C, Silva P, Fontes N, Dias ACP, Tavares RM, Sousa MJ, Agasse A, Delrot S, Gerós H. 2007b. Biochemical changes throughout grape berry development and fruit and wine quality. *Food* **1**, 1–22.

Cordoba E, Salmi M, León P. 2009. Unravelling the regulatory mechanisms that modulate the MEP pathway in higher plants. *Journal of Experimental Botany* **60**, 2933–2943.

Costa JM, Ortuño MF, Lopes CM, Chaves MM. 2012. Grapevine varieties exhibiting differences in stomatal response to water deficit. *Functional Plant Biology* **39**, 179–189.

Delrot S, Bonnemain JL. 1981. Involvement of protons as a substrate for the sucrose carrier during phloem loading in *Vicia faba* leaves. *Plant Physiology* **67**, 560-564.

Fetter K, Wilder V Van, Moshelion M, Van Wilder V, Moshelion M, Chaumont F. 2004. Interactions between plasma membrane aquaporins modulate their water channel activity. *The Plant Cell* **16**, 215–228.

Fillion L, Ageorges a, Picaud S, Coutos-Thévenot P, Lemoine R, Romieu C, Delrot S. 1999. Cloning and expression of a hexose transporter gene expressed during the ripening of grape berry. *Plant Physiology* **120**, 1083–1094.

Fischer K. 2011. The import and export business in plastids: transport processes across the inner envelope membrane. *Plant Physiology* **155**, 1511–1519.

Fischer K, Kammerer B, Gutensohn M, Arbinger B, Weber a, Häusler RE, Flügge UI. 1997. A new class of plastidic phosphate translocators: a putative link between primary and secondary metabolism by the phosphoenolpyruvate/phosphate antiporter. *The Plant Cell* **9**, 453–462.

Flügge U-I. 1999. Phosphate translocators in plastids. *Annual Review of Plant Physiology and Plant Molecular Biology* **50**, 27–45.

Flügge UI, Häusler RE, Ludewig F, Gierth M. 2011. The role of transporters in supplying energy to plant plastids. *Journal of Experimental Botany* **62**, 2381–2392.

Flügge UI, Weber APM. 1994. A rapid method for measuring organelle-specific substrate transport in homogenates from plant tissues. *Planta* **194**, 181–185.

Fontes N, Gerós H, Delrot S. 2011. Grape berry vacuole: A complex and heterogeneous membrane system specialized in the accumulation of solutes. *American Journal of Enology and Viticulture* **62**, 270–278.

Fouquet R, Léon C, Ollat N, Barrieu F. 2008. Identification of grapevine aquaporins and expression analysis in developing berries. *Plant Cell Reports* **27**, 1541–1550.

Gambetta GS, Fei J, Rost TL, Knipfer T, Matthews MA, Shackel KA, Walker MA, McElrone AJ. 2013. Water uptake along the length of grapevine fine roots:

Developmental anatomy, tissue-apecific aquaporin expression, and pathways of water transport. *Plant Physiology* **163**, 1254–1265.

Gomes D, Agasse a, Thiébaud P, Delrot S, Gerós H, Chaumont F. 2009. Aquaporins are multifunctional water and solute transporters highly divergent in living organisms. *Biochimica et Biophysica Acta - Biomembranes* **1788**, 1213–28.

De Groot BL, Engel A, Grubmüller H. 2001. A refined structure of human aquaporin-1. *FEBS Letters* **504**, 206–211.

Guo W-J, Nagy R, Chen H-Y, Pfrunder S, Yu Y-C, Santelia D, Frommer WB, Martinoia E. 2013. SWEET17, a facilitative transporter, mediates fructose transport across the tonoplast of Arabidopsis roots and leaves. *Plant Physiology* **164**, 777–789.

Gupta AB, Sankararamakrishnan R. 2009. Genome-wide analysis of major intrinsic proteins in the tree plant Populus trichocarpa: characterization of XIP subfamily of aquaporins from evolutionary perspective. *BMC Plant Biology* **9**, 134.

Hachez C, Moshelion M, Zelazny E, Cavez D, Chaumont F. 2006. Localization and quantification of plasma membrane aquaporin expression in maize primary root: A clue to understanding their role as cellular plumbers. *Plant Molecular Biology* **62**, 305–323.

Hampel D, Mosandl A, Wüst M. 2005. Induction of de novo volatile terpene biosynthesis via cytosolic and plastidial pathways by methyl jasmonate in foliage of *Vitis vinifera* L. *Journal of Agricultural and Food Chemistry* **53**, 2652–2657.

Hayes M a., Davies C, Dry IB. 2007. Isolation, functional characterization, and expression analysis of grapevine (*Vitis vinifera* L.) hexose transporters: Differential roles in sink and source tissues. *Journal of Experimental Botany* **58**, 1985–1997.

Hayes M a, Feechan A, Dry IB. 2010. Involvement of abscisic acid in the coordinated regulation of a stress-inducible hexose transporter (*VvHT5*) and a cell wall invertase

in grapevine in response to biotrophic fungal infection. *Plant Physiology* **153**, 211–21.

Herrmann KM, Weaver LM. 1999. The shikimate pathway. *Annual Review of Plant Physiology and Plant Molecular Biology* **50**, 473–503.

Hill LM, Smith AM. 1991. Evidence that glucose 6-phosphate is imported as the substrate for starch synthesis by the plastids of developing pea embryos. *Planta* **185**, 91–96.

Horsefield R, Nordén K, Fellert M, Backmark A, Törnroth-Horsefield S, Terwisscha van Scheltinga AC, Kvassman J, Kjellbom P, Johanson U, Neutze R. 2008. High-resolution x-ray structure of human aquaporin 5. *Proceedings of the National Academy of Sciences, USA* **105**, 13327–13332.

Hub JS, de Groot BL. 2008. Mechanism of selectivity in aquaporins and aquaglyceroporins. *Proceedings of the National Academy of Sciences, USA* **105**, 1198–1203.

Hunter JJ, De Villiers OT, Watts JE. 1991. The effect of partial defoliation on quality characteristics of *Vitis vinifera* L. cv. Cabernet Sauvignon grapes. II. Skin color, skin sugar, and wine quality. *American Journal of Enology and Viticulture* **42**, 13–18.

Jaillon O, Aury J-M, Noel B, *et al*. 2007. The grapevine genome sequence suggests ancestral hexaploidization in major angiosperm phyla. *Nature* **449**, 463–467.

Johanson U, Karlsson M, Johansson I, Gustavsson S, Sjövall S, Fraysse L, Weig a R, Kjellbom P. 2001. The complete set of genes encoding major intrinsic proteins in Arabidopsis provides a framework for a new nomenclature for major intrinsic proteins in plants. *Plant Physiology* **126**, 1358–1369.

Kühn C, Grof CPL. 2010. Sucrose transporters of higher plants. *Current Opinion in Plant Biology* **13**, 288–298.

Lalonde S, Wipf D, Frommer WB. 2004. Transport mechanisms for organic forms of carbon and nitrogen between source and sink. *Annual Review of Plant Biology* **55**, 341–372.

Larronde F, Krisa S, Decendit a., Chèze C, Deffieux G, Mérillon JM. 1998. Regulation of polyphenol production in *Vitis vinifera* cell suspension cultures by sugars. *Plant Cell Reports* **17**, 946–950.

Laur J, Hacke UG. 2013. Transpirational demand affects aquaporin expression in poplar roots. *Journal of Experimental Botany* **64**, 2283–2293.

Lecourieux F, Kappel C, Lecourieux D, Serrano A, Torres E, Arce-Johnson P, Delrot S. 2014. An update on sugar transport and signalling in grapevine. *Journal of Experimental Botany* **65**, 821–832.

Leitão L, Prista C, Moura TF, Loureiro-Dias MC, Soveral G. 2012. Grapevine aquaporins: Gating of a tonoplast intrinsic protein (TIP2;1) by cytosolic pH. *PLoS ONE* **7**, e33219.

Lichtenthaler HK. 1999. The 1-deoxy-D-xylulose-5-phosphate pathway of isoprenoid biosynthesis in plants. *Annual Review of Plant Physiology and Plant Molecular Biology* **50**, 47–65.

Lin IW, Sosso D, Chen L-Q, *et al.* 2014. Nectar secretion requires sucrose phosphate synthases and the sugar transporter SWEET9. *Nature* **508**, 546–9.

Linka N, Weber a. PM. 2010. Intracellular metabolite transporters in plants. *Molecular Plant* **3**, 21–53.

Maisels CK. 1993. The Nearest - Archaeology in the 'Cradle of Civilization' (CK Maisels, Ed.). Routledge Books.

Manning K, Davies C, Bowen HC, White PJ. 2001. Functional characterization of two ripening-related sucrose transporters from grape berries. *Annals of Botany* **87**, 125–129.

Maurel C. 2007. Plant aquaporins: novel functions and regulation properties. *FEBS Letters* **581**, 2227–36.

Maurel C, Reizer J, Schroeder JI, Chrispeels MJ. 1993. The vacuolar membrane protein gamma-TIP creates water specific channels in *Xenopus oocytes*. *The EMBO Journal* **12**, 2241–2247.

May B, Lange BM, Wüst M. 2013. Biosynthesis of sesquiterpenes in grape berry exocarp of *Vitis vinifera* L.: Evidence for a transport of farnesyl diphosphate precursors from plastids to the cytosol. *Phytochemistry* **95**, 135–144.

Maynard JW, Lucas JW. 1982. A reanalysis of the two-component phloem loading system in *Beta vulgaris. Plant Physiology* **69**, 734-739

Murata K, Mitsuoka K, Hirai T, Walz T, Agre P, Heymann JB, Engel A, Fujiyoshi Y. 2000. Structural determinants of water permeation through aquaporin-1. *Nature* **407**, 599–605.

Neuhaus HE, Batz O, Thom E, Scheibe R. 1993. Purification of highly intact plastids from various heterotrophic plant tissues: analysis of enzymic equipment and precursor dependency for starch biosynthesis. *The Biochemical Journal* **296,** 395–401.

Niewiadomski P, Knappe S, Geimer S, Fischer K, Schulz B, Unte US, Rosso MG, Ache P, Flügge U-I, Schneider A. 2005. The *Arabidopsis* plastidic glucose 6-phosphate/phosphate translocator GPT1 is essential for pollen maturation and embryo sac development. *The Plant Cell* **17**, 760–775.

Niittylä T, Messerli G, Trevisan M, Chen J, Smith AM, Zeeman SC. 2004. A previously unknown maltose transporter essential for starch degradation in leaves. *Science* **303**, 87–89.

Park W, Scheffler BE, Bauer PJ, Campbell BT. 2010. Identification of the family of aquaporin genes and their expression in upland cotton (*Gossypium hirsutum* L.). *BMC Plant Biology* **10**, 142.

Pirie A, Mullins M. 1977. Interrelationships of sugars, anthocyanins, total phenols, and dry weight in the skin of grape berries during ripening. *American Journal of Enology and Viticulture* **28**, 204–209.

Prabhakar V, Löttgert T, Gigolashvili T, Bell K, Flügge UI, Häusler RE. 2009. Molecular and functional characterization of the plastid-localized Phosphoenolpyruvate enolase (ENO1) from *Arabidopsis thaliana*. *FEBS Letters* **583**, 983–991.

Preston GM, Carrol TP, Guggino WB, Agre P. 1992. Apperance of water channels in *Xenopus oocytes* expressing red cell CHIP28 protein. *Science* **256**, 385–387.

Quick WP, Neuhaus HE. 1996. Evidence for two types of phosphate translocators in sweet-pepper (*Capsicum annum* L.) fruit chromoplasts. *The Biochemical Journal* **320**, 7–10.

Reuscher S, Akiyama M, Mori C, Aoki K, Shibata D, Shiratake K. 2013. Genome-wide identification and expression analysis of aquaporins in tomato. *PLoS ONE* **8**, e79052.

Riesmeier JW, Willmitzer L, Frommer WB. 1992. Isolation and characterization of a sucrose carrier cDNA from spinach by functional expression in yeast. *The EMBO Journal* **11**, 4705–4713.

Sabir F, Leandro MJ, Martins AP, Loureiro-Dias MC, Moura TF, Soveral G, Prista C. 2014. Exploring three PIPs and three TIPs of grapevine for transport of water

and atypical substrates through heterologous expression in aqy-null yeast. *PLoS ONE* **9**, e102087.

Sakurai J, Ahamed A, Murai M, Maeshima M, Uemura M. 2008. Tissue and cell-specific localization of rice aquaporins and their water transport activities. *Plant and Cell Physiology* **49**, 30–39.

Sakurai J, Ishikawa F, Yamaguchi T, Uemura M, Maeshima M. 2005. Identification of 33 rice aquaporin genes and analysis of their expression and function. *Plant and Cell Physiology* **46**, 1568–1577.

Salas JJ, Sánchez J, Ramli US, Manaf AM, Williams M, Harwood JL. 2000. Biochemistry of lipid metabolism in olive and other oil fruits. *Progress in Lipid Research* **39**, 151–180.

Sauer N, Friedländer K, Gräml-Wicke U. 1990. Primary structure, genomic organization and heterologous expression of a glucose transporter from *Arabidopsis thaliana*. *The EMBO Journal* **9**, 3045–3050.

Schunemann D, Borchert S. 1994. Specific transport of inorganic phosphate and C3- and C6-sugar-phosphates across the envelope membranes of tomato (*Lycopersicon esculentum*) leaf-chloroplasts, tomato fruit-chloroplasts and fruit-chromoplasts. *Botanica Acta* **107**, 461–467.

Shannon JC, Pien FM, Cao H, Liu KC. 1998. Brittle-1, an adenylate translocator, facilitates transfer of extraplastidial synthesized ADP--glucose into amyloplasts of maize endosperms. *Plant Physiology* **117**, 1235–1252.

Shelden MC, Howitt SM, Kaiser BN, Tyerman SD. 2009. Identification and functional characterisation of aquaporins in the grapevine, *Vitis vinifera*. *Functional Plant Biology* **36**, 1065–1078.

Slewinski TL, Meeley R, Braun DM. 2009. Sucrose transporter1 functions in phloem loading in maize leaves. *Journal of Experimental Botany* **60**, 881–892.

Soler E, Claste M, Bantignies B, Marigo G, Ambid C. 1993. Uptake of iso pentenyl diphosphate by plastids isolated from *Vitis vinifera* L. cell suspensions. *Planta* **191**, 324–329.

Soler E, Feron G, Clastre M, Dargent R, Gleizes M, Ambid C. 1992. Evidence for a geranyl-diphosphate synthase located within the plastids of *Vitis vinifera* L. cultivated *in vitro*. *Planta* **187**, 171–175.

Steudle E. 2001. The cohesion-tension mechanism and the aquisition of water by plant roots. *Annual Review of Plant Physiology and Plant Molecular Biology* **52**, 847–875.

Steudle E, Peterson CA. 1998. How does water get through roots? *Journal of Experimental Botany* **49**, 775–788.

Terral JF, Tabard E, Bouby L, *et al*. 2010. Evolution and history of grapevine (*Vitis vinifera*) under domestication: new morphometric perspectives to understand seed domestication syndrome and reveal origins of ancient European cultivars. *Annals of Botany* **105**, 443–455.

Tournaire-Roux C, Sutka M, Javot H, Gout E, Gerbeau P, Luu D-T, Bligny R, Maurel C. 2003. Cytosolic pH regulates root water transport during anoxic stress through gating of aquaporins. *Nature* **425**, 393–397.

Turgeon R, Wolf S. 2009. Phloem transport: cellular pathways and molecular trafficking. *Annual Review of Plant Biology* **60**, 207–221.

Tyerman SD, Chaves MM, Barrieu F. 2012. Water Relations of the Grape Berry and Aquaporins. In: Gerós H, Chaves MM, Delrot S, eds. The biochemistry of the grape berry. Bentham Books, 3–22.

Vega A, Gutiérrez R a., Peña-Neira A, Cramer GR, Arce-Johnson P. 2011. Compatible GLRaV-3 viral infections affect berry ripening decreasing sugar accumulation and anthocyanin biosynthesis in *Vitis vinifera*. *Plant Molecular Biology* **77**, 261–274.

Vignault C, Vachaud M, Cakir B, Glissant D, Dédaldéchamp F, Büttner M, Atanassova R, Fleurat-Lessard P, Lemoine R, Delrot S. 2005. *VvHT1* encodes a monosaccharide transporter expressed in the conducting complex of the grape berry phloem. *Journal of Experimental Botany* **56**, 1409–1418.

Weber APM. 2004. Solute transporters as connecting elements between cytosol and plastid stroma. *Current Opinion in Plant Biology* **7**, 247–253.

Weber AP. 2007. Synthesis, export and partitioning of the end products of photosynthesis. In: Wise RR, Hoober JK, eds. The structure and function of plastids. Elsevier, 273–292.

Weber a, Servaites JC, Geiger DR, Kofler H, Hille D, Gröner F, Hebbeker U, Flügge UI. 2000. Identification, purification, and molecular cloning of a putative plastidic glucose translocator. *The Plant Cell* **12**, 787–802.

Weise SE, Weber APM, Sharkey TD. 2004. Maltose is the major form of carbon exported from the chloroplast at night. *Planta* **218**, 474–482.

Wise RR. 2007. The diversity of plastid form and function. In: Wise RR, Hoober JK, eds. The structure and function of plastids. Springer, 3–27.

Zapata C, Deléens E, Chaillou S, Magné C. 2004. Partitioning and mobilization of starch and N reserves in grapevine (*Vitis vinifera* L.). *Journal of Plant Physiology* **161**, 1031–1040.

Zhang DY, Ali Z, Wang CB, *et al*. 2013. Genome-Wide sequence characterization and expression analysis of major intrinsic proteins in soybean (*Glycine max* L.). *PLoS ONE* **8**, e56312.

Zhang X-Y, Wang X-L, Wang X-F, Xia G-H, Pan Q-H, Fan R-C, Wu F-Q, Yu X-C, Zhang D-P. 2006. A shift of phloem unloading from symplasmic to apoplasmic pathway is involved in developmental onset of ripening in grape berry. *Plant Physiology* **142**, 220–232.

Zhou Y, Qu H, Dibley KE, Offler CE, Patrick JW. 2007. A suite of sucrose transporters expressed in coats of developing legume seeds includes novel pH-independent facilitators. *The Plant Journal* **49**, 750–764.

Chapter 2

Identification and functional characterization of grapevine transporters that mediate glucose-6-phosphate uptake into plastids

The work presented in this chapter has been accepted for publication:

Noronha H, Conde C, Delrot S, Gerós H. 2015. Identification and functional characterization of grapevine transporters that mediate glucose-6-phosphate uptake into plastids. *Planta.*

Authors´ contributions: HN and HG raised the hypothesis underlying this work. HN, CC, SD and HG design the experiments. HN and CC performed the experiments. HN analyzed the data. HN and HG wrote the paper. CC, SD and HG directed the study.

Abstract

In grapevine, starch accumulation in the trunk is important for winter storage of carbon and in the flower for reproductive development. Berries also accumulate starch in their plastids, which are also involved in the synthesis of aroma compounds important for fruit quality. The present work characterizes two glucose-phosphate translocators (VvGPT1 and VvGPT2) that control the accumulation of starch in grape amyloplasts. Three different splicing variants identified for *VvGPT2* (*VvGPT2α*, *VvGPT2β* and *VvGPT2*Ω) were more expressed in the leaves than in other organs. In contrast, *VvGPT1* transcripts were more abundant in mature berries, canes and flowers than in the leaves. Expression of *35S-VvGPT1-GFP* and *35S-VvGPT2*Ω*-GFP* in tobacco leaf epidermal cells showed that the fusion proteins localized at the plastidial envelope. Complementation of the *Arabidopsis pgi1-1* mutant impaired in leaf starch synthesis restored its ability to synthesize starch, demonstrating that VvGPT1 and VvGPT2Ω mediate the transport of glucose-6-Pi across the plastidial envelope. In grape cell suspensions, ABA, light and galactinol, together with sucrose and fructose, significantly increased the transcript abundance of *VvGPT1*, whereas *VvGPT2*Ω expression was affected only by sucrose. In addition, elicitation with MeJA strongly upregulated *VvGPT1*, *VvGPT2*Ω and *VvPAL1*, suggesting a role for GPTs in the production of secondary compounds in grapevine. Moreover, in grapevines cultivated in field conditions, *VvGPT1* expression was higher in berries more exposed to the sun and subjected to higher temperatures. Although both VvGPT1 and VvGPT2 mediate the same function at the molecular level, they exhibit different expression levels and regulation in plant organs and in response to environmental and hormonal signals.

2.1 Introduction

The berries of grapevine (*Vitis vinifera* L.) may be consumed as table fruits, dried raisins, and they are also used to prepare juices, wines and spirits. Grapevine is thus a fruit species with an utmost economic importance in many countries. The accumulation of glucose and fructose in the vacuoles of the mesocarp cells is one of the markers used to monitor berry ripening, and a determinant of berry quality. This accumulation, which starts at veraison, depends on several plasma membrane and tonoplast transporters whose identity, activity and regulation have been partially characterized (Conde *et al*., 2006; Chong *et al*., 2014; Lecourieux *et al*., 2014).

In addition to soluble sugars, grape berries also accumulate starch (Fortes *et al*., 2011). Starch is also present in grapevine flowers, where its abundance depends on the genotype and on the developmental stage (Lebon *et al*., 2005). However, accumulation of starch in the reproductive structures of grapevine is marginal and transitory when compared with trunk and root starch. As other perennial species, grapevine accumulates very large amounts of starch in the trunk at the end of summer and beginning of autumn. In spring, hydrolysis and remobilization of this storage carbon is important to ensure the early phases of vegetative development that occur prior to the emergence of photosynthetically active leaves (Zapata *et al*., 2004). The whole process of starch accumulation and remobilization heavily depends on the climatic conditions that control photosynthetic activity and phloem transport in autumn, and amylase activity and transport from the ray cells in the spring. The climate change that significantly affects the summer water regime and the temperatures all over the year may significantly impact these processes and alter the long-term vigor of grapevines. In spite of potential threats resulting from climate change on viticulture (Hannah *et al*., 2013; Van Leeuwen *et al*., 2013), relatively little has been done on the long term effects of climate change on vine physiology.

Plastids from heterotrophic tissues are generally unable to generate hexoses-phosphate from C_3-compounds due to the lack of fructose 1,6-bisphosphatase activity (Entwistle and ap Rees, 1990), therefore they must import cytosolic hexoses-Pi through GPT (Weber and Linka, 2011). In the amyloplast, glucose-6-Pi is a precursor for starch and fatty acid synthesis and may be involved in the production of reducing equivalents (NADPH) via the oxidative pentose phosphate pathway (OPPP) (Fischer *et al*., 2011). The

first molecular identification of GPT was achieved from maize kernels (Kammerer *et al*., 1998). Two *GPT* genes are present in *Arabidopsis thaliana* genome code for glucose-6-Pi antiporters displaying different expression patterns (Knappe *et al*., 2003; Niewiadomski *et al*., 2005). *AtGPT1* is ubiquitously expressed whereas *AtGPT2* is restricted to few tissues including senescent leaves and responds to the pathogen *Pseudomonas syringae* (Niewiadomski *et al*., 2005). Only the loss of *AtGPT1* function causes a visible phenotype in t-DNA mutants of *Arabidopsis*, displaying an arrest of pollen and ovule development, probably due to an impairment of the plastidial OPPP that affects fatty acid metabolism (Niewiadomski *et al*., 2005).

In the present study, *GPT* members of grapevine were identified and two, *VvGPT1* and *VvGPT2*Ω, were cloned and molecularly characterized. Functional complementation of *Arabidopsis* mutants showed that both proteins mediate the uptake of cytosolic glucose-6-Pi into the plastid. *VvGPTs* showed different expression levels and regulation in plant organs and in response to environmental and hormonal signals. Elicitation of suspension-cultured cells with methyl jasmonate (MeJA) increased the expression of *VvGPT1*, *VvGPT2*Ω and *VvPAL1*, suggesting that these plastidial phosphate translocators (pPT) may play an important role in the secondary metabolism pathways. In field conditions, *VvGPT1* transcripts were more abundant in berries sampled from the western side of the canopy (more exposed to the sun) than in berries from the eastern side.

2.2 Results

2.2.1 Identification of GPTs in grapevine and analyses of VvGPTs protein sequences

A phylogenetic tree constructed with 13 pPTs from grapevine, *Zea mays* and *Arabidopsis thaliana* showed that this protein family clusters in 4 different groups (Fig. 2.1). Two *GPT* genes were identified in *V. vinifera*, *VvGPT1*, localized in chr. 19, and *VvGPT2*, in chr. 10. *VvGPT1* transcript shares the general *GPT* structure including 5 exons, and the last one was very small with only 12 bp (Fig. 2.2). Shortly after the cloning of *VvGPT1* and *VvGPT2*, we were able to identify three different splicing variants for *VvGPT2*: *VvGPT2α*, *VvGPT2β* and *VvGPT2*Ω (Fig. 2.2). The cloned *VvGPT2* was renamed *VvGPT2*Ω and *VvGPT2β* was also successfully cloned. To our knowledge, this is the first time that such splice variants for plastid phosphate translocators were identified. *VvGPT1*

and the two splicing variants of *VvGPT2*, *VvGPT2β* and *VvGPT2*Ω, were subsequently studied in more detail regarding their subcellular localization and function. *VvGPT2α* has a similar structure to *VvGPT1* but *VvGPT2β* skips the 3rd exon, which results in a frame shift and the appearance of a stop codon at the beginning of exon 4. Also, *VvGPT2β* displays a splicing in the 3´UTR in the same location as *VvGPT2α* (Fig. 2.2). *VvGPT2*Ω retains the 4th intron which prolongs the 4th exon until the stop codon (Fig. 2.2). The 1000 bp region upstream of the initial ATG codon of the ORF was used to study promoter cis-acting regulatory elements. Several significant motifs associated with light regulation, pollen expression and plant specific transcription factors were identified (Table 2.1).

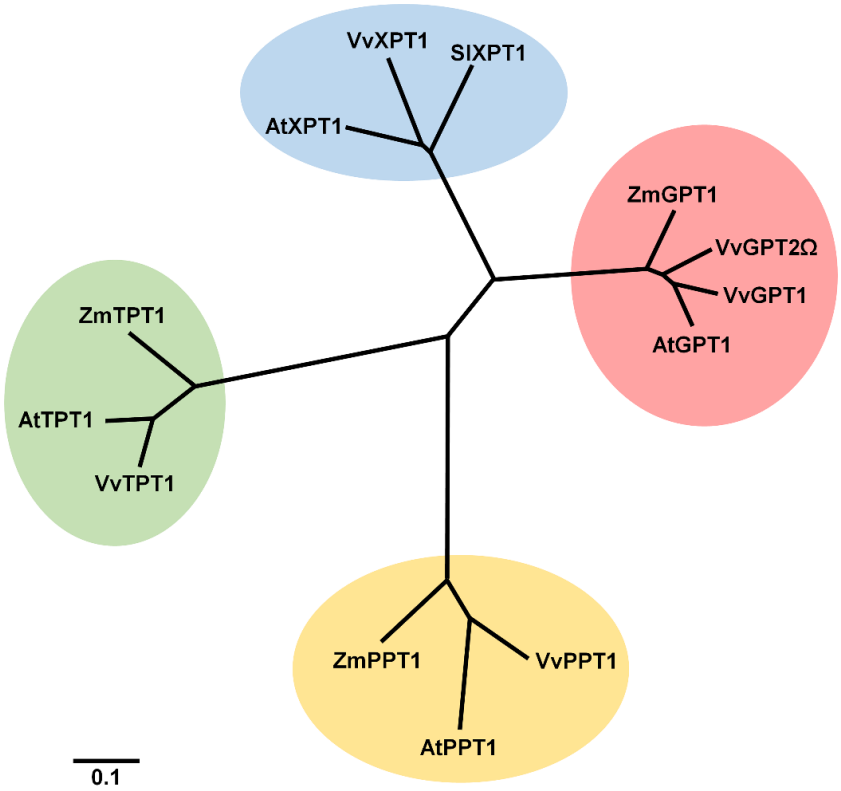

Figure 2.1 Phylogenetic tree of pPT grapevine transporter family after aligning sequences from XPTs, GPTs, PPTs and TPTs from *Vitis vinifera*, maize (*Zea mays*), tomato (*Solanum lycopersicum*) and *Arabidopsis*.

Cis-acting element	Number of copies	
	VvGPT1	*VvGPT2*
Light regulated motif	44 7	20 4
Pollen expression	20 10	21 -
ARR1 binding	21	20
Pathogen response	17	-
MYC motif	-	12
WRKY motif	-	11
Dof motif	36	30

Table 2.1 Cis-acting elements identified by PlantPAN database in *VvGPT1* and *VvGPT2* promoter sequences.

VvGPT1 (389 aa long), VvGPT2α (393 aa), VvGPT2β (252 aa) and VvGPT2Ω (456 aa) proteins were aligned with GPTs from different species, without transit peptides (Fig. 2.3 and 2.4) that were detected by online ChloroP 1.1 Server (Emanuelsson *et al*., 1999) and by alignment with the mature peptides of AtGPT1, AtGPT2, and ZmGPT1 (Kammerer *et al*., 1998). VvGPT1 and all VvGPT2 (-α, -β, and -Ω) proteins have transit peptides of approximately 69 aa (Fig. 2.3). The mature peptides of the analyzed GPT proteins are highly conserved, showing 47.10-96.91% similarity (Table 2.2) and 8 putative transmembrane domains (Fig. 2.3). Two conserved serines that may be targets for phosphorylation, the typical GPT domain TMKRISVIV (Knappe *et al*., 2003; Fig. 2.5) and the two conserved domains EamA (pfam00892) and TPT (pfam03151) were all identified (Fig. 2.3), except in VvGPT2β that lacks the TPT motif.

2.2.2 Transcriptional analyses of VvGPT1, VvGPT2α, VvGPT2β and VvGPT2Ω

The expression of *VvGPT1* and *VvGPT2* was studied by qRT-PCR in different grapevine organs (cv. Vinhão) (Fig. 2.6). *VvGPT1* transcripts were more abundant in sink tissues, including berries, than in leaves (Fig. 2.6A).

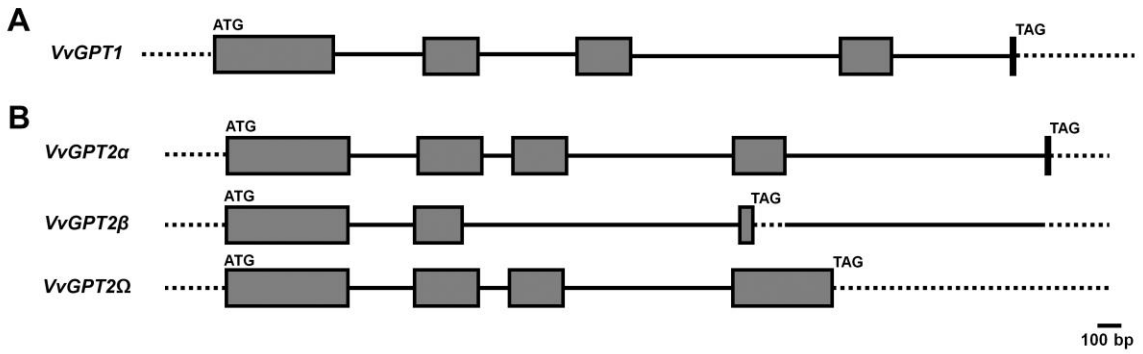

Figure 2.2 Transcript structure of *GPT1* and *GPT2* genes from grapevine. Grey boxes represent exons, black lines show introns and dashed lines depict 5' and 3' UTRs.

In berries, *VvGPT1* transcript levels decreased from the green stage to veraison and increased again in mature fruits (Fig. 2.6B). Contrarily to *VvGPT1*, *VvGPT2α* and -Ω were more expressed in leaves than in sink tissues (Fig. 2.6C). The expression of *VvGPT2β* was marginal in all organs when compared to *VvGPT2α* and -Ω.

2.2.3 Regulation of VvGPT1 expression in response to environmental and hormonal signals in heterotrophic tissues

Because *VvGPT1* expression analysis suggested a more important role for this pPT in heterotrophic tissues than in leaves, we studied its expression in berries sampled from cv. Aragonez vines cultivated in the field under well-established stress conditions (Fig. 2.7). As described in Materials and methods, grapevines subjected to RDI were irrigated with 50% less water than those subjected to SDI, but results showed that *VvGPT1* expression in SDI and RDI conditions was not statistically different. In addition, average daily maximal temperatures were 4–5ºC higher in grapes facing the west (RDI-W and SDI-W) than in those exposed to the east (RDI-E and SDI-E). The steady-state transcript levels of *VvGPT1* increased after veraison (Fig. 2.8), just as in cv. Vinhão, and its expression followed the trend SDI-W > SDI-E and RDI-W > RDI-E, suggesting a positive effect of sun exposure on *VvGPT1* transcript accumulation. To gain further insights on the regulation of *VvGPT1* by environmental and hormonal stimuli, the expression of *VvGPT1* was studied in heterotrophic CSB cultured cells.

AtGPT1	100															
VvGPT1	88.62	100														
VvGPT2α	88.15	91.94	100													
VvGPT2β	54.50	56.39	62.32	100												
VvGPT2Ω	72.98	76.77	84.83	47.39	100											
AtGPT2	86.49	88.62	91.23	57.58	76.06	100										
SlGPT1	84.83	85.3	83.17	50.23	68.24	81.75	100									
SlGPT2	82.22	84.83	85.30	53.08	70.37	83.88	79.14	100								
MtGPT1	89.81	90.75	88.38	55.45	73.22	87.67	84.83	82.70	100							
Am.trGPT1	85.71	89.09	89.57	55.21	74.64	86.01	80.56	81.99	86.49	100						
OsGPT1	85.78	89.57	88.62	54.73	73.45	87.44	81.75	82.46	88.62	87.91	100					
ZmGPT1	85.3	87.91	87.44	53.79	72.27	87.20	80.56	82.70	87.20	89.06	96.91	100				
	AtGPT1	**VvGPT1**	**VvGPT2α**	**VvGPT2β**	**VvGPT2Ω**	AtGPT2	SlGPT1	SlGPT2	MtGPT1	Am.trGPT1	OsGPT1	ZmGPT1				

Table 2.2 Protein identity of several GPT members.

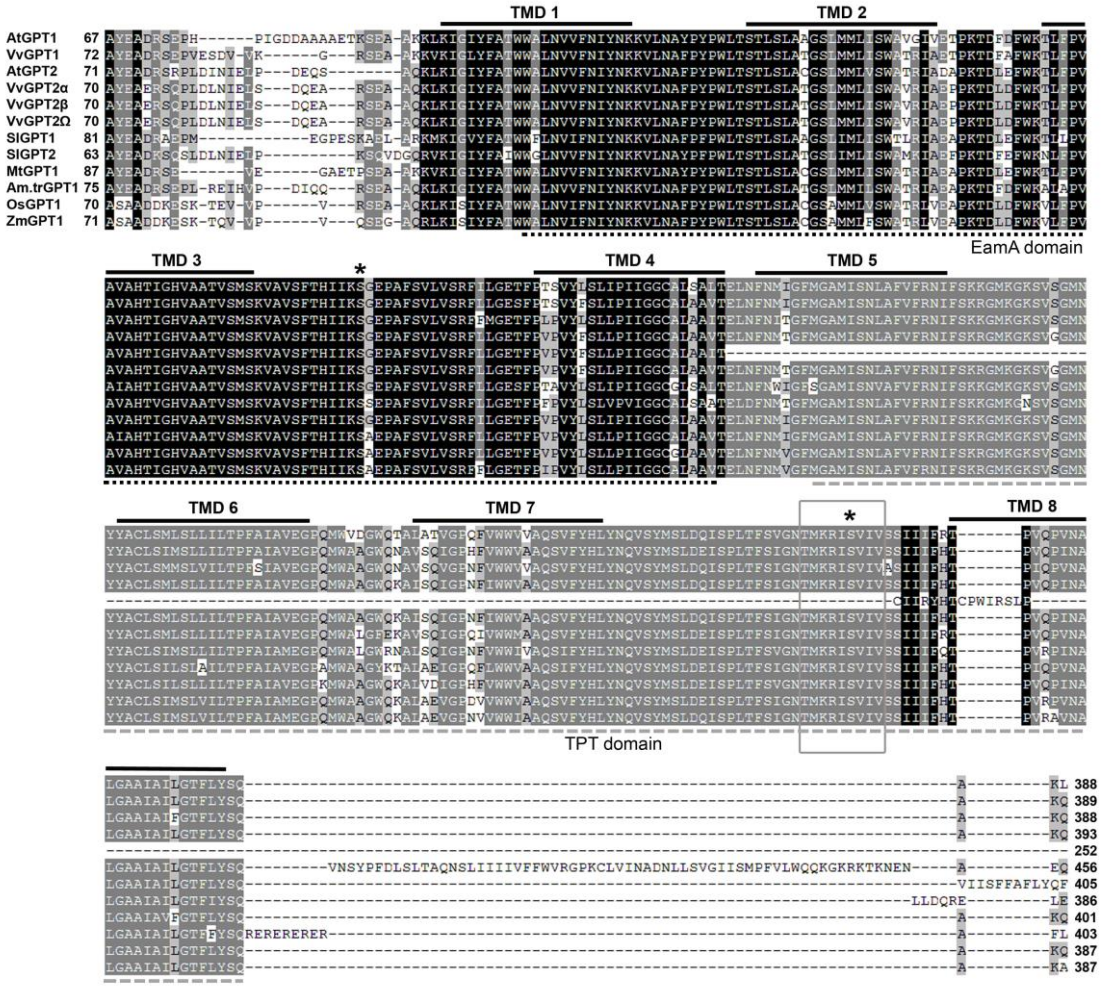

Figure 2.3 Alignment of GPT proteins from different species. The transmembrane domains for AtGPT1 predicted in the ARAMEMNON database are depicted as black lines. EamA and TPT conserved domains are marked with black and grey dashed lines, respectively. Asterisk shows putative phosphorylation sites for all GPT members, and typical GPT domain TMKRISVIV is enclosed by a grey box.

VvGPT1 expression changed 12 h after treatment with hormones, light or several sugars (Fig. 2.8A-D). Abscisic acid (ABA), light and galactinol increased the expression of *VvGPT1* by 1.68, 1.85 and 1.3-fold respectively, and elicitation with MeJA strongly upregulated *VvGPT1* transcription by 9-fold (Fig. 2.8A). Sucrose and fructose, which are very abundant in the mature berries, also upregulated *VvGPT1* by 1.37 and 1.32-fold, respectively (Fig. 2.8C). The expression of *VvPAL1*, a gene coding for a phenylalanine ammonia-lyase, a key enzyme of the phenylpropanoid pathway, was also measured in response to MeJA to evaluate if the increased expression of *VvGPTs* could somehow be involved in the stimulation of secondary metabolism. Figure 2.8c shows that *VvPAL1*

expression was indeed strongly upregulated in response to 20 µM MeJA. Although the transcript levels of *VvGPT2* splicing variants were less abundant in berries than in autotrophic leaves, we also studied the expression of *VvGPT2*Ω in heterotrophic CSB cells. The addition of MeJA and sucrose caused a 74 and 1.83-fold increase of *VvGPT2*Ω transcript levels, respectively (Fig. 2.9).

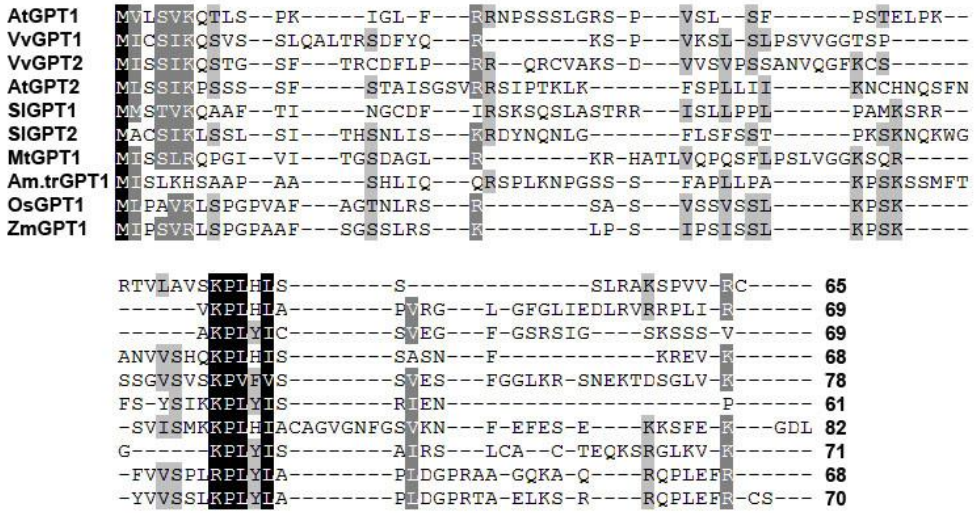

Figure 2.4 Alignment of GPT transit peptides identified by the ChloroP software and protein alignment.

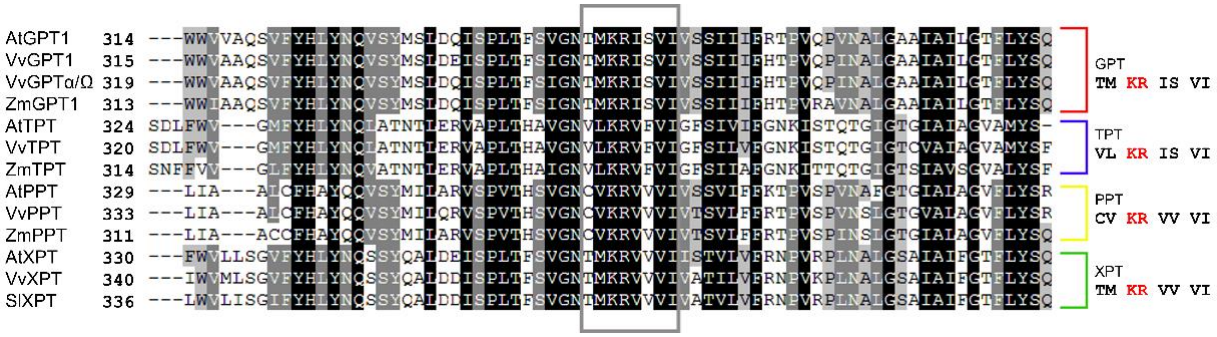

Figure 2.5 Comparison of a highly conserved region of pPT transporters from grapevine. On the right side of the figure it's depicted the conserved domains that identify different groups of the pPT family (Knappe *et al*., 2003).

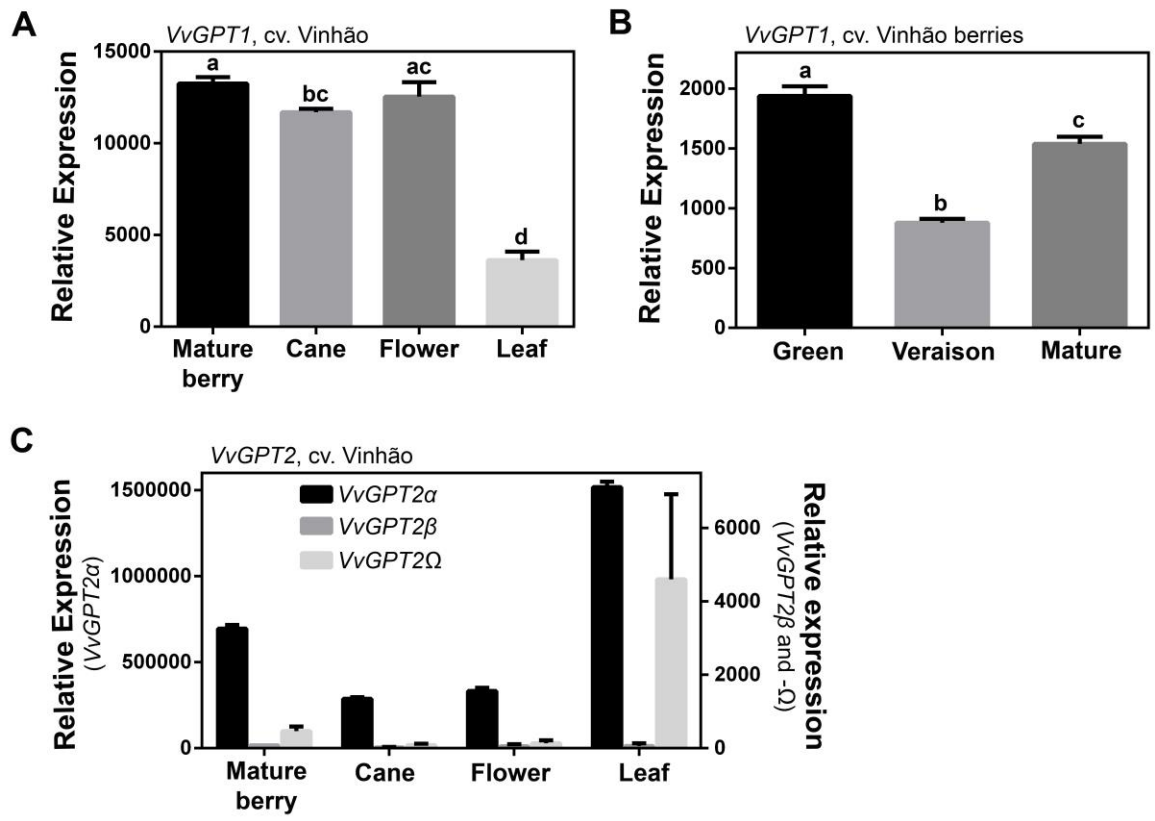

Figure 2.6 *VvGPT1* and *VvGPT2* expression in cv. Vinhão. Quantitative Real-Time PCR was used to study *VvGPT* expression in different grapevine organs (A and C) and during berry maturation (B). Results indicate the mean ± SD of three independent experiments. Letters denote significant differences.

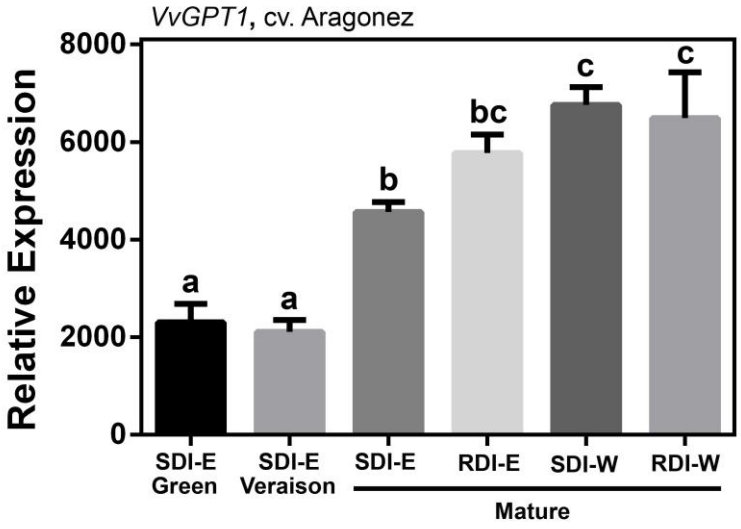

Figure 2.7 *VvGPT1* expression in berries from cv. Aragonez grown under different irrigation regimes and sun exposures. Vines subjected do RDI (regulated deficit irrigation) and SDI (sustained deficit irrigation) were used to study the *VvGPT1* expression in response to water stress and grapes

were sampled accordingly to their higher (W, row facing west) or lower (E, row facing east) sun exposure. Results indicate the mean ± SD of three independent experiments. Letters denote significant differences.

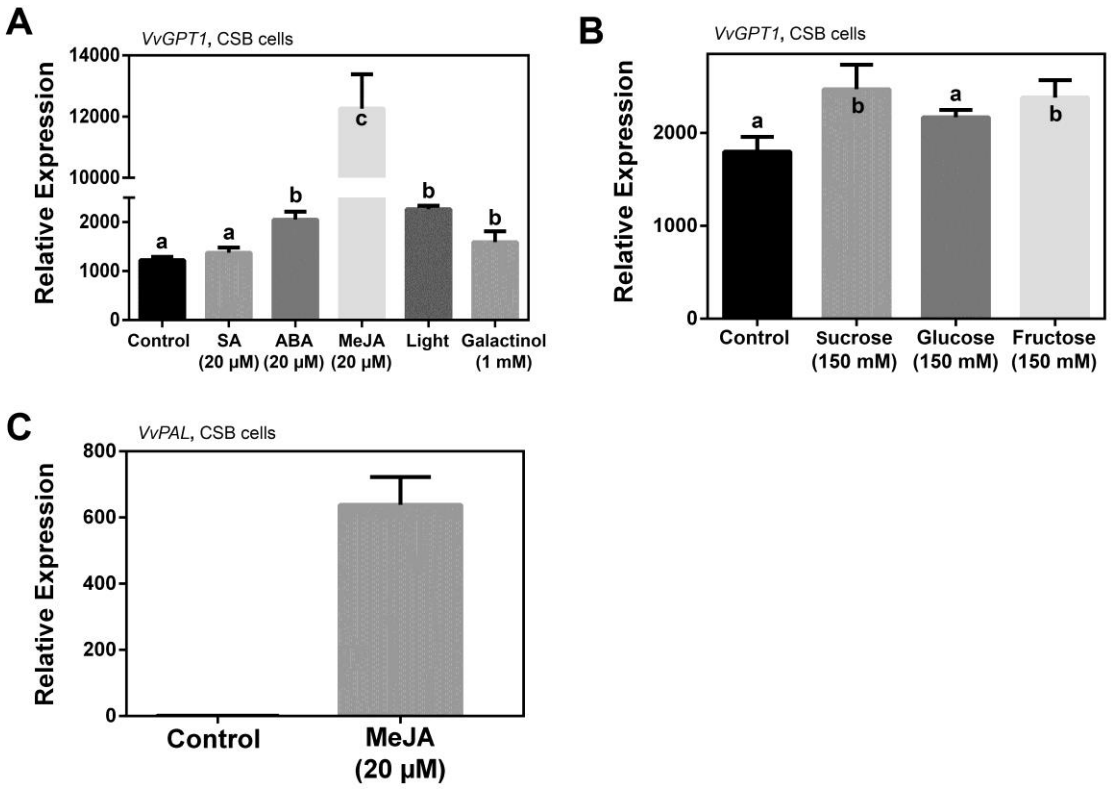

Figure 2.8 Effects of sugars, hormones and light on *VvGPT1* transcript levels in Cabernet Sauvignon Berry cell suspensions. Results indicate the mean ± SD of three independent experiments. Letters denote significant differences.

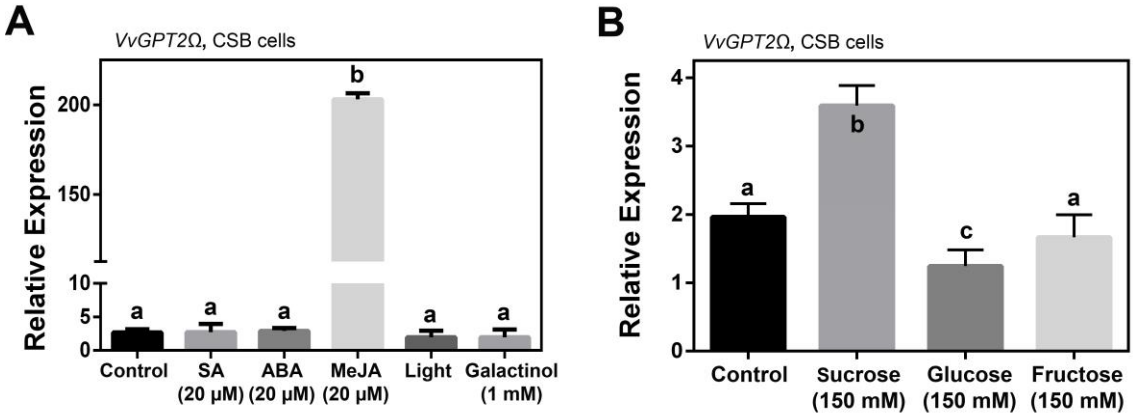

Figure 2.9 Effect of sugars, hormones and light on *VvGPT2*Ω transcript levels in Cabernet Sauvignon Berry cell suspensions. Results indicate the mean ± SD of three independent experiments. Letters denote significant differences.

2.2.4 Starch accumulation in heterotrophic tissues and starch synthase (VvSS) and α-amylase (VvAMY) expression

The amount of starch in the berry and the steady-state transcript levels of starch synthase (*VvSS*) and α-amylase (*VvAMY*) were developmentally affected in cv. Vinhão. (Fig. 2.10a, d and e). Starch content of the berry sharply decreased from the green stage (66.4 ± 2.5 µg/g FW) to veraison, and then increased again in the mature phase (47.4 ± 1.6 µg/g FW) (Fig. 2.10a).

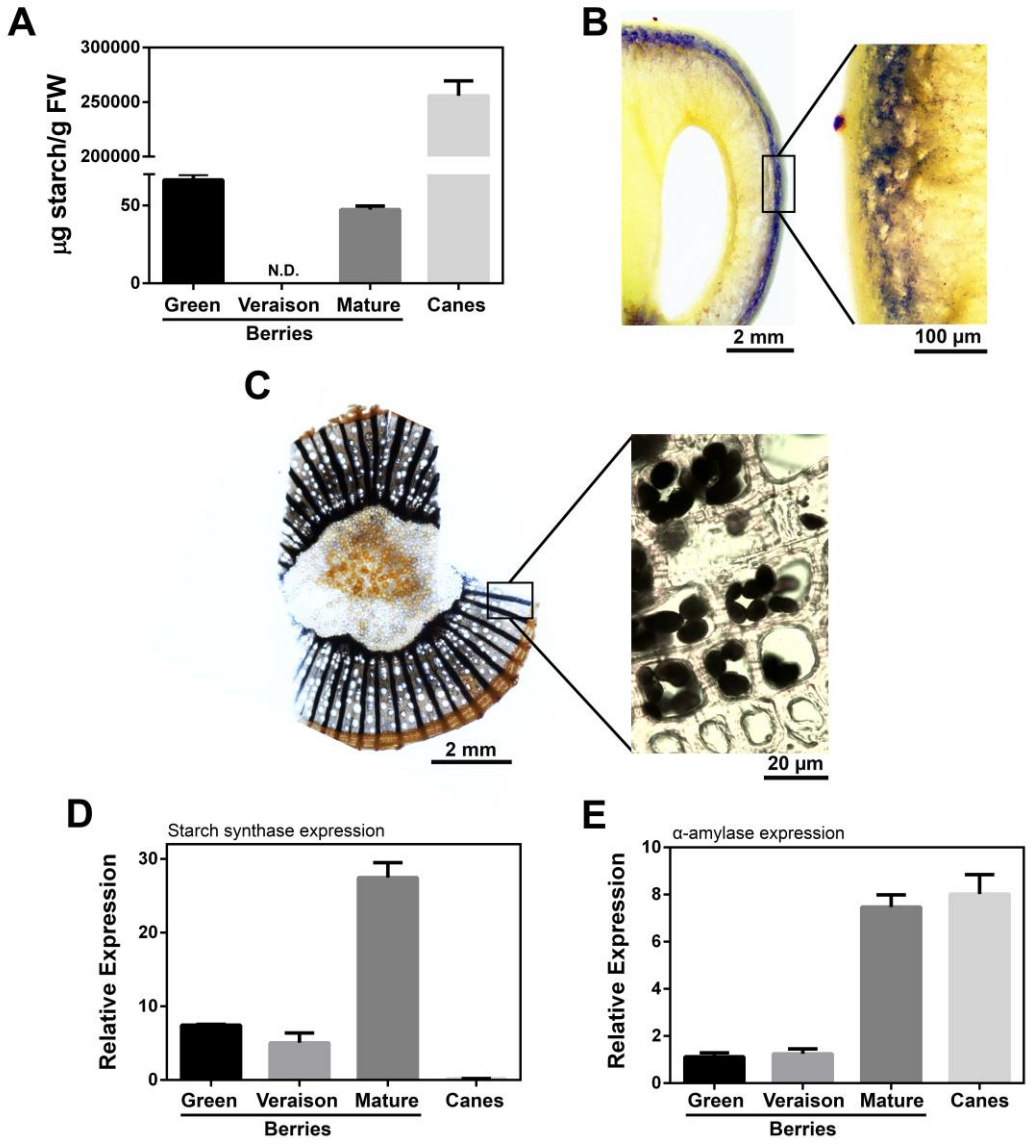

Figure 2.10 Starch in berries and canes. Starch was quantified during berry development and in canes (A), and free-hand slices from green berries (B) and canes (C) showing sites of starch accumulation after iodine staining. The expression of *starch synthase* (D) and *α-amylase* (E) was

studied by qRT-PCR during grape berry maturation and in canes. Results indicate the mean ± SD of three independent experiments. Letters denote significant differences.

Iodine staining of transversal sections of green berries showed that starch accumulated preferentially in the peripheral vascular bundle near the pedicel (Fig. 2.10B and 2.11). The increase in the expression of *VvSS* and *VvAMY* from veraison to mature phase correlated with the observed higher amounts of starch in the mature berries (Fig. 2.10D and E). As shown before, a similar trend was followed by the expression levels of *VvGPT1* (Fig. 2.6B).

Starch levels in canes collected 2 weeks after harvest were much higher than in berries (Fig. 6A, 255.8 ± 11.1 mg/g FW), and accumulated in well-defined amyloplasts of parenchyma ray cells (Fig. 2.10c). *α-amylase* was highly expressed in canes, contrarily to *starch synthase*.

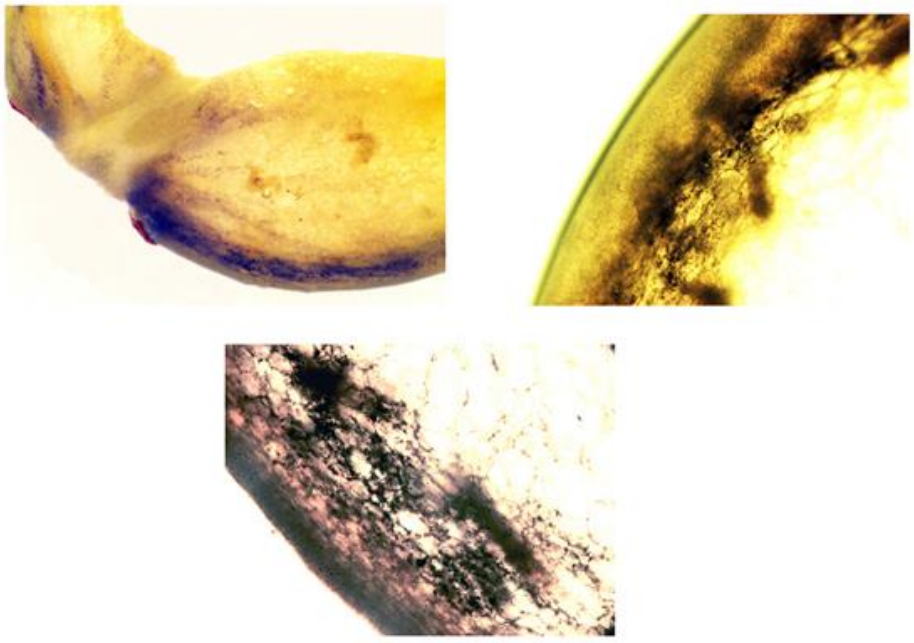

Figure 2.11 Grape berry slices stained with Lugol's solution. Starch accumulates predominately in the peripheral vascular bundle, and near the grape pedicel.

2.2.5 Subcellular localization and function of VvGPTs

We cloned *VvGPT1* and two splicing variants of *VvGPT2* (*VvGPT2β* and *VvGPT2*Ω), which, contrarily to *VvGPT2α*, structurally differ from *VvGPT1* (Fig. 2.2 and Fig. 2.4). To study the subcellular localization of VvGPT1, VvGPT2β and VvGPT2Ω, the corresponding GPT-GFP fusion were transiently expressed in tobacco epidermal cells. The pattern of fluorescence distribution around the plastid clearly suggested that both VvGPT1-GFP and VvGPT2Ω-GFP fusion proteins were localized in the plastidial envelope (Fig. 2.12), as previously shown with the same approach for other plastidial transporters (Gigolashvili *et al*., 2009, 2012).

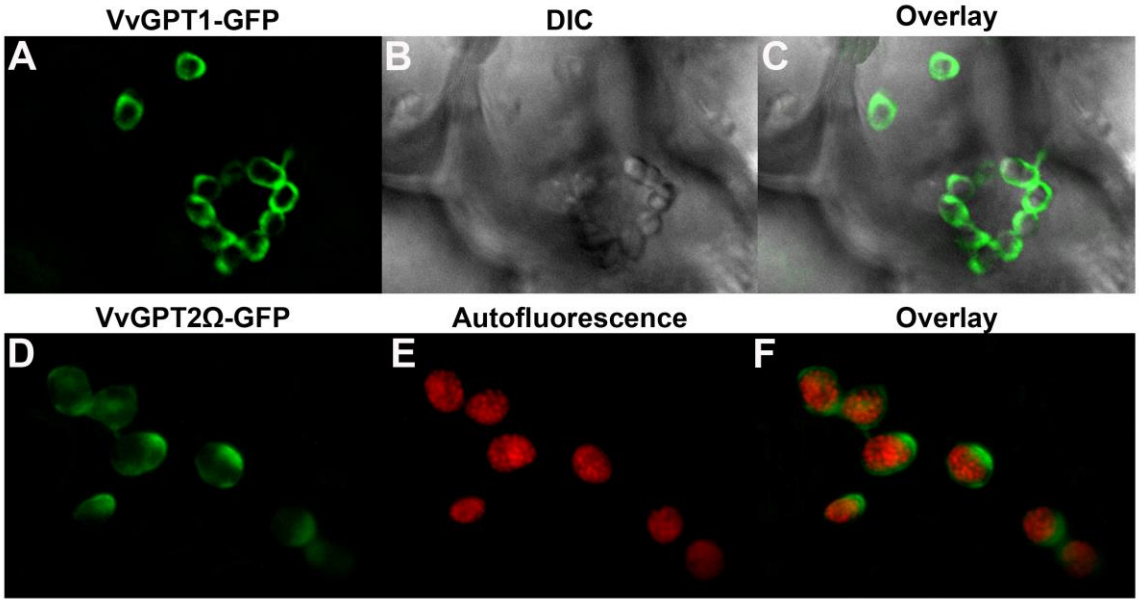

Figure 2.12. Subcellular localization of VvGPT1 (A, B and C) and VvGPT2Ω (D, E and F) in tobacco leaves. *Nicotiana benthamiana* leaves were infiltrated with *Agrobacterium tumefaciens* harboring the VvGPT1-GFP and VvGPT2Ω-GFP and after 2 days were observed in the confocal (A, B and C) and epifluorescence (D, E and F) microscopes.

Contrarily, when tobacco cells were transformed with the *35S-VvGPT2β-GFP* construct no fluorescence signal was observed (not shown), suggesting that the corresponding protein may be non-functional. This is in agreement with the sequence analysis of Fig. 2.4 showing that VvGPT2β lacks the characteristic TPT motif. As shown below, a clear GFP labeling of the plastidial membrane was also observed when

Arabidopsis thaliana was stably transformed with *35S-VvGPT1-GFP* and *35S-VvGPT2*Ω*-GFP* constructs (Fig. 2.13, insets).

Because the *Arabidopsis* homozygous mutant lacking *GPT1* is lethal and the one lacking *GPT2* does not show an obvious phenotype (Niewiadomski *et al*., 2005), the capacity of VvGPTs to transport glucose-6-Pi *in planta* was studied in the *pgi1-1* mutant. The leaves from *pgi1-1* are unable to accumulate starch due to the lack of plastidial phosphoglucose isomerase (PGI) activity (Fig. 2.13) and, as a result, they show a pale yellow color when stained with iodine (Yu *et al*., 2000; Niewiadomski *et al*., 2005). In the present study, when the *pgi1-1* mutant was complemented with *35S-VvGPT1-GFP* and *35S-VvGPT2*Ω*-GFP* constructs leaves recovered the typical strong iodine blue staining of the wild type (Fig. 2.14), suggesting that the capacity of chloroplasts to synthesize and accumulate starch was recovered, as shown before when the same mutant was complemented with *AtGPT1* and *AtGPT2* (Niewiadomski *et al*., 2005). Furthermore, the transformation with *35S-VvGPT2β-GFP* did not recover the capacity of the leaves to synthesize starch (Fig. 2.15), in agreement with the probable non-functional nature of VvGPT2β.

2.3 Discussion

2.3.1 VvGPTs share typical features of GPT family and VvGPT2 is alternatively spliced

Two *GPT* genes were identified in the grapevine genome, *VvGPT1* and *VvGPT2*, and soon after the cloning of both genes three different splicing variants of *VvGPT2* were found and named *VvGPT2α*, *-β* and -Ω. Alternative splicing is one of the main mechanisms underlying transcriptome and proteome plasticity. Recent studies pointed out to the extensive occurrence of these phenomena in plants and their importance in gene expression and stress response (Reddy *et al*., 2013). In grapevine, 30% of the genes with 2 or more exons produce different transcript isoforms, and 64% of the alternative spliced genes produced more than two isoforms (Vitulo *et al*., 2014).

The GPT signature motif TMKRISVIV is present in VvGPT1, VvGPT2α and VvGPT2Ω, which shared with other GPTs a high degree of similarity. This motif contains

a serine that can be phosphorylated and has been associated with substrate specificity because it varies between groups of the pPT family (Fig. 2.4 and 2.5; Knappe *et al.*, 2003).

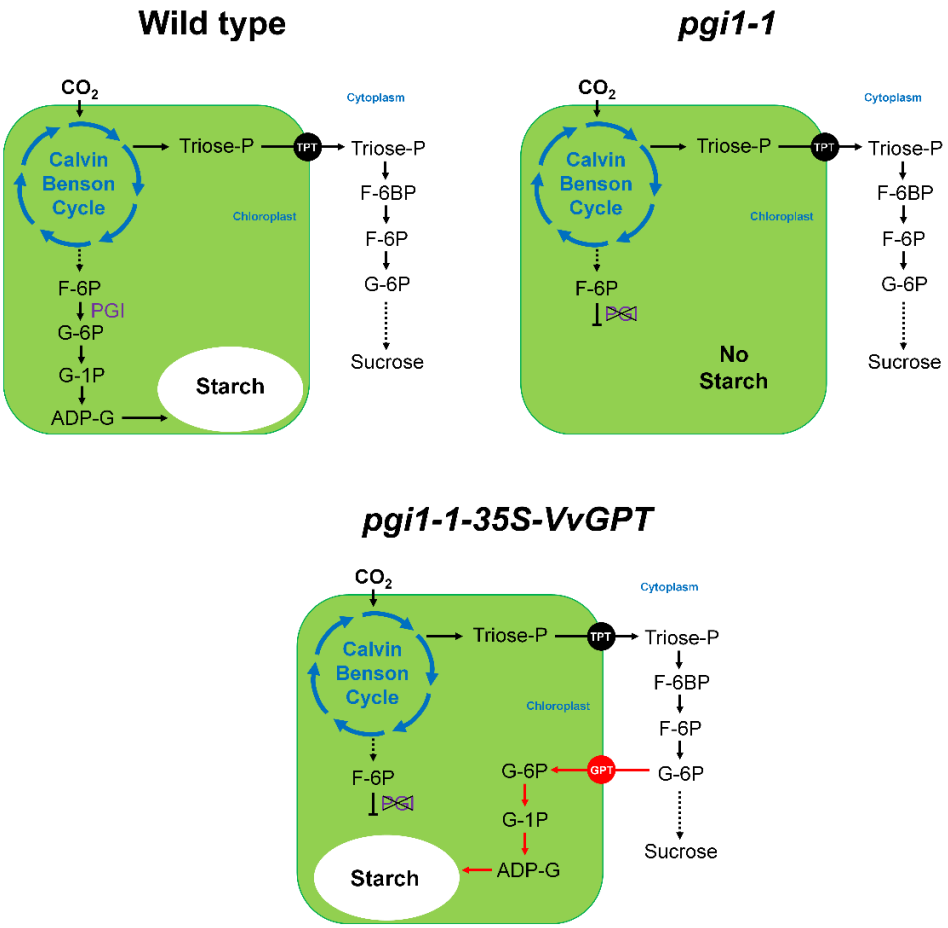

Figure 2.15 Schematic model of the strategy used to study glucose-6-Pi transport in the low-starch *Arabidopsis* mutant *pgi1-1*.

2.3.2 VvGPTs are glucose-6-Pi translocators

VvGPT1 and VvGPT2Ω have plastidial transit peptides and the localization of the mature protein in the chloroplast envelope was confirmed by transient expression of *GPT–GFP* fusion proteins in tobacco epidermal cells (Fig. 2.12). Although to the best of our knowledge this is the first time that a GPT-GFP is transiently expressed in tobacco leaves, the same pattern of fluorescence distribution around the plastid was observed for the plastidial transporters AtTPT (Gigolashvili *et al.*, 2012) and AtBAT5 (Gigolashvili *et al.*, 2009).

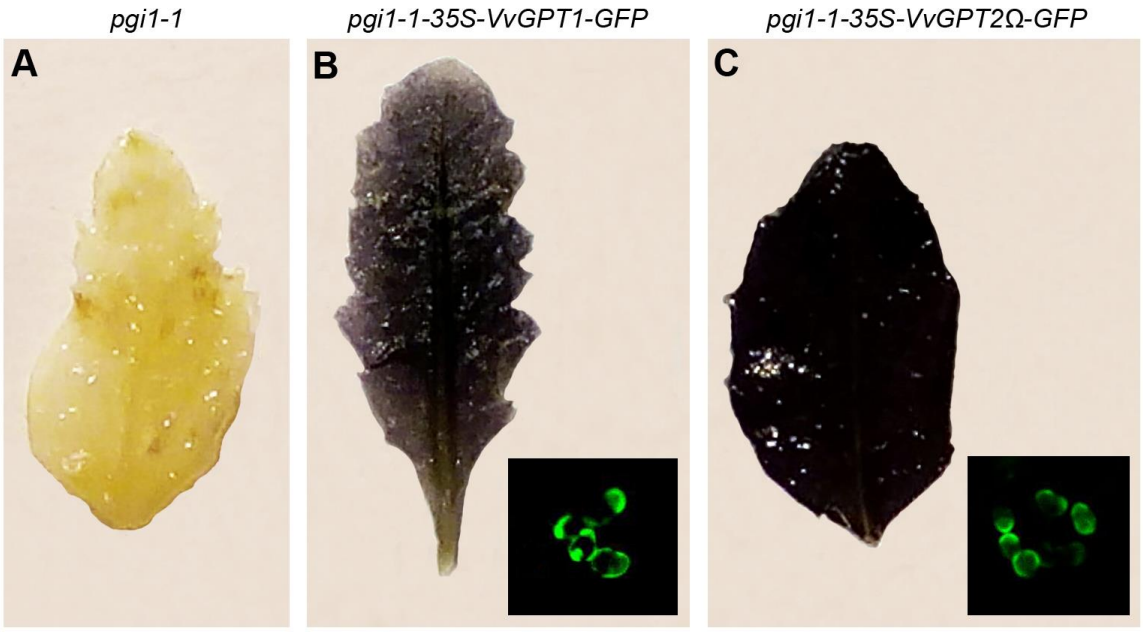

Figure 2.14 VvGPT1 and VvGPT2Ω transport glucose-6Pi *in planta*. The *pgi1-1 Arabidopsis* mutant, lacking phospho-glucose isomerase activity, is unable to convert fructose-6-Pi to glucose-6-Pi leading to a low-starch phenotype in the leaves (A) (Yu *et al*. 2000). Plants transformed with *35S-VvGPT1-GFP* (B) and *35S-VvGPT2*Ω*-GFP* (C) are able to accumulate starch by import cytosolic glucose-6-Pi and finishing the biosynthetic pathway (Niewiadomski *et al*., 2005). Representative experiment showing *Arabidopsis* leaves stained with iodine solution at the end of a 12 h photoperiod. Insets, confocal images of *Arabidopsis* leaves, showing the localization of VvGPT1-GFP and VvGPT2Ω-GFP in the chloroplast envelope.

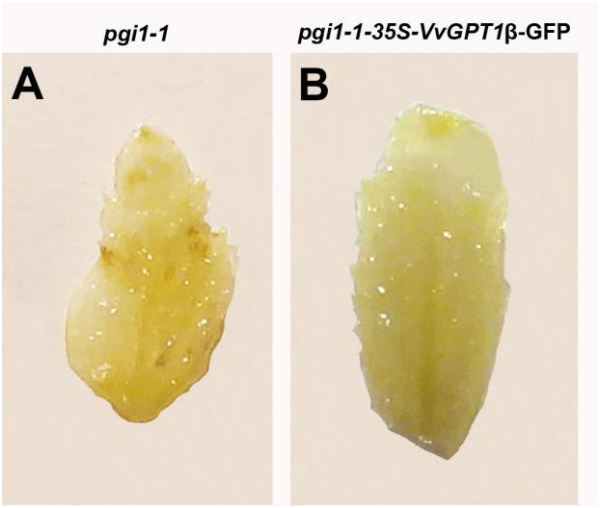

Figure 2.15 *VvGPT2*Ω does not transport glucose-6-Pi *in planta*. For details see Fig. 2.13 and legend of Fig 2.14.

Moreover, *Arabidopsis pgi1-1* mutants expressing *35S-VvGPT1-GFP and 35S-VvGPT2*Ω*-GFP* constructs displayed a clear GFP labeling of the chloroplast envelope (Fig. 2.14). As previously mentioned, *these pgi1-1* mutants are unable to accumulate transient starch in the leaves, which upon iodine staining show a pale yellow color (Yu *et al*. 2000). In our experimental conditions these observations were reproduced, but leaves from stably transformed plants overexpressing *pgi1-1-35S-VvGPT1-GFP* or *pgi1-1-35S-VvGPT2*Ω*-GFP* showed a typical strong iodine blue staining (Fig. 2.14), demonstrating that the chloroplasts recovered their capacity to accumulate starch. Altogether, these findings clearly demonstrate that VvGPT1 and VvGPT2Ω are indeed glucose-6-Pi transporters.

Regarding *VvGPT2β*, the results obtained in both *Arabidopsis* and tobacco suggests that this splicing version, which lacks the TPT motif, codes for a protein that has no function or is rapidly degraded. This phenomenon is sometimes observed in transcripts that undergo alternative splicing (Uversky, 2014). Much like the remaining *VvGPT2* splicing variants, *VvGPTα* is mostly expressed in autotrophic tissues. Because the present study was more focused on the role of *VvGPTs* in heterotrophic tissues we centered the work on *VvGPT1*. Nonetheless, both the localization and function of VvGPTα are good targets for future work, as the discovery of different functional or regulatory roles among splicing variants is of great scientific interest. Interestingly, in *Arabidopsis*, *GPT2* seems to be involved in the dynamic acclimation of leaves to increased light intensities, possibly by altering the sugar partitioning between the cytosol and the chloroplast or by altering the phosphate balance of the cell (Athanasiou *et al*., 2010).

2.3.3 VVGPT1 is likely involved in starch accumulation in heterotrophic tissues

In berries of cv. Vinhão, *VvGPT1* expression, which decreased from the green stage to the veraison before increasing again in the mature state, correlated well with the variation of starch levels along berry development. In tomato fruit, a relationship between starch, sucrose, sucrose synthase and symplastic loading has been suggested (N'tchobo *et al*., 1999; Nguyen-Quoc and Foyer, 2001). Also, starch and malate levels present in the green fruit were related with the content in soluble sugars of the ripe tomato (Centeno *et al*., 2011). In green berries of grape, starch may also be involved in the regulation of fruit loading since it accumulates preferentially in the outer layers of the mesocarp in the peripheral vascular bundle near the pedicel. *VvSS*, *VvAMY* and *VvGPT1* expressions peaked

at the mature stage when starch amount were also high. This suggests that a high turnover of starch occurs at this stage, involving an upregulation of carbon compartmentation into the amyloplast, paralleled by starch synthesis and degradation.

As a woody perennial plant, grapevine relies on carbohydrate reserves accumulated in the canes, roots and trunk to sustain rapid seasonal growth phases (Zapata *et al*., 2004). Even several weeks after bud burst, carbon assimilation is low and growth is maintained by sugars assimilated in the previous season that are mobilized from storage organs to sink tissues (Zapata *et al*., 2004). Canes from cv. Vinhão showed a high steady-state expression of *VvGPT1* and accumulated high amounts of starch in well-defined amyloplasts present in xylem rays (Fig. 2.12). Given the plastidial localization of VvGPT1 and its capacity to transport glucose-6-Pi, it is likely that this protein is fundamental for carbohydrate accumulation in grapevine storage tissues, an important parameter of plant productivity.

2.3.4 VvGPT1 provides glucose-6-Pi for the secondary metabolism within plastids

In grapevine, stress conditions increase the production of secondary metabolites that are synthesized in the plastid (Chaves *et al*., 2010), which may require additional glucose-6-Pi to increase the availability of reducing power via the OPPP. Our results showed that *VvGPT1* expression was slightly increased by ABA and galactinol but was strongly upregulated by MeJA in heterotrophic CSB cells growing in the dark. Because MeJA also strongly upregulated the expression of *VvPAL1*, pPT transporters may be important to feed the plastids with precursors for the secondary metabolism. In agreement with this hypothesis, sucrose, which has been associated with the production of secondary compounds in grape cells (Cormier *et al*., 1989; Larronde *et al*., 1998), also stimulated the expression of *VvGPT1* (Fig. 2.8). MeJA is an important plant regulator involved in fruit ripening, senescence, vegetative growth, cell cycle regulation, and plant defense mechanisms in response to herbivores, pathogen attack, and environmental stresses (Creelman and Rao, 2002; Wasternack and Hause, 2002; Liechti and Farmer, 2002; Castillo and Léon, 2008; Pauwels and Goosens, 2011). The observed strong upregulation of *VvPAL1* mediated by MeJA, is in line with previous reports showing that this hormone promotes the accumulation of several phenolic compounds including phytoalexins, anthocyanins, resveratrol and viniferins, and also induces sesquiterpene biosynthesis in grape cells (Krisa *et al*., 1999; Qu *et al*., 2011; Righetti *et al*., 2007; Santamaria *et al*., 2011;

Santamaria *et al*., 2012; D'Onofrio *et al*., 2009). In addition, MeJA was shown to activate the biosynthesis of terpenoids in the leaves of *Vitis* cv. Morio Muskat (Hampel *et al*., 2005). Furthermore, the observation that in cv. Aragonez cultivated under well-controlled field conditions *VvGPTs* expression was higher in west-exposed berries – subjected to higher temperatures and light intensities – is also in agreement with a possible role of *VvGPT1* on secondary metabolism, since water deficit, high berry temperature and sun exposure can promote the synthesis of some secondary compounds in grapevine (Chaves *et al*., 2010; Carbonell-Bejerano *et al*., 2014).

2.3.5 Other possible roles of VvGPTs

VvGPT1 showed a high steady-state expression in grapevine flowers, which may account for a higher influx into the plastid of precursors of fatty acid metabolism and secondary metabolism. There is a strong relationship between starch and flower development in grapevine (Lebon *et al*., 2005). In *Arabidopsis*, *AtGPT1* t-DNA insertion mutants displayed altered pollen and ovule development caused by the disruption of the plastidial OPPP, most likely affecting fatty acid metabolism during gametogenesis (Niewiadomski *et al*., 2005).

When compared to heterotrophic tissues, steady-state levels of *VvGPT1* in leaves were relatively low, contrarily to *VvGPT2* (Fig. 2.6a and b). Similarly to plastids from heterotrophic tissues, guard-cell chloroplasts are unable to convert triose-phosphates into hexose-phosphates (Hedrich *et al*., 1985) and rely on the import of cytosolic glucose-6-Pi to synthesize starch (Overlach *et al*., 1993), which is mobilized during the day and converted to malate and used as a counter-ion for potassium (Flügge *et al*., 1999). VvGPT2 may thus play an important role on the import of G-6-Pi into the plastids of guard cells.

As previously mentioned, besides its role in the accumulation of several secondary metabolites, MeJa is also involved in leaf senescence (Castillo and Léon, 2008; Pauwels and Goosens, 2011). The expression of *AtGPT2* increase in senescent leaves (Niewiadomski *et al*., 2005; Pourtau *et al*., 2006). In agreement, *VvGPT2α* and *VvGPT2*Ω showed higher expression levels in leaves and were additionally upregulated by MeJA in cultured cells, which together might suggest a possible involvement of VvGPT2 in leaf senescence. Finally, a recent study assigned GPT2 with a fundamental role in the

development of *Arabidopsis* seedlings, controlling the sugar partitioning and/or phosphate between the plastids and the cytosol (Dyson *et al*., 2014).

In conclusion, the present work provides the first characterization of plastid glucose-6-Pi transporters from grapevine, with a special emphasis given to *VvGPT1* that plays an important role in starch accumulation in heterotrophic tissues. Although both *VvGPT1* and *VvGPT2* appear to mediate the same function at the molecular level, they are differentially expressed and regulated in plant organs and in response to environmental and hormonal signals.

2.4 Material and Methods

2.4.1 Plant Material

Field-grown grapevines (*Vitis vinifera* L.) of cv. Aragonez and Vinhão were used in the present study. cv. Aragonez vines were collected from commercial vineyards in Reguengos de Monsaraz and Estremoz (south of Portugal) and cv. Vinhão from a commercial vineyard in Guimarães (north of Portugal). Rows had north–south orientation. The cv. Aragonez vines cultivated in Reguengos de Monsaraz were subjected to RDI (regulated deficit irrigation) and SDI (sustained deficit irrigation), within the scope of the European Project KBBE Innovine. RDI vines were supplied with 50% less water than SDI vines, and berries from SDI vines were collected from the green to mature phase to study gene expression during maturation. At the mature stage, the following values for leaf water potential were measured: –0.7 MPa (RDI) and –0.5 MPa (SDI). The oscillations in berry temperature were continuously monitored. Average daily maximal temperatures in grapes from clusters exposed to the west (RDI-W and SDI-W) were 4-5ºC higher than in east-exposed clusters (RDI-E and SDI-E). Grape berry clusters from 4–6 plants, located in three different rows, were collected, and grapes from three different berry clusters per plant were harvested and immediately frozen in liquid nitrogen. Berries were sampled at green (4 weeks after flowering (WAF)), veraison (9 WAF), and mature (15 WAF) stages of development and ripening. Mature leaves, flowers and canes from cv. Vinhão were used to study *VvGPT* expression.

Cultured cells from grape berry pulp (CSB, Cabernet Sauvignon Berry) were grown in liquid MS medium (Murashige and Skoog, 1962) supplemented with 2% (w/v) sucrose, and maintained in 250 mL flasks on a rotatory shaker at 100 rpm in the dark at 25ºC, according to Decendit *et al*. (1996). To study the effect of different treatments on *VvGPT* expression, 5 mL aliquots were incubated for 12 h with 20 µM ABA, 20 µM salicylic acid (SA), 20 µM methyl jasmonate (MeJA), 1 mM galactinol, 150 mM sucrose, 150 mM glucose and 150 mM fructose. Also, to study the effect of light exposure, cell aliquots were exposed to light (90 µmol m^{-2} s^{-1}) for 12 h. Cells were immediately frozen in liquid nitrogen and stored at -80 °C.

2.4.2 In silico studies

VvGPTs were identified in grapevine genome (V. vinifera cv. Pinot Noir clone PN40024 genome sequence; Jaillon *et al*., 2007) by homology search with *AtGPT1*. Protein sequences were obtained from the database of the National Center for Biotechnology Information (NCBI). Sequences from the grapevine genome were used to perform a promoter analysis using the Plant Promoter Analysis Navigator - PlantPAN software (Chang *et al*. 2008). Protein alignment was performed by Prankster and the result visualized in Genedoc (Nicholas *et al*., 1997). Phylogenetic trees were obtained with Phylip-3.69 software package (Felsenstein, 1986), and bootstrap values from 1000 trials were used. Chloroplast transit peptides were detected using the software ChloroP (Emmanuelson *et al*., 1999) and phosphorylation sites predicted by NetPhos 2.0 Server (Blom *et al*., 1999). Detection of conserved domains was performed using the CDD method available online at the NCBI website (Marchler-Bauer *et al*., 2013).

2.4.3 RNA isolation and cDNA synthesis

Total RNA was isolated with RNeasy Plant Mini Kit (QIAGEN) following manufacturer's instructions, except that the extraction buffer was changed to 2% CTAB, 2% soluble polyvinylpyrrolidone K-30, 300 mM Tris-HCl (pH 8.0), 25 mM EDTA, 2.0 M NaCl and 2% (v/v) β-mercaptoethanol (Reid *et al*., 2006). After DNAse treatment, RNA integrity was checked in a 1% agarose gel, and first strand cDNA synthesis was performed with the Omniscript RT kit (QIAGEN), following the manufacturer's instructions.

2.4.4 Subcellular localization of VvGPT1 and VvGPT2Ω

The *35S-VvGPT1-GFP*, *35S-VvGPT2β-GFP* and *35S-VvGPT2Ω-GFP* constructs were prepared using GATEWAY as described previously using the primers given on Table 3 (Noronha *et al*., 2014). Constructs were introduced in *Agrobacterium tumefaciens* (GV3101) and transient transformation *Nicotiana benthamiana* leaf epidermal cells was performed according to Sparkes *et al*. (2006). Briefly, overnight grown bacterial cultures were diluted to OD_{600nm} = 0.1 with infiltration buffer (50 mM MES pH 5.6, 2 mM Na_3PO_4, 0.5% glucose and 100 µM acetosyringone). Four-weeks-old tobacco plants were infiltrated with the bacterial cultures and leaf discs were examined under the confocal and epifluorescence microscope 3 days after.

	Primer forward (5'- 3')	Primer reverse (5'- 3')
pH7FWG2-VvGPT1-GFP	GGGGACAAGTTTGTACAAA AAAGCAGGCTTCATGATCTG CTCGATAAAGCAATCCG	GGGGACCACTTTGTACAAG AAAGCTGGGTCCTGCTTTG CCTGAGAATACAAGAAAG
pH7FWG2-VvGPT2β-GFP	GGGGACAAGTTTGTACAAAAA AGCAGGCTGAAATATGATTTC TTCAATTAAACAATCAACTGGG	GGGGACCACTTTGTACA AGAAAGCTGGGTGAGGG AGAGATCTGATCCAGG
pH7FWG2-VvGPT2Ω-GFP	GGGGACAAGTTTGTACAAAAA AGCAGGCTGAAATATGATTTC TTCAATTAAACAATCAACTGGG	GGGGACCACTTTGTACAAGA AAGCTGGGTGCTGTTCTGC ATTTTCATTTTTAGTTTTCC
qRT-PCR *VvGPT*1	TCAATGCTCTTGGAGCTGCCATC	CTTCCTCACTGCTTTGCCTGAG
qRT-PCR *VvGPT2α*	ACCAAATTTCATATGGTGGGT	TTTGCCTGCGAATAGAGAAA
qRT-PCR *VvGPT2β*	GCACTGGCTGCTATCACTTG	TGACAGAAATCCGCTTCATC
qRT-PCR *VvGPT2*Ω	ACACCTGTTCAACCCATCAA	GGGATAAGAATTTACCTGCGA
qRT-PCR *starch synthase*	TCGGATACTGACAGTTAGCAAGGG	ATGCAGACCATATCCACCTTCGG
qRT-PCR *α-amylase*	GGTTCTACTCAGGGTCACTGG	TGATGCAATTTCAGATCGGT
qRT-PCR *VvPAL1*	CCGAACCGAATCAAGGACTG	GTTCCAGCCACTGAGACAAT
PCR detection *VvGPT2α*	GGGATGAAGGGGAAGTCTGT	TCACTGCTTTGCCTGCGAATAGAGAA
PCR detection *VvGPT2β*	GCACTGGCTGCTATCACTTGTAT	TCACTGCTTTGCCTGCGAATAGAGAA
PCR detection *VvGPT2*Ω	CACATCATCAAGAGTGGTGAGC	GGGATAAGAATTTACCTGCGA

Table 3 Primers used in this study

2.4.5 Transformation of Arabidopsis pgi1-1 plants

Arabidopsis pgi1-1 homozygous line (Yu *et al*., 2000) was transformed by floral dipping (Clough and Bent 1998) with *35S-VvGPT1-GFP*, *35S-VvGPT2β-GFP* and *35S-VvGPT2*Ω*-GFP* constructs. Transformed plants were self-pollinated and homozygous lines were obtained. The presence of *VvGPT1*, *VvGPT2β* and *VvGPT2*Ω in the genome of transformed *Arabidopsis* was confirmed by PCR and confocal microscopy. Plants were maintained in a growth chamber with 12 h light period.

2.4.6 Starch staining

Free-hand slices of grape berries and canes were stained with Lugol's solution (1% (w/v) KI, 0.5% (w/v) I_2) and observed in a light microscope. *Arabidopsis* leaves from *pgi1-1* mutants overexpressing *VvGPT1, VvGPT2β* and *VvGPT2*Ω were sampled 4 weeks after germination from different positions, placed in a boiling bath with 80% ethanol (v/v) to remove chlorophylls, stained with iodine and incubated in deionized water to remove unspecific labelling. Images of Fig. 2.13 are representative of several experiments with similar results.

2.4.7 Starch quantification

Starch was quantified in berries and canes following the method by Smith and Zeeman (2006) with slight modifications. Frozen berry (1 g FW) and cane (0.1 g FW) tissues were washed 3 times with 5 mL 80% ethanol to remove soluble sugars, and the starch grains were gelatinized with 15 min incubation in a boiling bath. Starch was enzymatically degraded by adding α-amylase (1U, Sigma-Aldrich) and β-glucosidase (10U, Sigma-Aldrich) in a medium containing 200 mM sodium acetate (pH 5.5) and glucose was quantified using the Glucose (HK) Assay Kit (Sigma).

2.4.8 Real-Time PCR studies

Quantitative real-time PCR reactions were prepared with a QuantiTect SYBR Green PCR Kit (QIAGEN) and were performed in a CFX96 Real-Time Detection System (Bio-Rad), at an annealing temperature of 50ºC. RNA and cDNA were obtained as mentioned

above. Experiments were done in triplicate (biological replicates) with the software Bio-Rad CFX Manager (Bio-Rad), using *VvGAPDH* as internal control. After each run, melting curves were performed to check for unspecific and primer dimer amplification. Data was analyzed using the CFX Manager Software (Bio-Rad), and comparison of gene expression was performed following the $2^{-\Delta\Delta CT}$ method (Livak and Schmittgen, 2001). The primers used to study gene expression are shown Table 2.3.

2.4.9 Statistical analysis

The results were statistically analyzed by Student's t-test and by Analysis of Variances tests (one-way ANOVA) using Prism vs. 5 (GraphPad Software, Inc.). For each condition, differences between mean values are identified with different letters.

2.4.10 Sequences accession numbers

Am.trGPT1 (U5DAK5), AtGPT1 (Q9M5A9), AtGPT2 (Q94B38), AtPPT (Q8RXN3), AtTPT (Q9ZSR7), AtXPT (Q9LF61), MtGPT1 (G7J1A0), OsGPT1 (Q94JS6), SlGPT1 (K4CHA8), SlGPT2 (K4BFE6), SlXPT1 (K4AY31), VvGPT1 (KP133859), VvGPT2 (KP133860), VvPAL1 (EC987386), VvPPT (D7SHQ5), VvTPT (D7TJE0), VvXPT (F6I5C8), ZmGPT1 (K7UEC7), ZmPPT1 (P93642), ZmTPT1 (B4FWC0).

2.5 Acknowledgments

This work was supported by European Union Funds (FEDER/COMPETE Operational Competitiveness Programme) and Portuguese national Funds (FCT-Portuguese Foundation for Science and Technology): KBBE-2012-6-3117 “Inovinne”, FCOMP-01-0124-FEDER-022692 and PTDC/AGR-ALI/100636/2008. HN was supported by a PhD grant from FCT (SFRH/BD/74257/2010). This work also benefited from the networking activities within the European funded COST ACTION FA1106 “QualityFruit”. We would like to thank Dr. Anja Schneider from the Ludwig-Maximilians, University of Munich for kindly providing *Arabidopsis* pgi1-1 seeds

2.6 References

Athanasiou K, Dyson BC, Webster RE, Johnson GN. 2010. Dynamic acclimation of photosynthesis increases plant fitness in changing environments. *Plant Physiology* **152**, 366-373.

Blom N, Gammeltoft S, Brunak S. 1999. Sequence- and structure-based prediction of eukaryotic protein phosphorylation sites. *Journal of Molecular Biology* **294**, 1351-1362.

Bölter B, Soll J. 2001. Ion channels in the outer membrane of chloroplasts and mitochondria, open doors or regulated gates? *EMBO Journal* **20**,935-940.

Bölter B, Soll J, Hill K, Hemmler R, Wagner R. 1999. A rectifying ATP-regulated solute channel in the choloplastic outer envelope from pea. *EMBO Journal* **18**, 5505-5516.

Bowsher CG, Tobin AK. 2000. Compartmentation of metabolism within mitochondria and plastids. *Journal of Experimental Botany* **52**, 513-527.

Carbonell-Bejerano P, Diago MP, Matínez-Abaigar J, Martínez-Zapater JM, Tardáguila J, Núñez-Olivera E. 2014. Solar ultraviolet radiation is necessary to enhance grapevine fruit ripening transcriptional and phenolic responses. *BMC Plant Biology* **14**, 183.

Castillo MC, León J. 2008. Expression of the β-oxidation gene *3-ketoacyl-CoA thiolase 2* (*KAT2*) is required for the timely onset of natural and dark-induced leaf senescence in *Arabidopsis*. *Journal of Experimental Botany* **59**, 2171-2179.

Centeno DC, Osorio S, Nunes-Nesi A, Bertolo ALF, Carneiro RT, Araújo WL, Steinhauser MC, Michalska J, Rohrmann J, Geigenberger P, Oliver SN, Stitt M, Carrari C, Rose JKC, Fernie AR. 2011. Malate plays a crucial role in starch metabolism, ripening, and soluble solid content of tomato fruit and affects postharvest softening. *The Plant Cell* **23**, 162-184.

Chang WC, Lee TY, Huang HD, Huang HY, Pan RL. 2008. PlantPAN: plant promoter analysis navigator, for identifying combinatorial cis-regulatory elements with distance constraint in plant gene group. *BMC Genomics* **9**, 561.

Chaves MM, Zarrouk O, Francisco R, Costa JM, Santos T, Regalado AP, Rodrigues ML, Lopes CM. 2010. Grapevine under deficit irrigation: hints from physiological and molecular data. *Annals of Botany* **105**, 661–676.

Chong J, Piron MC, Meyer S, Merdinoglu D, Bertsch C, Mestre P. 2014. The SWEET family of sugar transporters in grapevine: VvSWEET4 is involved in the interaction with *Botrytis cinerea*. *Journal of Experimental Botany* **65**, 6589-601.

Clough SJ, Bent AF. 1998. Floral dip: a simplified method for *Agrobacterium*-mediated transformation of Arabidopsis thaliana. *The Plant Journal* **16**, 735-743.

Conde C, Agasse A, Glissant D, Tavares R, Gerós H, Delrot S. 2006. Pathways of glucose regulation of monosaccharide transport in grape cells. *Plant Physiology* **141**, 1563-1577.

Cormier F, Crevier HA, Do CB. 1989. Effects of sucrose concentration on the accumulation of anthocyanins in grape (*Vitis vinifera*) cell suspension. *Canadian Journal of Botany* **68**,1822-1825.

Creelman RA, Rao MV. 2002. The oxylipin pathway in Arabidopsis. In The Arabidopsis Book (Somerville, C.R.and Meyerowitz, E.M., eds), doi: 10.1199/tab.0012, American Society of Plant Biologists.

D'Onofrio C, Cox A, Davies C, Boss PK. 2009. Induction of secondary metabolism in grape cell cultures by jasmonates. *Functional Plant Biology* **36**, 323-338.

Decendit A, Ramawat KG, Waffo P, Deffieux G, Badoc A, Merillon JM. 1996. Anthocyanins, catechins, condensed tanins and piceid production in Vitis vinifera cell bioreactor cultures. *Biotechnology Letters* **18**, 659–662.

Deluc LG, Grimplet J, Wheatley MD, Tillett RL, Quilici DR, Osborne C, Schooley DA, Schlauch KA, Cushman JC, Cramer GR. 2007. Transcriptomic and metabolite analyses of Cabernet Sauvignon grape berry development. *BMC Genomics* **8**, 429.

Dyson BC, Webster RE, Johnson GN. 2014. GPT2: a glucose 6-phosphate/phosphate translocator with a novel role in the regulation of sugar signaling during seedling development. *Annals of Botany* **113**, 643-652.

Eicks M, Maurino V, Knappe S, Flügge UI, Fischer K. 2002. The plastidic pentose phosphate translocator represents a link between the cytosolic and the plastidic pentose phosphate pathways in plants. *Plant Physiology* **128**, 512-522.

Eisenreich W, Bacher A, Arigoni D, Rohdich F. 2004. Biosynthesis of isoprenoids via the non-mevalonate pathway. *Cellular and Molecular Life Sciences* **61**, 1401-1426.

Emmanuelson O, Nielsen H, von Heijne G. 1999. ChloroP, a neural network-based method for predicting chloroplast transit peptides and their cleavage sites. *Protein Science* **8**, 978-984.

Entwistle G, ap Rees T. 1990. Lack of fructose-1,6-bisphosphatase in a range of higher plants that store starch. *Biochemical Journal* **271**, 467-472.

Felsenstein J. 1986. PHYLIP – Phylogeny inference package (Version 3.2). *Cladistics* **5**, 164-166.

Fischer K, Kammerer B, Gutensohn M, Arbinger B, Weber A, Häusler R, Flügge UI. 1997. A new class of plastidic phosphate translocators: a putative link between primary and secondary metabolism by the phosphoenolpyruvate/phosphate antiporter. *Plant Cell* **9**, 453-62.

Fischer K. 2001. The import and export business of plastids, transport processes across the inner envelope membrane. *Plant Physiology* **155**, 1511-1519.

Fliege R, Flügge UI, Werdan K, Heldt HW. 1978. Specific transport of inorganic phosphate, 3-phosphoglycerate and triosephosphates across the inner membrane of the envelope in spinach chloroplasts. *Biochimica et Biophysica Acta* **502**, 232-247.

Flügge UI. 1999. Phosphate translocators in plastids. *Annual Reviews in Plant Physiology and Plant Molecular Biology* **50**, 27-45.

Flügge UI, Benz R. 1984. Pore-forming activity in the outer membrane of the chloroplast envelope. *FEBS letters* **169**, 85-89.

Flügge UI, Häusler RE, Ludewig F, Gierth M. 2011. The role of transporters in supplying energy to plant plastids. *Journal of Experimental Botany* **62**, 2381-2392.

Fortes AM, Agudelo-Romero P, Silva MS, Ali K, Sousa L, Maltese F, Choi YH, Grimplet J, Martinez-Zapater JM, Verpoorte R, Pais MS. 2011. Transcript and metabolite analysis in Trincadeira cultivar reveals novel information regarding the dynamics of grape ripening. *BMC Plant Biology* **11**, 149.

Gigolashvili T, Geier M, Ashykhmina N, Frerigmann H, Wulfert S, Krueger S, Mugford SG, Kopriva S, Haferkamp I, Flügge UI. 2012. The Arabidopsis thylakoid ADP/ATP carrier TAAC has an additional role in supplying plastidic phosphoadenosine 5'-phosphate to the cytosol. *Plant Cell* **24**, 4187-4204.

Gigolashvili T, Yatusevich R, Rollwitz I, Humphry M, Gershenzon J, Flügge UI. 2009. The plastidic bile acid transporter 5 is required for the biosynthesis of methionine-derived glucosinolates in *Arabidopsis thaliana*. *Plant Cell* **21**, 1813-1829.

Hampel D, Mosandl A, Wüst M. 2005. Induction of de novo volatile terpene biosynthesis via cytosolic and plastidial pathways by methyl jasmonate in foliage of *Vitis vinifera* L. *Journal of Agriculture and Food Chemistry* **53**, 2652-2657.

Hannah L, Roehrdanz PR, Ikegami M, Shepard AV, Shaw MR, Tabor G, Zhi L, Marquet PA, Hijmans RJ. 2013. Climate change, wine, and conservation. *Proceedings of the National Academy of Sciences, USA* **110**, 6907-6912.

Hardie WJ, O´Brien TP, Jaudzems VG. 1996. Morphology, anatomy and development of the pericarp after anthesis in grape, *Vitis vinifera* L. *Australian Journal of Grape Wine Research* **2**, 97-142.

Hedrich R, Raschke K, Stitt M. 1985. A role for fructose-2,6-bisphosphate in regulating carbohydrate metabolism in guard cells. *Plant Physiology* 79, 977-982.

Herrmann KM, Weaver LM. 1999. The shikimate pathway. *Annual Reviews in Plant Physiology and Plant Molecular Biology* **50**, 473-503.

Hill LM, Smith AM. 1991. Evidence that glucose 6-phosphate is imported as the substrate for starch biosynthesis by the plastids of developing pea embryos. *Planta* 185, 91-96.

Hill LM, Smith AM. 1995. Coupled movements of glucose 6-phosphate and triose phosphate through the envelopes of plastids from developing embryos of pea (*Pisum sativum* L.). *Journal of Plant Physiology* **146**, 411-417.

Jaillon O, Aury JM, Noel B, Policriti A, Clepet C, *et al*. 2007. The grapevine genome sequence suggests ancestral hexaploidization in major angiosperm phyla. *Nature* **449**, 463-467.

Kammerer B, Fischer K, Hilpert B, Schubert S, Gutensohn M, Weber APM, Flügge UI. 1998. Molecular characterization of a carbon transporter in plastids from heterotrophic tissues: the glucose 6-phosphate/phosphate antiporter. *Plant Cell* **10**,105-117.

Knappe S, Flügge UI, Fischer K. 2003. Analysis of the *plastidic phosphate* translocator gene family in Arabidopsis and identification of new *phosphate translocator*-homologous transporters, classified by their putative substrate-binding site. *Plant Physiology* **131**, 1178-1190.

Krisa S, Larronde F, Budzinski H, Decendit A, Deffieux G, Mérillon JM. 1999. Stilbene production by *Vitis vinifera* cell suspension cultures, methyl jasmonate induction and ^{13}C biolabeling. *Journal of Natural Products* **62**, 1688-1690.

Kruger NJ, von Schaewen A. 2003. The oxidative pentose phosphate pathway, structure and organisation. *Current Opinion in Plant Biology* **6**, 236-246.

Larronde F, Krisa S, Decendit A, Chèze C, Deffieux G, Mérrillon JM. 1998. Regulation of polyphenol production in *Vitis vinifera* cell suspension cultures by sugars. *Plant Cell Reports* **17**, 946-950.

Lebon G, Duchêne E, Brun O, Clément C. 2005. Phenology of flowering and starch accumulation in grape (*Vitis vinifera* L.) cuttings and vines. *Annals of Botany* **95**, 943-948.

Lecourieux F, Kappel C, Lecourieux D, Serrano A, Torres E, Arce-Johnson P, Delrot S. 2014. An update on sugar transport and signaling in grapevine. *Journal of Experimental Botany* **65**, 821-832.

Liechti R, Farmer EE. 2002. The jasmonate pathway. Science **296**, 1649-1650.

Linka N, Weber APM. 2010. Intracellular Metabolite Transporters in Plants. Molecular Plant **3**, 21-53.

Livak KJ, Schimittgen TD. 2001. Analysis of relative gene expression data using real-time quantitative PCR and the $2^{-\Delta\Delta CT}$ method. *Methods (San Diego, Calif.)* **25**, 402-408.

Luan F, Wüst M. 2002. Differential incorporation of 1-deoxy-d-xylulose into (3S)-linalool and geraniol in grape berry exocarp and mesocarp. *Phytochemistry* **60**, 451-459.

Marchler-Bauer A, Zheng C, Chitsaz F, Derbyshire MK, Geer LY, Geer RC, Gonzales NR, Gwadz M, Hurwitz DI, Lanczycki CJ, Lu F, Lu S, Marchler GH, Song JS, Thanki N, Yamashita RA, Zhang D, Bryant SH. 2013. CDD, conserved

domains and protein three-dimensional structure. *Nucleic Acids Research*, doi: 10.1093/nar/gks1243.

Martin DM, Toub O, Chiang A, Lo BC, Ohse S, Lund ST, Bohlmann J. 2009. The bouquet of grapevine (*Vitis vinifera* L. cv. Cabernet Sauvignon) flowers arises from the biosynthesis of sesquiterpene volatiles in pollen grains. *Proceedings of the National Academy of Sciences, USA* **106**, 7245-7250.

May B, Lange BM, Wüst M. 2013. Biosynthesis of sesquiterpenes in grape berry exocarp of *Vitis vinifera* L.: evidence for a transport of farnesyl diphosphate precursors from plastids to the cytosol. *Phytochemistry* **95**, 135-144.

N'tchobo H, Dali N, Nguyen-Quoc B, Foyer CH, Yelle S. 1999. Starch synthesis in tomato remains constant throughout fruit development and is dependent on sucrose supply and sucrose synthase activity. *Journal of Experimental Botany* **50**, 1457-1463.

Neuhaus HE, Thom E, Batz O, Scheibe R. 1993. Purification of highly intact plastids from various heterotrophic plant tissues. Analysis of enzyme equipment and precursor dependency for starch biosynthesis. *Biochemical Journal* **296**, 395-401.

Nguyen-Quoc B, Foyer CH. 2001. A role for "futile cycles" involving invertase and sucrose synthase in sucrose metabolism in tomato fruit. *Journal of Experimental Botany* **52**, 881-889.

Nicholas KB, Nicholas HB Jr, Deerfield DW II (1997) GeneDoc, analysis and visualization of genetic variation. *EMBNET.NEWS* **4**, 14.

Niewiadomski P, Knappe S, Geimer S, Fisher K, Schulz B, Unte US, Rosso MG, Ache P, Flügge U, Schneider A. 2005. The Arabidopsis plastidic glucose 6-phosphate/phosphate translocator GPT1 is essential for pollen maturation and embryo sac development. *Plant Cell* **17**, 760-775.

Noronha H, Agasse A, Martins AP, Berny MC, Gomes D, Zarrouk O, Thiebaud P, Delrot S, Chaumont F, Gerós H. 2014. The grape aquaporin VvSIP1 transports water across the ER membrane. *Journal of Experimental Botany* **65**, 981-993.

Overlach S, Diekmann W, Raschke K. 1993. Phosphate translocator of isolated guard-cell chloroplasts from *Pisum sativum* L. transports glucose-6-phosphate. *Plant Physiology* **101**, 1201-1207.

Pauwels L, Goossens A. 2011. The JAZ proteins: a crucial interface in the jasmonate signaling cascade. *Plant Cell* **23**, 3089-3100

P**ohlmeyer K, Soll J, Grimm R, Hill K, Wagner R**. 1998. A high-conductance solute channel in the chloroplastic outer envelope from pea. *Plant Cell* **10**, 1207-1216.

Pohlmeyer K, Soll J, Steinkamp T, Hinnah S, Wagner R. 1997. Isolation and characterization of an amino acid-selective channel protein present in the chloroplastic outer envelope membrane. *Proceedings of the National Academy of Sciences, USA* **94**, 9504-9509.

Qu J, Zhang W, Yu X. 2011. A combination of elicitation and precursor feeding leads to increased anthocyanin synthesis in cell suspension cultures of *Vitis vinifera*. *Plant Cell, Tissue and Organ Culture* **107**, 261-269.

Quick WP, Neuhaus HE. 1996. Evidence for two types of phosphate translocators in sweet-pepper (*Capsicum annuum* L.) fruit chromoplasts. *Biochemical Journal* **320**, 7-10.

Reddy ASN, Marquez Y, Kalyna M, Barta A. 2013. Complexity of the alternative splicing landscape in plants. *Plant Cell* **25**, 3657-3683.

Reid KE, Olsson N, Schlosser J, Peng F, Lund ST. 2006. An optimized grapevine RNA isolation procedure and statistical determination of reference genes for real-time RT-PCR during berry development. *BMC Plant Biology* **6**, 27.

Righetti L, Franceschetti M, Ferri M, Tassoni A, Bagni N. 2007. Resveratrol production in *Vitis vinifera* cell suspensions treated with several elicitors. *Caryologia* **60**, 169-171.

Rolletschek H, Nguyen TH, Häusler R, Rutten T, Göbel C, Feussner I, Radchuk R, Tewes A, Claus B, Klukas C, Linemann U, Weber H, Wobus U, Borisjuk L. 2007. Antisense inhibition of the plastidial glucose-6-phosphate/phosphate translocator in *Vicia* seeds shifts cellular differentiation and promotes protein storage. *Plant Journal* **51**, 468–484.

Roth C, Menzel G, Petetot JM, Rochat-Hacker S, Poirier Y. 2004. Characterization of a protein of the plastid inner envelope having homology to animal inorganic phosphate, chloride and organic-anion transporters. *Planta* **218**, 406-416.

Santamaria AR, Innocenti M, Mulinacci N, Melani F, Valletta A, Sciandra I, Pasqua G. 2012. Enhancement of viniferin production in *Vitis vinifera* L. cv. Alphonse Lavallée cell suspensions by low-energy ultrasound alone and in combination with methyl jasmonate. *Journal of Agriculture and Food Chemistry* **60**, 11135-11142.

Santamaria AR, Mulinacci N, Valletta A, Innocenti M, Pasqua G. 2011. Effects of elicitors on the production of resveratrol and viniferins in cell cultures of *Vitis vinifera* L. cv. Italia. *Journal of Agriculture and Food Chemistry* **59**, 9094-9101.

Schott K, Borchert S, Müller-Röber B, Heldt HW, 1995, Transport of inorganic phosphate and C3- and C6-sugar phosphates across the envelope membranes of potato tuber amyloplasts. *Planta* **196**, 647-652.

Smith AM, Zeeman SC. 2006. Quantification of starch in plant tissues. *Nature Protocols* **1**, 1342-1345.

Smith AM, Zeeman SC, Smith SM. 2005. Starch degradation. *Annual Reviews in Plant Biology* **56**, 73-98.

Soler E, Clastre M, Bantignies B, Marigo G, Ambid C. 1993. Uptake of isopentenyl diphosphate by plastids isolated from *Vitis vinifera* L. cell suspensions. *Planta* **191**, 324-329.

Soler E, Feron G, Clastre M, Dargent R, Gleizes M, Ambid C. 1992. Evidence for a geranyl-diphosphate synthase localized within the plastids of *Vitis vinifera* L. cultivated *in vitro*. *Planta* **187**, 171-175.

Sparkes IA, Runions J, Kearns A, Hawes C. 2006. Rapid, transient expression of fluorescent fusion proteins in tobacco plants and generation of stably transformed plants. *Nature Protocols* **1**, 2019-2025.

Streatfield SJ, Weber APM, Kinsman EA, Häusler RE, Li J, Post-Beittenmiller D, Kaiser WM, Pyke KA, Flügge UI, Chory J. 1999. The phosphoenolpyruvate/phosphate translocator is required for phenolic metabolism, palisade cell development, and plastid-dependent nuclear gene expression. *Plant Cell* **11**, 1609-1621.

Suzuki N, Sakuta M, Shimizu S, Komamine A. 1995. Changes in the activity of 3-deoxy-D-arabino-heptulosonate 7-phosphate (DAHP) synthase in suspension-cultured cells of *Vitis*. *Physiologia Plantarum* **94**, 591-596.

Teixeira A, Eiras-Dias J, Castellarin SD, Gerós H. 2013. Berry phenolics of grapevine under challenging environments. *International Journal of Molecular Sciences* **14**, 18711-18739.

Teixeira A, Martins V, Noronha H, Eiras-Dias J, Gerós H. 2014. The first insight into the metabolite profiling of grapes from three *Vitis vinifera* L. cultivars of two controlled appellation (DOC) regions. *International Journal of Molecular Sciences* **15**, 4237-4254.

Van Leeuwen C, Schultz HR, Garcia de Cortazar-Atauri I, Duchêne E, Ollat N, Pieri P, Bois B, Goutouly JP, Quénol H, Touzard JM, Malheiro AC, Bavaresco L and Delrot S. 2013. Why climate change will not dramatically decrease viticultural

suitability in main wine-producing areas by 2050. *Proceedings of the National Academy of Sciences, USA* **110**, 3051-3052.

Vitulo N, Forcato C, Carpinelli EC, Telatin A, Campagna D, D'Angelo M, Zimbello R, Corso M, Vannozzi A, Bonghi C, Lucchin M, Valle G. 2014. A deep survey of alternative splicing in grape reveals changes in the splicing machinery related to tissue, stress condition and genotype. *BMC Plant Biology* **14**, 99.

Wasternack C, Hause B. 2002. Jasmonates and octadecanoids, signals in plant stress responses and development. *Progress in Nucleic Acid Research and Molecular Biology* **72**, 165-221.

Weber APM, Linka N. 2011. Connecting the plastid: transporters of the plastid envelope and their role in linking plastidial with cytosolic metabolism. *Annual Reviews in Plant Biology* **62**, 53-77.

Yu T, Lue W, Wang S, Chen J. 2000. Mutation of Arabidopsis plastid phosphoglucose isomerase affects leaf starch synthesis and floral initiation. *Plant Physiology* **123**, 319-325.

Zapata C, Deléens E, Chaillou S, Magné C. 2004. Partitioning and mobilization of starch and N reserves in grapevine (*Vitis vinifera* L.). *Journal of Plant Physiology* **161**, 1031-1040.

Zhang ZZ, Li XX, Zhu BQ, Wen YQ, Duan CQ, Pan QH. 2010. Molecular characterization and expression analysis on two isogenes encoding *3-deoxy- D -arabino-heptulosonate 7-phosphate synthase* in grapes. *Molecular Biology Reports* **38**, 4739-47

Chapter 3

The grape aquaporin VvSIP1 transports water across the ER membrane

The work presented in this chapter has been published:

Noronha H**,** Agasse A, Martins AP, Berny MC, Gomes D, Zarrouk O, Thiebaud P, Delrot S, Soveral G, Chaumont F and Gerós H. 2014. The grape aquaporin VvSIP1 transports water across the ER membrane. *Journal of Experimental Botany* **65**, 981–993.

Authors´ contributions: HN, AA and HG raised the hypothesis underlying this work. HN, AA, PT, SD, GS, FC and HG design the experiments. HN, AA, DG, APM, MCB and OZ performed the experiments. HN and AA analyzed the data. HN and HG wrote the paper. CC, SD and HG directed the study.

Abstract

Water diffusion through biological membranes is facilitated by aquaporins, members of the widespread Major Intrinsic Proteins (MIPs). In the present study, the localization, expression and functional characterization of a SIP from the grapevine were assessed. *VvSIP1* was expressed in leaves and berries from field-grown vines, and in leaves and stems from *in vitro* plantlets, but not in roots. When expressed in tobacco mesophyll cells and in *Saccharomyces cerevisiae*, fluorescent-tagged VvSIP1 was localized at the endoplasmic reticulum (ER). Stopped-flow spectroscopy showed that VvSIP1-enriched ER membrane vesicles from yeast exhibited higher water permeability and lower E_a for water transport than control vesicles, indicating the involvement of protein mediated water diffusion. This aquaporin was able to transport water but not glycerol, urea, sorbitol, glucose and inositol. *VvSIP1* expression in *Xenopus* oocytes failed to increase the water permeability of the plasma membrane. VvSIP1-His-tag was solubilized and purified to homogeneity from yeast ER membranes and the reconstitution of the purified protein in phosphatidylethanolamine liposomes confirmed its water channel activity. To provide further insights into gene function, the expression of *VvSIP1* in mature grapes was studied when vines were cultivated in different field conditions, but its transcript levels did not increase significantly in water stressed plants and western-exposed berries. However, the expression of the aquaporins *VvSIP1*, *VvPIP2;2* and *VvTIP1;1* was upregulated by heat in cultured cells.

3.1 Introduction

The physiological role of intracellular aquaporins (AQP) in plants is not yet clear and remains a stimulating matter of debate (for reviews see Ishibashi, 2006; Nozaki *et al*., 2008; Maeshima and Ishikawa, 2008; Gomes *et al*., 2009; Wudick *et al*., 2009; Conde *et al*., 2010). Intracellular AQPs may play important roles in organelle water transport and intracellular water homeostasis, but they may also transport small solutes important for cell signaling (Gomes *et al*., 2009).

Comparatively to other organisms, plants appear to have a remarkable large number of aquaporins ubiquitously expressed (Javot and Maurel, 2002; Javot *et al*., 2003). Following the identification of *Arabidopsis thaliana* AtTIP1;1 as the first plant water channel (Höfte *et al*., 1992; Maurel *et al*., 1993), several intracellular aquaporins have been described, particularly at the tonoplast (reviewed by Wudick *et al*., 2009). However, three SIPs (Small Basic Intrinsic Protein) and one NIP (Nodulin-like Intrinsic Protein) from *Arabidopsis* have shown to localize at the ER (Ishikawa *et al*., 2005; Mituzani *et al*., 2006). Also, an aquaporin able to transport CO_2, NtAQP1, was shown to be localized at the chloroplast membranes (Uehlein *et al*., 2003, 2008). AQP8 and AQP9 from mammals were localized in the membrane system of the mitochondria (Calamita *et al*., 2005; Amiry-Moghaddam *et al*., 2005), and more recently *Arabidopsis* AtTIP5;1 was specifically found in the mitochondria of pollen tubes (Soto *et al*., 2010).

SIPs constitute a subfamily of MIPs that was identified for the first time by database mining and phylogenetic analyses (Johanson and Gustavsson, 2002), and are related to mammalian AQP11 and AQP12 in their intracellular localization and function (reviewed by Ishibashi, 2006). Each SIP member may exhibit a particular pattern of expression in the plant and play a role specific to each cell. *Arabidopsis thaliana SIP1;1* is expressed in the roots and flowers, especially in stamens, and pollens, and in trichomes of rosette leaves. *AtSIP1;2* is expressed in the cotyledon and hydathode tissue of rosette leaves. *AtSIP2;1* is expressed in the vascular tissue of roots and the leaf veins, in flowers, pollen and siliques (Ishikawa *et al*., 2005).

Regarding key distinctive structural characteristics of SIPs, the first NPA motif of the loop B, which participates in the formation of an essential constriction region, is

changed to NPT, NPC, or NPL in AtSIP1;1, AtSIP1;2, and AtSIP2;1, respectively, and to NPC or NPT in human aquaporins AQP11 and AQP12, respectively. The two NPA motifs are involved in the selection of substrate through the hydrogen bond formation between a water molecule and the asparagine residue. Thus, any variation of the NPA motif might directly reflect the substrate specificity and/or velocity of the water transport (reviewed by Ishibashi, 2006; Maeshima and Ishikawa, 2008; Gomes *et al*., 2009). The SIP members are also relatively rich in basic residues such as lysine, and their isoelectric points are higher than in aquaporins from other subfamilies.

Grape berries are sophisticated biochemical factories of major economic importance. They import and accumulate water, minerals, sugars and amino acids, and synthesize organic acids, tannins, anthocyanins as well as flavor and aroma compounds. The development and maturation of grape berries have received considerable scientific scrutiny because of both the uniqueness of such processes to plant biology and the importance of these fruits as a significant component of the human diet and wine industry (Conde *et al*., 2007). The grape genome has only two *SIP* genes, *VvSIP1* and *VvSIP2*, encoding a SIP1 and SIP2 subtype, respectively. The present study investigates the expression of *VvSIP1* in leaves and grape berries throughout the season and the subcellular localization of the protein fused to a fluorescent tag both in tobacco leaves and yeast. Expression of *VvSIP1* in *Xenopus* oocytes did not increase the water permeability of the plasma membrane. In contrast, when expressed in yeast, VvSIP1-enriched ER membrane vesicles exhibited higher water permeability than control vesicles, as determined by stopped-flow spectroscopy, and the protein was unable to accept other substrates, including glycerol, urea, sorbitol, glucose and inositol. VvSIP1 protein was also purified to homogeneity and its water transport activity was reconstituted in phosphatidylethanolamine artificial vesicles. The potential role of VvSIP1 in stress response was studied in field-grown grapevines and grape cell cultures.

3.2 Results

3.2.1 Analysis of SIP1s protein sequences

The amino acid sequence of *Vitis vinifera* VvSIP1 was compared to SIP1 aquaporins from *A. thaliana*, *Zea mays* (maize), *Olea europaea* (olive), *Oryza sativa* (rice),

Medicago truncatula and the moss *Physcomitrella patens* (Fig. 3.1). All proteins share 6 transmembrane domains and two intracellular and extracellular loops that fold into the membrane and interact with each other through two "NPA" motifs. A 3D computer simulation of VvSIP1 using SoPIP2;1 as a template (Thornroth-Horesfiel *et al*., 2006) confirmed that these "NPA" motives form a central constriction. Except for MtSIP1;1 and AtSIP1;2, the first "NPA" motive is changed to NPT (Fig. 3.1). The R1 (I, L,V or N), R2 (I, L or V), R3 (P) and R4 (I or N) residues, which form the Ar/R filter meet proximal to the central constriction formed by the two "NPA" motives. Contrarily to most PIPs, TIPs and NIPs, which contain an arginine (R) in R4 residue, the SIP1 proteins analyzed show a conserved asparagine (N), except in the case of AtSIPs. In SIP1 sequences, the R3 residue is a conserved proline (P), which seems a characteristic of SIP1 members. Furthermore, a highly conserved AFGWAYI motif is present in the Loop E of all SIP1s.

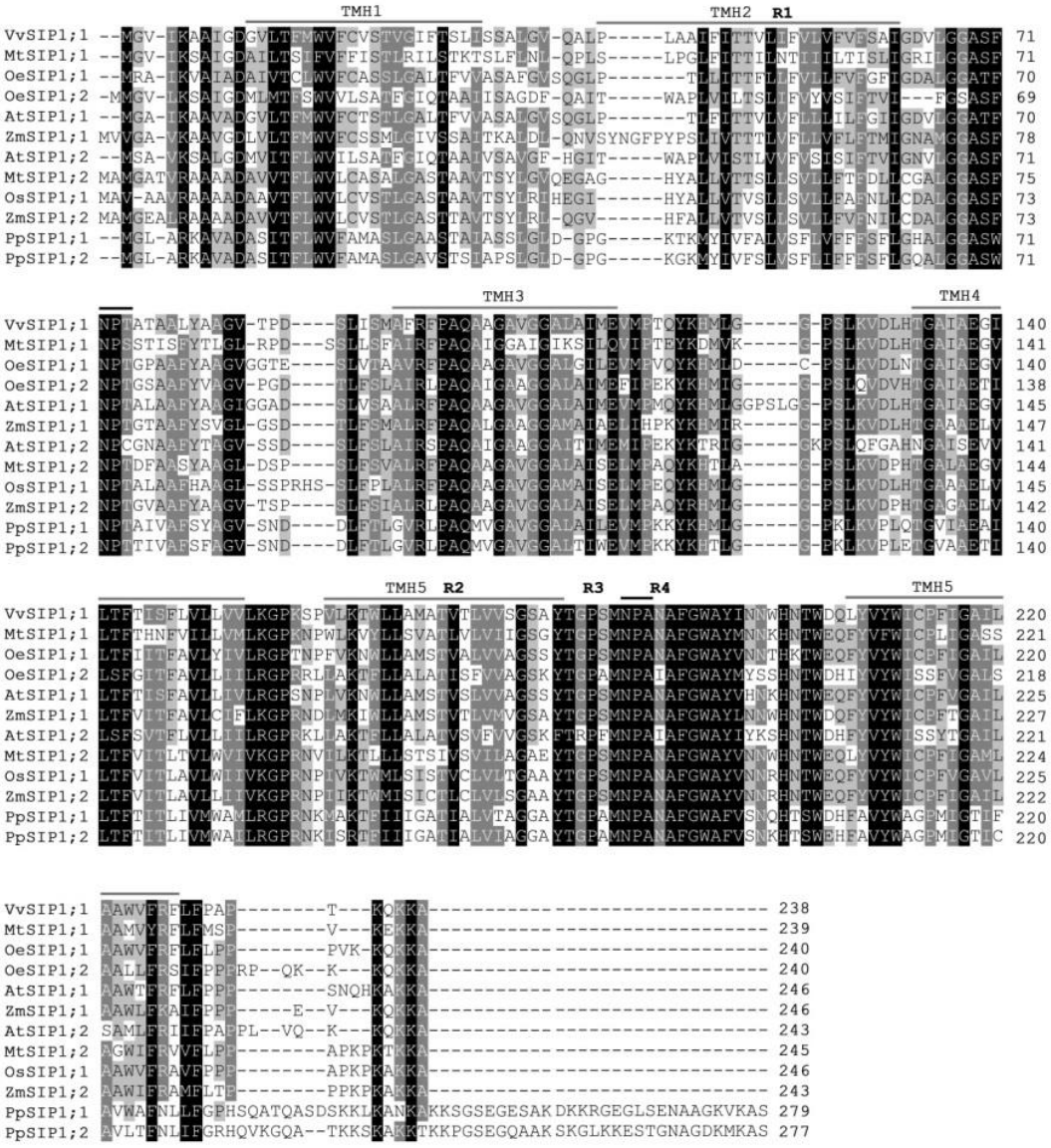

Figure 3.1 Alignment of seven SIP1 proteins showing six transmembrane domains (TMH1-6) and two intracellular and extracellular loops containing the conserved "NPA" motives (black lines) and the four amino acids corresponding to the Ar/R filter (R1-4).

3.2.2 Expression studies of VvSIP1

To study the expression of *VvSIP1*, total RNA was isolated from cv. Vinhão leaves and berries and from grape berries of cv. Aragonez at three different developmental stages. RNAs from grapevine plantlets growing *in vitro* and from liquid cultured cells were also isolated to study the transcript levels of *VvSIP1*. In cv. Vinhão, *VvSIP1* transcripts were detected in all samples, but were more abundant at the end of the season, both in leaves and mature grapes (Fig. 3.2A and B). Conversely, in berries from cv. Aragonez *VvSIP1* expression decreased during maturation (Fig. 3.2C). In 3-months old grapevine plantlets growing *in vitro VvSIP1* transcripts were very abundant in leaves and stem but were not detected in roots (not shown). Aragonez vines cultivated under field conditions were also used to study *VvSIP1* expression in berries in response to water deficit and different sun exposures (Fig. 3.2D and E). As described in material and methods, grapevines subjected to regulated deficit irrigation (RDI) were irrigated with 50% less water than those subjected to sustained deficit irrigation (SDI). In addition, average daily maximum temperatures were 4-5ºC higher in grapes exposed to west (RDI-W and SDI-W) than in those exposed to east (RDI-E and SDI-E). Results showed that transcript levels of *VvSIP1* did not increase significantly in berries from water stressed plants and in berries from western-exposed clusters. The expression of *VvSIP1* was also studied in mature berries from vines cultivated under more pronounced water deficit conditions (non-irrigation), but again, the expression of *VvSIP1* did not increase significantly (Fig. 3.2E). In suspension-cultured cells (CSB, Cabernet Sauvignon Berry), *VvSIP1* expression (Fig. 3.2F) did not change after treatments with salt (150 mM NaCl) and osmotic stresses (2% (w/v) PEG), as well as after elicitation with the stress-related hormones abscisic acid (150 µM) and salicylic acid (150 µM). These stress conditions have been reported to induce physiological changes in plant cells.

In contrast, *VvSIP1* transcript levels were significantly increased after an overnight incubation at 37ºC, while the expression of *VvGPT* (Vitis vinifera Glucose-Pi Transporter) decreased in the same experimental conditions (Fig. 3.3; negative control). Heat seems to

be a positive signal for the expression of aquaporins, because plasma membrane *VvPIP2;2* and tonoplast *VvTIP1;1* were also upregulated (Fig. 3.4).

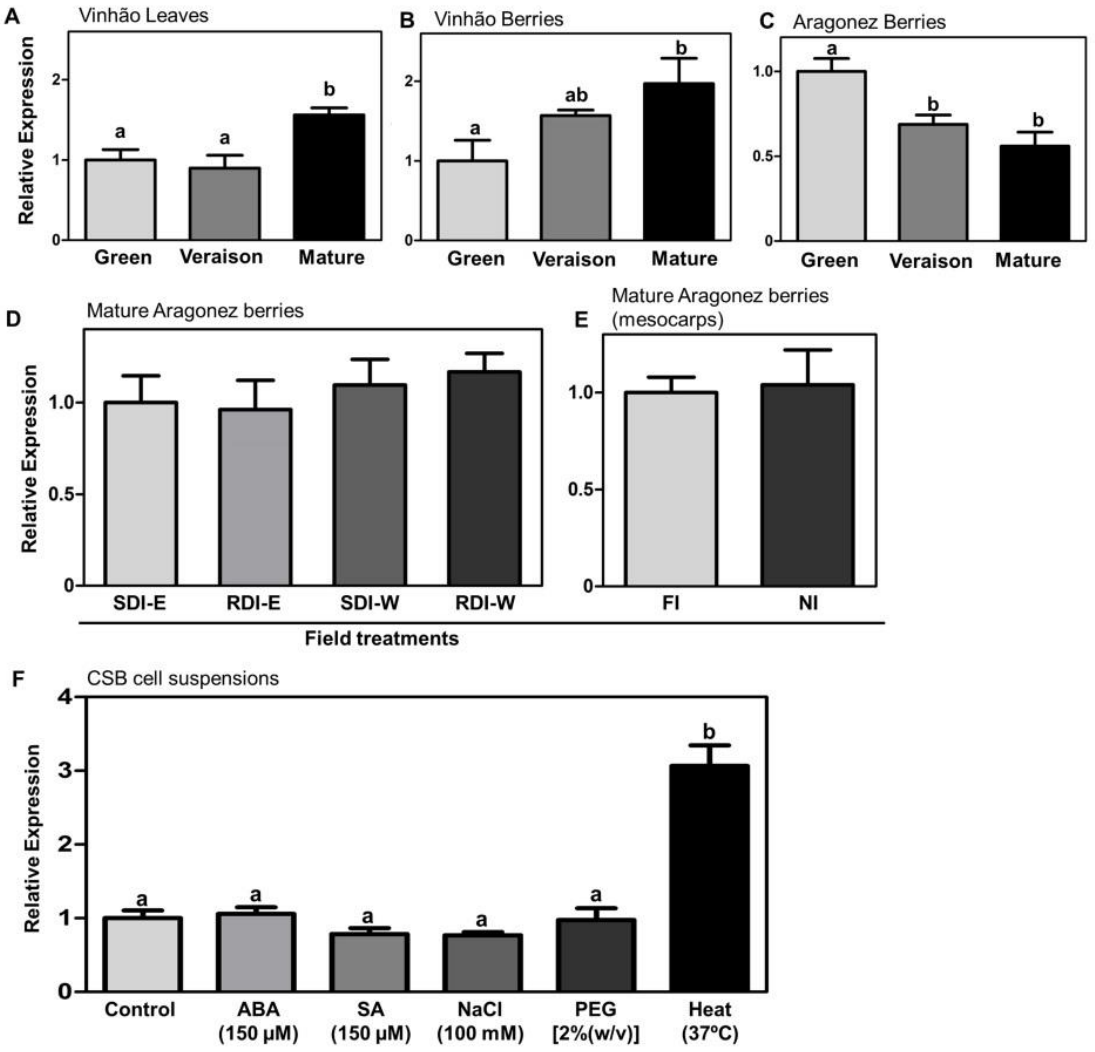

Figure 3.2 VvSIP1 expression determined by RT-qPCR. Transcript levels in leaves (A) and berries (B) from cv. Vinhão and cv. Aragonez (C) during development. *VvSIP1* expression in mature berries from cv. Aragonez under different irrigation regimes and sun exposures (D, E). Expression of *VvSIP1* in cultured cells in response to ABA and SA, and salt, osmotic and heat stresses. Results indicate mean ± SD of three independent experiments. Letters denote significant differences.

3.2.3 Subcellular localization of VvSIP1

The subcellular localization of VvSIP1-RFP was studied after transient expression in tobacco epidermal cells. Fig. 3.5 shows that VvSIP1-RFP co-localized with the ER marker GFP-HDEL (Batoko *et al.*, 2000). This reticular nature of the ER of tobacco cells has been clearly shown in other reports (Más and Beachy, 1999). VvSIP1 also localized in

yeast internal membranes resembling the ER after transformation with *VvSIP1-GFP* (Fig. 3.6A). Western-blot analysis with anti-ZmSIP and anti-calreticulin antibodies confirmed that VvSIP1 co-purified with the marker calreticulin, further corroborating that VvSIP1 is localized at the ER of transformed yeast.

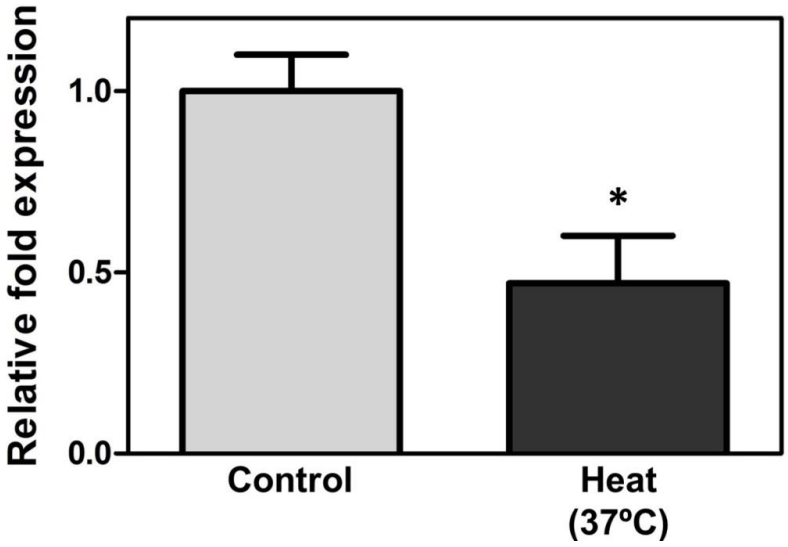

Figure 3.3 *VvGPT* expression determined by RT-PCR in CSB (Cabernet Sauvignon Berry) suspension cells incubated overnight at 37ºC and in control cells incubated at 23ºC (for details see material and methods). Results indicate mean ± SEM of three independent experiments. Asterisks denote significant differences compared to the control: * = $P \leq 0.01$.

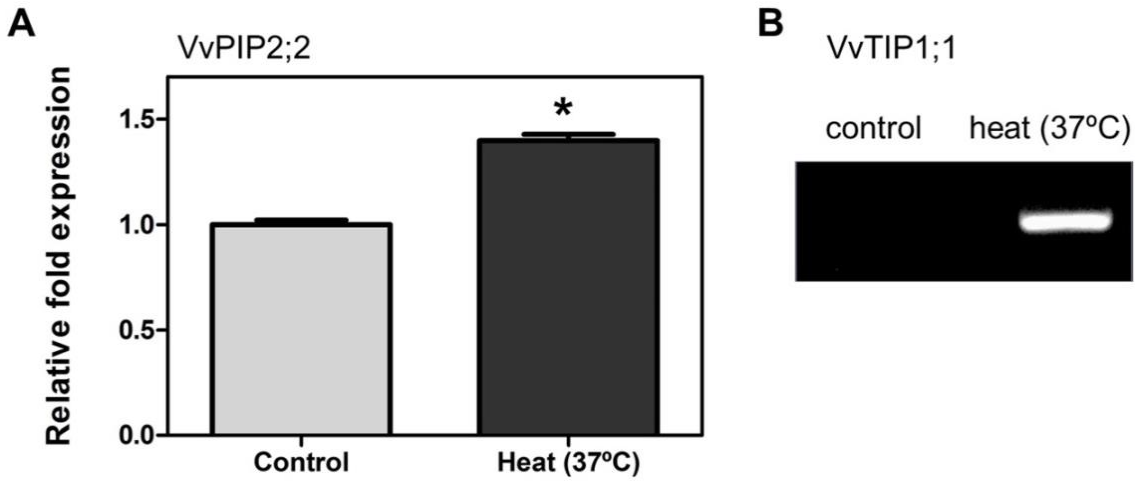

Figure 3.4 *VvPIP2;2* and *VvTIP1;1* expression determined by RT-PCR in (Cabernet Sauvignon Berry) suspension cells and incubated overnight at 37ºC and in control cells incubated at 23ºC (for details see material and methods). Results indicate mean ± SEM of three independent experiments. Asterisks denote significant differences compared to the control: * = $P \leq 0.05$.

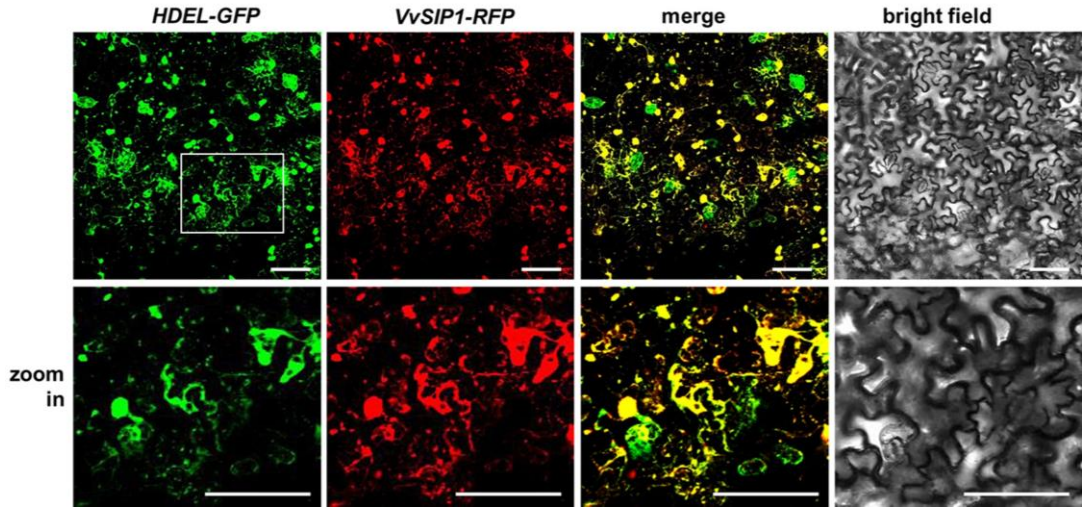

Figure 3.5 Subcellular localization of VvSIP1;1 in tobacco. Transgenic plants expressing the ER marker GFP-HDEL (Batoko *et al*., 2000) were infiltrated with *Agrobacterium* strains containing the *pH7RWG2-VvSIP1-RFP* plasmid. Images were acquired two days after infiltration using a confocal microscope and showed the green fluorescence (GFP-HDEL), red fluorescence (VvSIP1;1-RFP) and the overlap of fluorescence signals (merge). White box zoom in; bar = 100 µm.

3.2.4 Water transport by VvSIP1

The osmotic permeability coefficient (P_f) of *Xenopus* oocytes injected with *VvSIP1* cRNA did not increase, contrary to the P_f of the positive control cells injected with tobacco *NtPIP2;1* cRNA (Fig. 3.7). These results suggest that VvSIP1 is not correctly targeted to the plasma membrane of oocytes or that it is inactive.

To study VvSIP1 function, ER vesicles were isolated from yeast cells expressing *VvSIP1*, and its water permeability monitored by stopped-flow light-scattering spectrophotometry. QELS analysis showed that the vesicle size in all batches was homogeneous. Unimodal distributions were observed with a mean hydrodynamic diameter of 379 ± 65 nm (n = 8) (not shown). To analyze VvSIP1 activity, vesicles were challenged with a hypertonic mannitol solution. The change in the light scatter signal due to water efflux was used to calculate the P_f and the activation energy (E_a) of water transport. As shown in Fig. 3.8A, the shrinking rate of ER vesicles from *VvSIP1* expressing yeast cells was twice as high as the control (Table 3.1). The increase in water permeability was consistent with the decrease in E_a (Fig. 3.8B; Table 3.1) clearly indicating the involvement of protein mediated water diffusion.

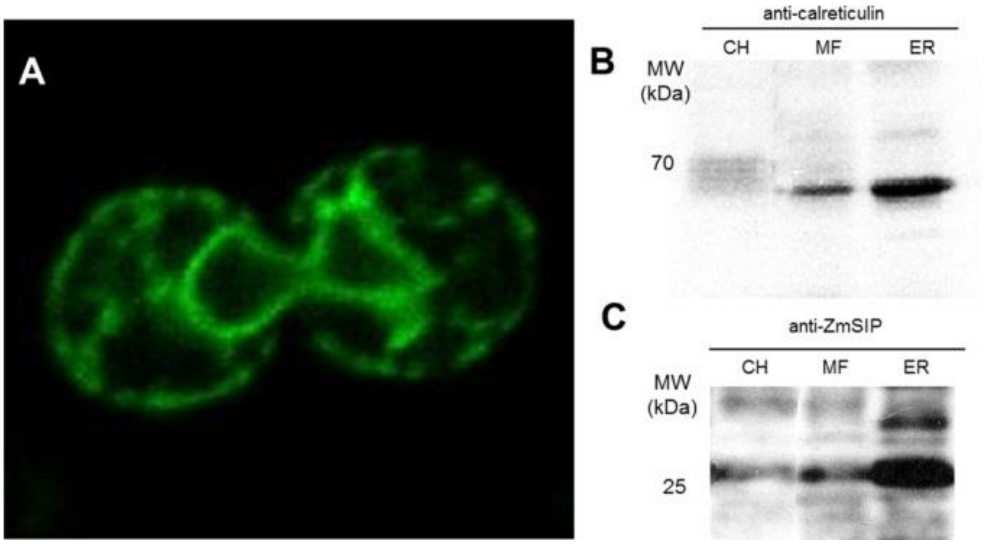

Figure 3.6 Subcellular localization of VvSIP1 in yeast. Cells were transformed with the *pUG35-VvSIP1-GFP* plasmid and observed under the confocal microscope (A). Membrane fractions from the crude homogenate (CH), microsomal fraction (MF) and endoplasmic reticulum (ER) were subjected to immunoblot with anti-calreticulin (B) and anti-ZmSIP (C) antibodies to study both ER and VvSIP1 enrichment.

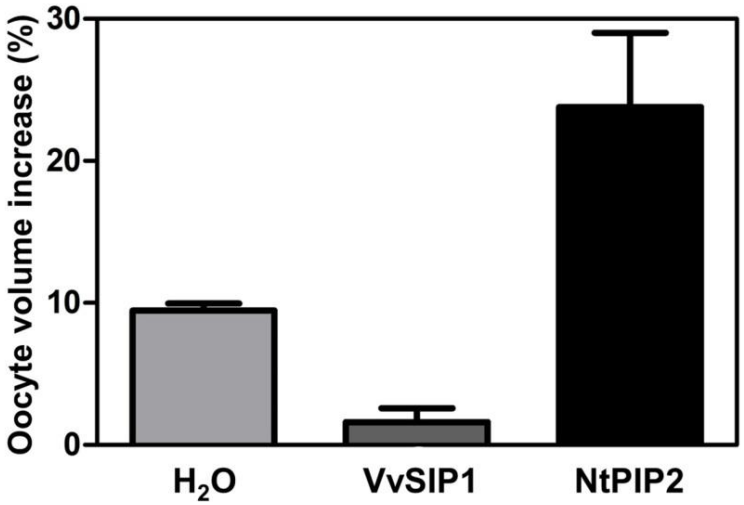

Figure 3.7 Study of aquaporin transport activity in *Xenopus* oocytes 2 days after injection of *NtPIP2;1* and *VvSIP1* cRNAs. Volume changes for individual oocytes were recorded after immersion in hyposmotic solutions. Control oocytes were injected with water. Results are the means ± SD of at least five cells.

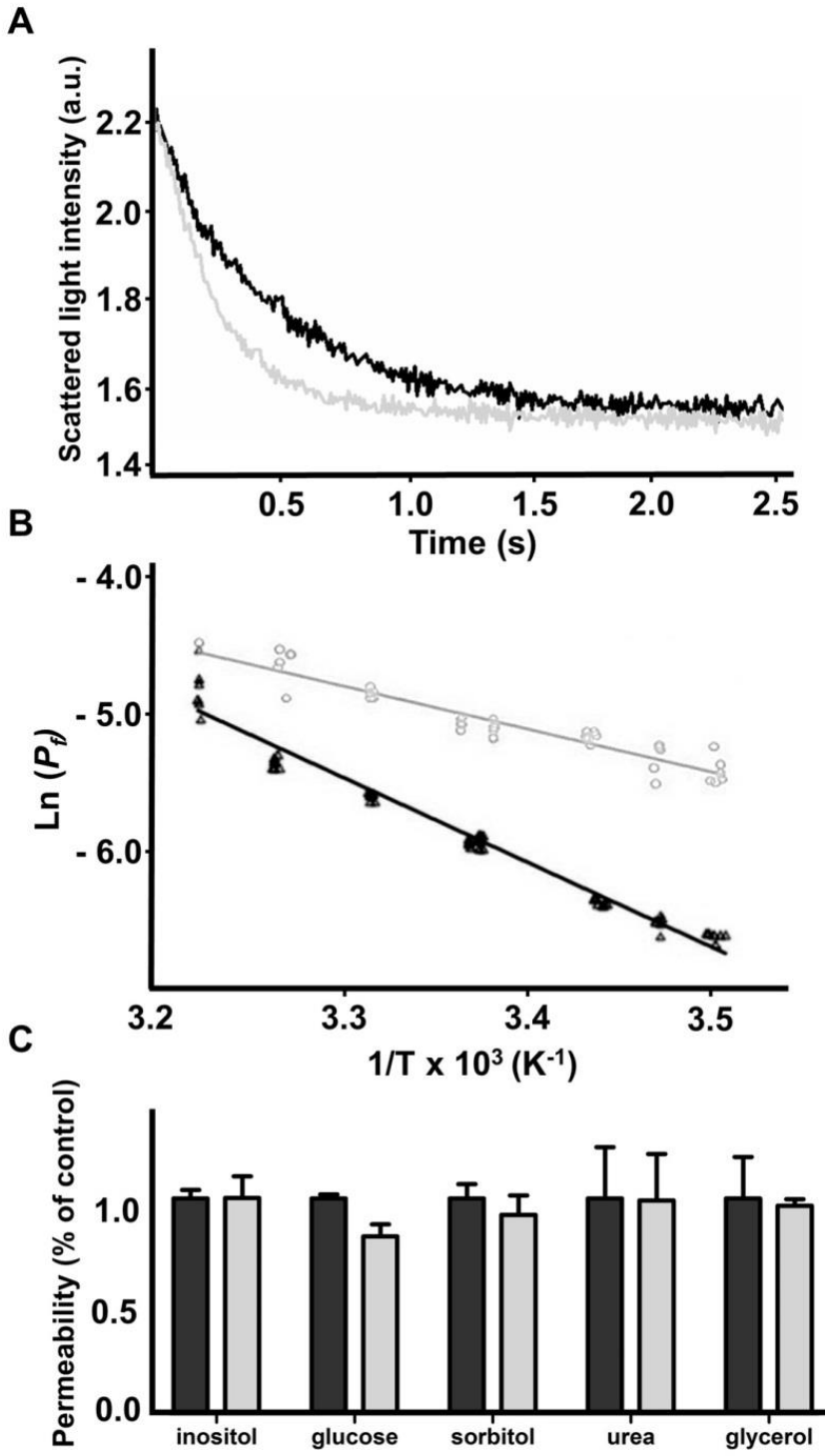

Figure 3.8 Stopped-flow experiment for evaluation of the water permeability in ER vesicles. Normalized scattered light intensity obtained from stopped-flow experiments with ER vesicles purified from yeast cells transformed with *pYESDES52-VvSIP1* (grey) or the empty vector (black) and suddenly exposed to an osmotic gradient of 120 mOsM with an impermeant solute (A) and the corresponding Arrhenius plots (B) used to calculate E_a. To test VvSIP1 specificity for water (C), mannitol was replaced by several solutes (glycerol, urea, glucose, sorbitol and inositol) with the same osmotic potential.

		P_f (10^{-3} cm s^{-1})	E_a (kcal mol^{-1})
ER vesicles	Empty vector	1.99 ± 0.23	13.7 ± 2.6
	VvSIP1	5.09 ± 0.77*	6.4 ± 1.5*
Liposomes	Empty	3.8 ± 0.1 x 10^{-1}	16.6 ± 0.5
	Proteoliposomes (1/50)	5.0 ± 0.4 x 10^{-1}*	12.2 ± 0.7*

Table 3.1 Permeability (P_f) and activation energy (E_a) for water transport in ER membranes and liposomes obtained by stopped-flow (for details see Material and Methods). Asterisks denote significant differences compared to the control: * = P ≤ 0.01

To purify VvSIP1, yeast cells were transformed with the construct *pYesDes52-VvSIP1-6his* followed by the purification of the ER fraction. Approximately, 7 mg of total ER protein was obtained from 1.5 L yeast culture at OD_{640}=1.5. After solubilization with 2% lysophosphatidylcholine at 1/10 protein to detergent ratio, VvSIP1 was eluted from the Ni-NTA column with 300 mM imidazole. Western blot analysis with the anti-ZmSIP1 antibody confirmed that VvSIP1 was purified to homogeneity (Fig. 3.9). In addition to a main band with a molecular mass of ~26 kDa, corresponding to the aquaporin monomer, a second band with ~52 kDa was detected, which probably corresponds to a VvSIP1 dimeric assembly (Bienert *et al*. 2012). Finally, a smaller band (~20 kDa) was also detected in fractions #3 and #4 that could correspond to VvSIP1 partially degraded. The preparation of phosphatidylethanolamine proteoliposomes was optimized for low protein to lipid ratios (1/50 lipid to protein ratio) to avoid the use of high amounts of purified protein.

Flow cytometry analysis showed that proteoliposomes formed a homogenous population and stained positively when loaded with the fluorescent sugar 2-NBDG, suggesting that sealed vesicles were formed, which is a prerequisite for transport experiments (Fig. 3.10). To confirm the water transport activity mediated by VvSIP1, the shrinkage rate of proteoliposomes resuspended in a hypertonic medium was assayed by stopped flow. These proteoliposomes displayed higher water transport activity and lower E_a than empty liposomes (Table 3.1), confirming that VvSIP1 is able to facilitate water diffusion.

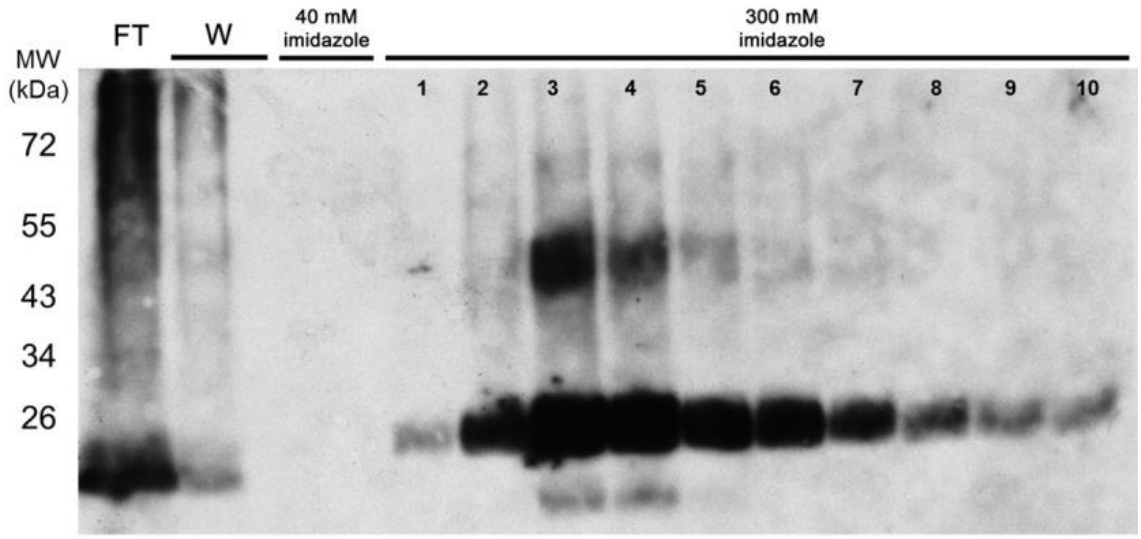

Figure 3.9 Purification of VvSIP1 from *S. cerevisiae*. ER membranes from yeast transformed with *pYESDES52-VvSIP1-6his* were isolated, solubilized with 2% LPC (w/v) at a protein:detergent ratio of 1/10 and purified in a Ni-NTA agarose column (for details see Material and Methods). VvSIP1 monomer (~26 kDa) and dimeric (~52) assembly can be observed. FT, flow-through of the column; W, eluates after washing the column. Eluates after addition of 300 mM imidazole (1-10).

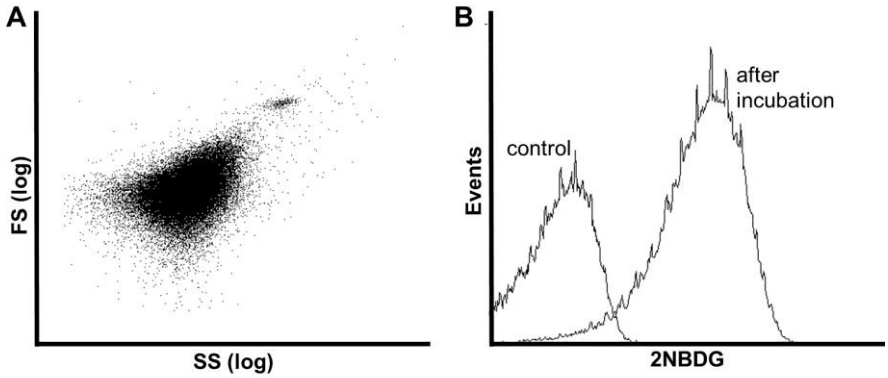

Figure 3.10 Flow cytometry analysis of phosphatidylethanolamine liposomes showing a homogeneous population (A) able to accumulate the fluorescent sugar analog 2-NBDG (B).

3.3 Discussion

3.3.1 Comparison of VvSIP1 to other SIP1 aquaporins

Three members of the SIP subfamily were found in *Arabidopsis* (SIP1;1, SIP1;2, and SIP2;1) (Johanson *et al*., 2001) and maize (Chaumont *et al*., 2001), and two in rice (OsSIP1;1 and OsSIP2;1) (Sakurai *et al*., 2005) and grape (VvSIP1;1 and VvSIP2;1)

(Fouquet *et al*. 2008). SIPs have also been described in *Populus trichocarpa* (Gupta and Sankararamakrishnan, 2009), the moss *P. patens* (Danielson and Johanson, 2008), and a putative ER aquaporin was described for the first time in the arbuscular mycorrhizal fungi *Glomus intraradices* (Aroca *et al*., 2009). As shown in Fig. 4.1, VvSIP1 amino acid sequence has a high degree of similarity with SIP1 aquaporins from monocots, dicots and moss. In particular, all the sequences analysed share R3 and R4 residues of the Ar/R filter, except AtSIP1;1 and AtSIP1;2 where asparagine is replaced by isoleucine in R4, and all the sequences contain the motif AFGWAYI in the loop E. The importance of the loop E for the oligomerization of aquaporins was already shown (Fetter *et al*., 2003; Duchesne *et al*., 2002), and a single amino acid substitution in the Loop E of AQP11 is responsible for a mice lethal phenotype (Tchekneva *et al*., 2008). Nonetheless, there is still little information on the oligomerization of intracellular aquaporins.

Three types of ER retention signals were identified at the C-termini of transmembrane proteins: dihydrophobic, diacidic and dibasic (reviewed by Barlowe, 2003; Giraudo and Maccioni, 2003). Interestingly, a dihydrophobic motif (LF) and a dibasic signal (KQKK) are present in the C-termini of VvSIP1, but their role in ER retention remains to be determined. The presence of a sequence rich in positively charged amino acids is a common feature of SIP aquaporins (reviewed by Gomes *et al*., 2009).

3.3.2 VvSIP1 co-localizes at the ER

So far, only one experimental study was dedicated to SIP localization and function (Ishikawa *et al*. 2005). AtSIP1;1, AtSIP1;2 and AtSIP2;1 are localized at the ER of *Arabidopsis* protoplasts. Likewise, VvSIP1 clearly co-localized at the ER of tobacco epidermal cells (Fig. 3.3). This ER localization was further demonstrated in yeast cells expressing *VvSIP1-GFP* and by ER purification followed by western blotting with an anti-ZmSIP1 (Fig. 3.4). A similar approach was performed to localize AtSIPs (Ishikawa *et al*., 2005), and mouse AQP11 and AQP12 (Itoh *et al*., 2005; Morishita *et al*., 2005) at the ER.

3.3.3 VvSIP1 facilitate membrane water diffusion in ER vesicles and in proteoliposomes

Oocytes have been often used as a tool to study the water channel activity of aquaporins, especially PIPs and TIPs (Gomes *et al*., 2009), but, in the present study, oocytes injected with *VvSIP1;1* cRNA did not show increased membrane water permeability (Fig. 3.5). This could be due to a failure in VvSIP1 protein expression or trafficking to the plasma membrane, which might indicate that this cell model is not suitable to study SIP aquaporins. However, we cannot exclude that VvSIP1 was targeted to the plasma membrane but the protein was inactive or was able to facilitate the diffusion of other substrates rather than water. In agreement, oocytes injected with the intracellular AQP11 did not show water transport although the protein was apparently targeted to the plasma membrane (Gorelick *et al*., 2006), contrarily to what was observed previously (Morishita *et al*., 2005).

To further clarify the function of VvSIP1, water transport activity was monitored by stopped-flow light-scattering spectrophotometry in ER membrane vesicles isolated from yeast cells expressing *VvSIP1* (Fig. 3.6). The observed increase of water permeability, together with the decrease of activation energy for water permeation, strongly supports that VvSIP1 mediates water fluxes. Furthermore, we showed that VvSIP1 does not transport other solutes, including urea, glycerol, glucose, inositol and sorbitol, suggesting that it is specific for water. In crude membranes from AtSIP expressing yeasts cells, AtSIP1;1 and AtSIP1;2, but not AtSIP2;1, also displayed water transport activity (Ishikawa *et al*., 2005). However, it was not excluded that AtSIP2;1 could facilitate water diffusion after heterodimerization with other SIPs.

Some AQPs, but none SIP member, were purified to homogeneity and reconstituted in liposomes (Zeidel *et al*., 1992; Tanimura *et al*., 2009; Yakata *et al*., 2007; Liu *et al*., 2006). Recently, the intracellular aquaporin AQP11 from mouse was shown to exhibit water channel activity after its reconstitution in proteoliposomes followed by stopped-flow measurements (Yakata *et al*., 2006). Here, we reported the solubilization of VvSIP1-6his from yeast ER membranes using lysophosphatidylcholine, its purification to homogeneity through a Ni-NTA column and its incorporation into phosphatidylethanolamine proteoliposomes by detergent dialysis (Fig. 3.7). As observed in ER vesicles, stopped-flow

studies with proteoliposomes (Table 3.1) suggested that VvSIP1 plays a role as an intracellular water channel.

3.3.4 VvSIP1 is not responsive to different vine water regimes and berry sun exposures

As already mentioned, *AtSIP1;1* and *AtSIP1;2* are expressed in a variety of *Arabidopsis* tissues, but low expression levels were detected in leaves and fruits (Ishikawa *et al*., 2005). In grapevine, expression of *VvSIP1* in leaves and berries of cv. Vinhão increased during development, peaking at the mature phase (Fig. 3.2A and B). Contrarily, *VvSIP1* expression in cv. Aragonez decreased during berry development (Fig. 3.2C), suggesting *VvSIP1* expression pattern may depend on the variety or be affected by the terroir.

It has been shown that water deficit is one of many environmental conditions that regulate plant aquaporins (Tyerman *et al*., 2002; Hachez *et al*., 2008). This is particularly relevant since grape berries are highly susceptible to excessive sun exposure and its quality is affected by temperature and water availability (Kliewer and Torres, 1972; Spayd *et al*., 2002; Pillet *et al*., 2012). Generally, plants modulate the expression of plasma membrane and tonoplast aquaporins in response to drought (Tyerman *et al*., 2002). In the present study, the transcript levels of VvSIP1 did not increase significantly in berries from vines subjected to water stress and in berries from western-oriented clusters (Fig. 3.2D and E), suggesting that *VvSIP1* does not play an important role in stress response under the field conditions tested. Contrarily, in *in vitro* cultures the expression of *VvSIP1* (Fig. 3.2D), *VvPIP2:2* and *VvTIP1;1* (Figure 3.4) was upregulated after an overnight incubation at 37ºC. This treatment did not affect the viability of the cells and induced HSPs. However, the cells kept their morphology substantially unchanged with a prominent central vacuole (not shown). Thus, the observed transcription profile of *AQPs* could be involved in the regulation of the intracellular water status under heat stress. In agreement, we cannot exclude that more extreme temperature conditions in the field can also promote the increase of *VvSIP1* expression and other *AQP* members in grapevine tissues.

Besides regulation at the transcriptional level, several factors may affect the gating of aquaporins, including phosphorylation, heteromerization, pH, Ca^{2+}, pressure, solute

gradients, and temperature (Chaumont *et al*., 2005). Post-transcriptional regulation of aquaporins by protonation was shown in AtPIP2;2 in response to anoxia (Tournaire-Roux *et al*., 2003). In this regard, the possible involvement of post-transcriptional regulation of VvSIP1 deserves further investigation.

Much work is also needed to clarify the specific physiological role of SIPs in the ER membrane. In mammals, it was observed that *AQP11*-knockout mice died before weaning due to advanced renal failure, and two important abnormalities were detected: vacuolization and cyst formation in the kidney proximal tubule. Because the observed vacuoles apparently originated from the ER, it was suggested that *AQP11* might have some role in vesicle homeostasis (Morishita *et al*., 2005). In plants, the analysis of *Arabidopsis* mutants followed by complementation experiments is a major tool for the assignment of a physiological role to a gene from a non-model plant. However, in preliminary experiments with T-DNA insertion mutants of *AtSIP1;1* and *AtSIP2;1* visible modifications in growth, morphology and stress responses were not observed (Maeshima and Ishikawa, 2008). In this regard, a thoroughly exploitation of phenotypes at the cellular level, including the study of ER ultrastructure, could provide important information on the role of SIPs.

3.3. Material and methods

3.3.1 Plant material

Field-grown grapevines (*Vitis vinifera* L.) of cv. Aragonez and Vinhão were used in the present study. Cv. Aragonez vines were collected from commercial vineyards in Reguengos de Monsaraz and Estremoz (south of Portugal) and cv. Vinhão from a commercial vineyard in Guimarães (north of Portugal). Rows were oriented north-south. Expression studies were also performed in 3-months old grapevine plantlets of the cv. Trincadeira growing *in vitro*.

The cv. Aragonez vines cultivated in Reguengos de Monsaraz were subjected to RDI (regulated deficit irrigation) and SDI (sustained deficit irrigation), in the scope of the European Project Innovine. RDI vines were supplied with 50% less water than SDI vines, and berries from SDI were collected from green to mature phase to study VvSIP1 expression during maturation. At the mature stage, the following values for leaf water

potential were measured: -0.7 MPa (RDI) and -0.5 MPa (SDI). Also, the oscillations in berry temperature were continuously monitored. Average daily maximum temperatures in grapes from clusters exposed to west (RDI-W and SDI-W) were 4-5ºC higher than in east–exposed clusters (RDI-E and SDI-E) because ambient temperatures are higher after mid-day. The expression of *VvSIP1* was also studied in berries from SDI-E, RDI-E, SDI-W and RDI-W.

The cv. Aragonez vines in Estremoz were subjected to full irrigation (FI, 100% evapotranspiration, ETc) and non-irrigation (NI, rain fed only). Watering was applied according to crop ETc and soil water content. Grape berry clusters from 4-6 plants, located in three different rows, were collected, and grapes from three different berry clusters per plant were harvested and immediately frozen in liquid nitrogen. Berries and leaves were sampled at green (4 WAF), veraison (9 WAF) and mature (15 WAF) stages of berry development and ripening.

Cells of *V. vinifera* L. (CSB, Cabernet Sauvignon Berry) were cultivated in liquid medium according to Decendit *et al*. (1996), and maintained in 250 mL flasks on a rotatory shaker at 100 rpm in the dark, at 25ºC. The mineral medium was supplemented with 2% (w/v) sucrose. Cells were subcultured weekly by transferring 10 mL aliquots into 40 mL of fresh medium. In order to study the effect of different treatments on *VvSIP1* expression, 5 mL aliquots were incubated overnight with 100 mM NaCl, PEG 2% (w/v), 150 µM ABA (Gagné *et al*., 2011) and 150 µM SA (Laura *et al*., 2007) at 23ºC. The effect of heat was evaluated after an overnight incubation at 38ºC. Cells were immediately frozen in liquid nitrogen and stored at -80ºC.

3.3.2 In silico studies

SIP sequences were obtained from the database of the National Center of Biotechnology (NCBI). Protein alignment was performed by Prankster and the result visualized in Genedoc (Nicholas *et al*., 1997). The 3D representation was performed by I-TASSER (Zhang, 2008) using SoPIP2;1 as a template (Thornroth-Horesfiel *et al*., 2006). The resulting 3D model was visualized using the PyMol software (DeLano, 2002).

3.3.3 RNA isolation from grape berries and leaves

Total RNA was isolated from grape berries and leaves with QIAGEN RNeasy Plant Mini Kit following manufacturer's instructions, except that the extraction buffer was changed to 2% CTAB, 2% soluble polyvinylpyrrolidone (PVP) K-30, 300 mM Tris HCl (pH 8.0), 25 mM EDTA, 2.0 M NaCl and 2% (v/v) β-mercaptoethanol. After an in column DNAse treatment, the RNA integrity was checked in a 1% agarose gel, and first strand cDNA synthesis was performed with the LongRange 2Step RT-PCR (QIAGEN), following the manufacturer's instructions.

3.3.4 Subcellular localization of VvSIP1

The *pH7RWG2-VvSIP1-RFP* construct was obtained using the GATEWAY (Qiagen) recombination technology. Briefly, the recombination sequences (forward: GGG GAC AAG TTT GTA CAA AAA AGC AGG CT; reverse: GGG GAC CAC TTT GTA CAA GAA AGC TGG GT) were introduced by PCR (primers are shown in Table 3.2) in the *VvSIP1* cDNA without stop codon and the fragment was recombined into the entry vector *pDONR221* using the BP clonase enzyme. The *VvSIP1* cDNA was recombined into the *pH7RWG2* vector by the LR clonase enzyme, introduced in *Agrobacterium tumefaciens* (GV3101), and transient transformation of tobacco (*Nicotiana tabacum*) leaf epidermal cells constitutively expressing GFP-HDEL (Batoko *et al*., 2000) was performed according to Sparkes *et al*. (2006). Bacterial cells were cultivated overnight in liquid LB medium up to the exponential-stationary phase and then diluted to $OD_{600nm} = 0.1$ with infiltration buffer (50 mM MES pH 5.6, 2 mM Na_3PO4, 0.5% glucose and 100 μM acetosyringone). Diluted cells were cultivated again until the culture reached an $OD_{600nm} = 0.2$. Four-weeks-old tobacco plants were infiltrated with the bacterial cultures and leaf discs were examined under the confocal microscope 3 days after.

VvSIP1 was cloned into *pUG35-GFP* behind the cDNA encoding *GFP*. Restriction sites for Bam HI were introduced by PCR (primers are shown in Table 3.2), and the fragment was cloned into *pUG35-GFP* vector after digestion with BamHI. *VvSIP1* expression was regulated by the inducible *MET25* promoter. *Saccharomyces cerevisiae* strain CEN.PK 135-5D (ura-) was transformed with the *pUG35-SIP1-GFP* vector with the LiAc/SS-DNA/PEG method (Gietz and Woods, 2002). To study fluorescence localization,

transformed yeast cells were cultivated overnight in YNB minimal medium without methionine and uracil, washed with deionized water, and observed with a Zeiss 710 confocal microscope (Carl Zeiss, Jena, Germany), with excitation at 488 nm and detection between 506 and 538 nm.

	Primer forward (5'-3')	Primer reverse (5'-3')
VvSIP1-GFP and pXT7-*VvSIP*	GCAGATCTATGGGTGTAATAAAGGC	GCACCGGTGCTTTCTTCTGCTTTG
pYES-DEST-VvSIP1	GGGGACAAGTTTGTACAAAAAAGC AGGCTGGAGGATGGGTGTAATAAA GGCGGCGATTG	GGGGACCACTTTGTACAAGAAAG CTGGGTCTCAGCTTTCTTCTGCTTT GTTGGTGCTGG
pYES-DEST-VvSIP1-6his	GGGGACAAGTTTGTACAAAAAAGC AGGCTGGAGGATGGGTGTAATAAA GGCGGCGATTG	GGGGACCACTTTGTACAAGAAAG CTGGGTCGGCTTTCTTCTGCTTTG TTGGTGCTGG
qVvSIP1	GTTTTCCTGCTCAGGCAGCTG	GCAACCATGTCTTCAATACTGGAC
q*VvGAPDH*	CACGGTCAGTGGAAGCATCATGAA CTC	CCTTGTCAGTGAACACACCAGTTG ACTC
q*VvGPT*	TCTTTCCTGTTGCAGTAGCTCA	CAGTGCGCAGCCTCCAATAA
RT-*VvPIP2;2*	TACCACCAGTACATACTGAGAGCAG	TATGGAACAAAAGATCCAAAGAA AG
RT-*VvTIP1;1*	AGGGGAACTTGGGCATTATT	CCCAAAGAAAAGCCCCTAAT
RT-*VvACT1*	GTGCCTGCCATGTATGTTGCCATTC AGGCTG	GCTCTTTGCAGTTTCCAGCTCTTG CTCGTAGTCAA

Table 3.2 Primers used in this study

3.3.5 Real-Time PCR studies

Quantitative real-time PCR reactions were prepared with a QuantiTect SYBR Green PCR Kit (QIAGEN) and were performed in a CFX96 Real-Time Detection System (Bio-Rad), at an annealing temperature of 50ºC. RNA and cDNA were obtained as mentioned above. Experiments were done in triplicate (biological replicates) with the software Bio-Rad CFX Manager (Bio-Rad), using *VvGAPDH* as internal control. After each run, melting curves were performed to check for unspecific and primer dimer amplification. The primers used to study the expression of *VvSIP1*, *VvGAPDH* and *VvGPT* are shown in Table 3.2.

3.3.6 Semi quantitative PCR studies

Semi quantitative PCR was performed with HotStarTaq DNA Polymerase (Qiagen) to study the effect of heat on aquaporin expression. Briefly, all the primers used were previously tested to determine the exponential phase of the amplification curve for each condition. Three reactions for each condition were run in the same gel and quantified with the software Quantity One (Biorad). The primers used for *VvGPT*, *VvPIP2;2*, *VvTIP1;1* and *VvACT1* are shown in Table 3.2.

3.3.7 Isolation of yeast endoplasmic reticulum

The recombination sequences of GATEWAY technology were introduced in the *VvSIP1* cDNA with the stop codon with the primers shown in Table 3.2. The fragment was introduced in the vector pDONR221, recombined with *pYES-DEST52*, and the resulting vector *pYES-DEST52-VvSIP1* introduced into yeast cells by the method described above. ER enriched vesicles were obtained following the method by Wuestehube and Schekman (1992), which has been routinely used to purify ER membranes from yeasts. Briefly, yeast cells were cultivated overnight in YNB medium without uracil supplemented with 2% galactose, and spheroplasts were obtained by digestion with zymolyase 20T (Rodrigues *et al*. 2013) dissolved in digestion buffer (1.35 M sorbitol, 10 mM citric acid, 30 mM Na_2HPO_4, 1 mM EGTA, pH 7.4). After 45 min of digestion, the spheroplasts were lysed in a Dounce tissue homogenizer in HEPES-lysis buffer (20 mM HEPES, 50 mM potassium acetate, 100 mM sorbitol, 2 mM EDTA, 1mM PMSF, 1 mM DTT, pH 6.8), and a crude membrane fraction was obtained by centrifugation at 18000 g for 15 min at 4ºC. This membrane fraction was resuspended in HEPES-lysis buffer, layered on top of a 1.2/1.5 M discontinuous sucrose gradient and centrifuged at 100000 g for 1 h at 4ºC. The enriched ER membrane fraction was collected from the 1.2/1.5 M sucrose interface, centrifuged at 18000 g for 15 min at 4ºC, and the pellet was resuspended in 100 mM mannitol, 10 mM Tris-HEPES (pH 7.5) and stored at -80ºC. The protein amount was estimated by the Lowry method (Lowry *et al*., 1951). The purity of the ER fraction was checked by immunoblot with an anti-calreticulin antibody.

3.3.8 Functional characterization by stopped flow spectroscopy

Water permeability of membrane vesicles was assessed with the stopped-flow technique (HI-TECH Scientific PQ/SF-53). Experiments were performed at 10 to 37°C to study activation energies. Five runs were usually stored and analyzed in each experimental condition, as described by Soveral *et al*. (1997). Briefly, vesicles resuspended in 100 mM mannitol, 10 mM Tris-HEPES (pH 7.5) (0.1 mL, 0.4 mg protein mL^{-1}) were mixed with an equal amount of hyperosmotic mannitol solutions at 23ºC to produce an inwardly directed gradient of impermeant solute (osmotic gradient 120 mOsmol). The kinetics of vesicle shrinkage was measured from the time course of 90° scattered light intensity at 400 nm until a stable light scatter signal was attained. The osmotic water permeability coefficient (P_f) was estimated by fitting the light scatter signal to a single exponential curve with the equation $P_f = k(V_o/A)(1/V_w/(osm_{out})_\infty)$, where V_w is the molar volume of water, V_o/A is the initial volume to area ratio of the vesicle population, and $(osm_{out})_\infty$ is the final medium osmolarity after the application of the osmotic gradient. The osmolarity of each solution was determined from freezing point depression by a semi-micro osmometer (Knauer GmbH, Germany). The activation energy of water transport was obtained from the slope of an Arrhenius plot (ln P_f as a function of 1/T) multiplied by the gas constant R. Vesicle size (initial volume) was determined by quasi-elastic light scattering (QELS) by a particle sizer (BI-90 Brookhaven Instruments) as described by Soveral *et al*. (1997). To determine VvSIP1 specificity for water, mannitol was replaced by several solutes (glycerol, urea, glucose, sorbitol and inositol) with the same osmotic potential, and solute uptake was measured as stated above.

3.3.9 VvSIP1 purification and reconstitution into phosphatidylethanolamine liposomes

The construct *pYES-DEST52-VvSIP1-His-tag* was obtained by GATEWAY recombination. Briefly, the *pDONR221-VvSIP1* without stop codon (see above) was recombined with *pYES-DEST52-His-tag* in front of *GAL1* promoter, and behind 6 histidines. This vector was used to transform *S. cerevisiae*, and purified ER membranes were obtained as described above. The sample was diluted to 0.2 mg protein mL^{-1} in Na_2CO_3, incubated for 30 min at 4ºC, and centrifuged for 40 min at 50000 g. The pellet

was washed with ice-cold water and resuspended in purification buffer (20 mM imidazole, 100 mM KCl, 10% (w/v) glycerol, pH 7.5) before protein solubilization. Three detergents were tested at different concentrations (1 and 2 % (w/v)) and protein:lipid ratios (1/10 and 1/20): octyl-glucoside (OTG), *n*-dodecyl *β*-D-maltoside (DDM) and lysophosphatidylcholine (LPC). The best results were obtained with 2% LPC at 1/10 protein:lipid ratio after incubation for 2 h at 42ºC under shaking. Non-digested proteins were pellet at 100000 g for 30 min at 4ºC. The purification step was started mixing the supernatant with Ni-NTA agarose (Qiagen), and, after incubation for 2 h at 37ºC under shaking, the mixture was loaded into an empty Bio-Spin Chromatography Column (Bio-Rad). The column was sequentially eluted with the following buffers: purification buffer supplemented with 0.05 % (w/v) LPC, 40 mM imidazole buffer (40 mM imidazole, 10% glycerol (v/v), 100 mM KCl, 0.05 % (w/v) LPC, pH 7.5), and 300 mM imidazole buffer (300 mM imidazole, 10% glycerol (v/v), 100 mM KCl, 0.05 % (w/v) LPC, pH 7.5). In each eluate, the purity of VvSIP1 was checked by western-blot with an anti-ZmSIP1 antibody raised in maize against the C-terminal peptide of ZmSIP1;1 (FLPPAPKPKTKKA). To reconstitute VvSIP1 in artificial vesicles, phosphatidylethanolamine lipids were mixed by sonication in a buffer with 100 mM mannitol, 10 mM Tris-HEPES (pH 7.5), and 2% (w/v) OTG before addition of the purified protein (protein:lipid ratio of 1/50). After 30 min incubation on ice, the mixture was dialyzed against 100 mM mannitol, 10 mM Tris-HEPES (pH 7.5) to remove LPC, and the proteoliposomes were frozen in liquid nitrogen and stored at -80 until used (Gerós *et al*., 1996).

3.3.10 Western blot analysis

Protein samples obtained as described above were separated on 10% acrylamide gels as described by Laemmli (1970). Proteins were transferred to a nitrocellulose membrane during 1 h 30 min at 100 V, and were blocked during 1 h in Tris-buffered saline containing 0.1% (v/v) Tween-20 (TBS-T) with 5% (w/v) skimmed milk powder, 1% (w/v) BSA, 0.1% goat serum and 0.05% (v/v) Tween-20. The membranes were probed against ZmSIP1 (1:1000 dilution) and calreticulin (1:10000) (Carqueijeiro *et al*. 2013) during 1 h at room temperature in blocking solution, followed by an incubation with an anti-rabbit peroxidase conjugated antibody (Sigma) at 1:160000 dilution in TBS-T, for 45 min. The immunodetection was accomplished with the chemiluminescent ECL detection substrate (Biorad).

3.3.11 Oocyte injection and permeability assays

NtPIP2;1 and *VvSIP1* cDNAs were cloned into the oocyte expression vector *pXT7* with the primers shown in Table 3.2, and *in vitro* complementary cRNAs were obtained with the Transcript Aid T7 High Yield Transcription Kit (Fisher, Thermo Scientific). *Xenopus laevis* oocytes were isolated and defolliculated by digestion at room temperature for 1.5 h with 4 mg/mL collagenase A in Barth's solution (88 mM NaCl, 1 mM KCl, 2.4 mM $NaHCO_3$, 10 mM Hepes-NaOH, 0.33 mM $Ca(NO_3)_2$, 0.41mM $CaCl_2$, 0.82 mM $MgSO_4$, pH 7.4, and 200 mosm/kg). *In vitro* transcripts or distilled water (50 nL) were injected and the oocytes were incubated at 18ºC in Barth's solution for 2 days. Oocyte swelling was measured by transferring the oocytes to 5-fold diluted Barth's solution and the changes in the cell volume were calculated as described before (Fetter *et al*., 2004).

3.3.12 Flow cytometry

Flow cytometry analysis of proteoliposomes was performed in an Epics XL Beckman Coulter flow cytometer equipped with an argon–ion laser with a beam emitting at 488 nm at 15 mW. Green fluorescence was collected through a 525 nm band-pass filter. Data were analyzed with Flowing Software 2.0 (Rodrigues *et al*., 2013).

3.3.13 Statistical analysis

The results were statistically analyzed by Student's t-test and by Analysis of Variances tests (one-way and two-way ANOVA) using Prism vs. 5 (GraphPad Software, Inc.). Post hocmultiple comparisons were performed using the HSD Tukey. For each condition differences between mean values are identified with different letters or asterisks.

3.3.14 Sequences accession numbers

VvSIP1(DQ086835), VvGPT (GSVIVT00006900001), VvPIP2;2 (EF364436), VvTIP1;1 (DQ834701), MtSIP1;1 (G7JDK7), MtSIP1;2 (G7KYE4), AtSIP1;1 (Q9M8W5), AtSIP1;2 (Q9FK43), ZmSIP1;1 (Q9ATM3), ZmSIP1;2 (Q9ATM2),

OeSIP1;1 (B0L1W3), OeSIP1;2 (B5KGP0), OsSIP1;1 (Q5VR89), PpSIP1;1 (A9RDU1), PpSIP1;2 (A9U3Q2).

3.5 Acknowledgements

This work was supported by European Union Funds (FEDER/COMPETE-Operational Competitiveness Programme and INNOVINE - ref. 311775), by Portuguese national funds (FCT-Portuguese Foundation for Science and Technology) under the project FCOMP-01-0124-FEDER-022692, the research projects PTDC/AGR-AAM/099154/2008 and PTDC/AGR-ALI/100636/2008, the Belgian National Fund for Scientific Research (FNRS), the Interuniversity Attraction Poles Programme-Belgian Science Policy, the "Communauté française de Belgique-Actions de Recherches Concertées" and the Francqui Fundation. HN was supported by a PhD grant no. SFRH/BD/74257/2010 from FCT and MCB was a Research Fellow at the "Fonds pour la Formation à la Recherche dans l'Industrie et dans l'Agriculture". This work also benefited from the networking activities within the European funded COST ACTION FA1106 QualityFruit".

3.6 References

Amiry-Moghaddam M, Lindland H, Zelenin S, Roberg BA, Gundersen BB, Petersen P, Rinvik E, Torgner IA and Ottersen OP. 2005. Brain mitochondria contain aquaporin water channels: evidence for the expression of a short AQP9 isoform in the inner mitochondrial membrane. *FASEB Journal* **9**, 1459-1467.

Bernsel A, Viklund H, Hennerdal A and Elofsson A. 2009. TOPCONS: consensus prediction of membrane protein topology. *Nucleic Acids Research* **37** (Webserver issue), W465-8.

Aroca R, Bago A, Sutka M, Paz JA, Cano C, Amodeo G and Ruiz-Lozano JM. 2009. Expression analysis of the first arbuscular mycorrhizal fungi aquaporin described reveals concerted gene expression between salt-stressed and nonstressed mycelium. *Molecular Plant-Microbe Interaction* **9**, 1169–1178.

Barlowe C. 2003. Signals for COPII-dependent export from the ER: what's the ticket out? *Trends in Cell Biology* **13**, 295-300.

Batoko H, Zheng HQ, Hawes C and Moore I. 2000. A Rab1 GTPase is required for transport between the endoplasmic reticulum and Golgi apparatus and for normal golgi movement in plants. *The Plant Cell* **12**, 2201–2217.

Calamita G, Ferri D, Gena P, Liquori GE, Cavalier A, Thomas D and Svelto M. 2005. The inner mitochondrial membrane has Aquaporin-8 water channels and is highly permeable to water. *Journal of Biological Chemistry* **280**, 17149–17153.

Carqueijeiro I, Noronha H, Duarte P, Gerós H and Sottomayor M. 2013. Vacuolar transport of the medicinal alkaloids from *Catharantus roseus* is mediated by a proton-driven antiport. *Plant Physiology* 162, 1486–1496.

Chaumont F, Barrieu F, Wojcik E, Chrispeels MJ and Jung R. 2001. Aquaporins constitute a large and highly divergent protein family in maize. *Plant Physiology* **125**, 1206–1215.

Chaumont F, Moshelion M and Daniels MJ. 2005. Regulation of plant aquaporin activity. *Biology of the Cell* **97**, 749–764.

Conde A, Diallinas G, Chaumont F, Chaves M and Gerós H. 2010. Transporters, channels or simple diffusion? Dogmas, atypical roles and complexity in transport systems. *The International Journal of Biochemistry & Cell Biology* **42**, 857-868.

Conde C, Silva P, Fontes N, Dias ACP, Tavares RM, Sousa MJ, Agasse A, Delrot S and Gerós H. 2007. Biochemical changes throughout grape berry development and fruit and wine quality. *Food* **1**, 1-22.

Danielson J and Johanson U. 2008. Unexpected complexity of the aquaporin gene family in the moss *Physcomitrella patens*. *BMC Plant Biology* **8**, doi:10.1186/1471-2229-8-45.

DeLano WL. 2002. The PyMOL molecular graphics system. DeLano Scientific, San Carlos, CA, USA. http://www.pymol.org.

Descendit A, Ramawat KG, Waffo P, Deffieux G, Badoc A and Merillon JM. 1996. Anthocyanins, catechins, condensed tanins and piceid production in *Vitis vinifera* cell bioreactor cultures. *Biotechnology Letters* **18**, 659–662.

Duchesne L, Pellerin I, Delemarche C, Deschamps S, Lagrée V, Froger A, Bonnec G, Thomas D and Hubert JF. 2002. Role of C-terminal domain and transmembrane helices 5 and 6 in function and quaternary structure of major intrinsic proteins. *The Journal of Biological Chemistry* **277**, 20598–20604.

Felsenstein J. 2005. PHYLIP (Phylogeny Inference Package) version 3.6. Distributed by the author. Department of Genome Sciences, University of Washington, Seattle.

Fetter K, Van Wilder V, Moshelion M and Chaumont F. 2004. Interactions between plasma membrane aquaporins modulate their water channel activity. *The Plant Cell* **16**, 215–228.

Fouquet R, Leon C, Ollat N, Barrieu F. 2008. Identification of grapevine aquaporins and expression analysis in developing berries. *Plant Cell Reports* **27**, 1541–1550.

Gagné S, Cluzet S, Mérillon J and Gény L (2011) ABA initiates anthocyanin production in grape cell cultures. *Journal of Plant Growth Regulation* **30**, 1-10.

Gasic K, Hernandez A and Korban SS. 2004. RNA extraction from different apple tissues rich in polyphenols and polysaccharides for cDNA library construction. *Plant Molecular Biology Reporter* **22**, 437–437.

Gerós H, Cássio F and Leão C. 1996. Reconstitution of lactate proton symport activity in plasma membrane vesicles from the yeast Candida utilis. *Yeast* **12**, 1263-1272.

Gietz RD and Woods RA. 2002. Transformation of yeast by the Liac/SS carrier DNA/PEG method. *Methods in Enzymology* **350**, 87-96.

Giraudo GC and Maccioni HJF. 2003. Endoplasmic reticulum export of glycosyl transferases depends on interaction of a cytoplasmic dibasic motif with Sar1. *Molecular Biology of the Cell* **14**, 3753–3766.

Gomes D, Agasse A, Thiébaud P, Delrot S, Gerós H, Chaumont F. 2009. Aquaporins are multifunctional water and solute transporters highly divergent in living organisms. *Biochimica et Biophysica Acta - Biomembranes* **1788**, 1213–1228.

Gorelick DA, Praetorius J, Tsunerari T, Nielsen S and Agre P .2006. Aquaporin-11: A channel protein lacking apparent transport function expressed in brain. *BMC Biochemistry***,** doi:10.1186/1471-2091-7-14.

Gupta AB and Sankararamakrishnan R. 2009. Genome-wide analysis of major intrinsic proteins in the tree plant *Populus trichocarpa*: characterization of XIP subfamily of aquaporins from evolutionary perspective. *BMC Plant Biology* **7**, doi:10.1186/1471-2229-9-134.

Hofte H, Hubberd L, Reizer J, Ludevid D, Herman EM and Chrispeels MJ. 1992. Vegetative and seed-specific forms of tonoplast intrinsic protein in the vacuolar membrane of *Arabidopsis thaliana*. *Plant Physiology* **99**, 561-570.

Ishibashi K. 2006. Aquaporin subfamily with unusual NPA boxes. *Biochimica et Biophysica Acta - Biomembranes* **1758**, 989–993.

Ishikawa F, Suga S, Uemura T, Sato MH and Maeshima M. 2005. Three SIP aquaporins of *Arabidopsis* are localized in the ER membrane and expressed in a tissue- and cell-specific manner. *FEBS Letters* **579**, 5814–5820.

Itoh T, Rai T, Kuwahara M, Ko SBH, Uchida S, Sasaki S and Ishibashi K. 2005. Identification of a novel aquaporin, AQP12, expressed in pancreatic acinar cells. *Biochemical and Biophysical Research Communications* **330**, 832–838.

Javot H, Lauvergeat V, Santoni V, Martin-Laurent F, Guclu J, Vinh J, Heyes J, Franck KI, Schäffner AR, Bouchez D and Maurel C. 2003. Role of a single aquaporin isoform in root water uptake. *The Plant Cell* **15**, 509–522.

Javot H and Maurel C. 2002. The role of aquaporins in root water uptake. *Annals of Botany* **90**, 301-313.

Johanson U and Gustavsson S. 2002. A new subfamily of major intrinsic proteins in plants. *Molecular Biology and Evolution* **19**, 456–461.

Johanson U, Karlsson M, Johansson I, Gustavsson S, Sjovall S, Fraysse L, Weig AR and Kjellbom P. 2001. The complete set of genes encoding major intrinsic proteins in Arabidopsis provides a framework for a new nomenclature for major intrinsic proteins in plants. *Plant Physiology* **126**, 1358–1369.

Kliewer WM and Torres RE. 1972. Effect of controlled say and night temperatures on grape coloration. *American Journal of Enology and Viticulture* **23**, 71-77.

Laemmli UK. 1970. Cleavage of structural proteins during the assembly of the head of bacteriophage T4. *Nature* **227**, 680–685.

Laura R, Franceschetti M, Ferri M, Tassoni A and Bagni N. 2007. Resveratrol production in *Vitis vinifera* cell suspensions treated with several elicitors. *Caryologia* **60**, 169-171.

Liu K, Nagasse H, Huang CG, Calamita G and Agre P. 2006. Purification and functional characterization of Aquaporin-8. *Biology of the Cell* **98**, 153–161.

Lowry OH, Rosebrough NJ, Farr AJ, Randall RJ. 1951. Protein measurement with the Folin reagent. *The Journal of Biological Chemistry* **193**, 265–275.

Maeshima M and Ishikawa F. 2008. ER membrane aquaporins in plants. *European Journal of Physiology* **456**, 709–716.

Más P and Beachy RN. 1999. Replication of tobacco mosaic virus on endoplasmic reticulum and role of the cytoskeleton and virus movement protein in intracellular distribution of viral RNA. *Journal of Cell Biology* **147**, 945–958

Mituzani M, Watanabe S, Nakagawa T and Maeshima M. 2006. Aquaporin NIP2;1 is mainly localized to the ER membrane and shows root-specific accumulation in *Arabidopsis thaliana*. *Plant Cell Physiology* **47**, 1420-1426.

Morishita Y, Matsuzaki T, Hara-Chikuma M, Andoo A, Shimono M, Matsuki A, Kobayashi K, Ikeda M, Yamamoto T, Verkman A, Kusano E, Ookawara S, Takata K, Sasaki S, Ishibashi K. 2005. Disruption of aquaporin-11 produces polycystic kidneys following vacuolization of the proximal tubule. *Molecular and Cellular Biology* **25**, 7770–7779.

Nicholas KB, Nicholas HB Jr, and Deerfield DW II. 1997. GeneDoc: analysis and visualization of genetic variation, *EMBNEW.NEWS* 4:14.

Nozaki K, Ishii D and Ishibashi K. 2008. Intracellular aquaporins: clues for intracellular water transport? *European Journal of Physiology* **456**, 701–707.

Pillet J, Egert A, Pieri P, Lecourieux F, Kappel C, Charon J, Gomès E, Keller F, Delrot S, Lecourieux D. 2012. VvGOLS1 and VvHsfA2 are involved in the heat stress responses in grapevine berries. *Plant Cell Physiology* **53**, 1776–1792.

Rodrigues J, Silva RD, Noronha H, Pedras A, Gerós H and Côrte-Real M. 2013. Flow cytometry as a novel tool for structural and functional characterization of isolated yeast vacuoles. *Microbiology* 159, 848–856.

Sakurai J, Ishikawa F, Yamaguchi T, Uemura M, Maeshima M. 2005. Identification of 33 rice aquaporin genes and analysis of their expression and function. *Plant Cell Physiology* **46**, 1568–1577.

Soto G, Fox R, Ayub N, Alleva K, Guaimas F, Erijman EJ, Mazzella A, Amodeo G and Muschietti J. 2010. TIP5;1 is an aquaporin specifically targeted to pollen

mitochondria and is probably involved in nitrogen remobilization in *Arabidopsis* thaliana. *The Plant Journal* **64**, 1038–1047.

Soveral G, Macey RI and Moura TF. 1997. Water permeability of brush border membrane vesicles from kidney proximal tubule. *Journal of Membrane Biology* **158**, 219-228.

Sparkles IA, Runions J, Kearns A and Hawes C. 2006. Rapid, transient expression of fluorescent fusion proteins in tobacco plants and generation of stably transformed plants. *Nature Protocols* **1**, 2019–2025.

Spayd SE, Tarara JM, Mee DL and Ferguson JC. 2002. Separation of sunlight and temperature effects on the composition of *Vitis vinifera* cv. Merlot berries. *American Journal of Enology and Viticulture* **53**, 171–182.

Suga S and Maeshima M. 2004. Water channel activity of radish plasma membrane aquaporins heterologously expressed in yeast and their modification by site-directed mutagenesis. *Plant Cell Physiology* **45**, 823–830.

Tamura K, Dudley J, Nei M and Kumar S. 2007. MEGA4: molecular evolutionary genetics analysis (MEGA) Software version 4.0. *Molecular Biology and Evolution* **24**, 1596–1599.

Tanimura Y, Hiroaki Y and Fujiyoshi Y. 2009. Acetazolamide reversibly inhibits water conduction by aquaporin-4. *Journal of Structural Biology* **166**, 16–21.

Tchekneva EE, Khuchua Z, Davis LS, Kadkina V, Dunn SR, Bachman S, Ishibashi K, Rinchik EM, Harris RC, Dikov MM and Breyer MD. 2008. Single amino acid substitution in aquaporin 11 causes renal failure. *Journal of the American Society of Nephrology* **19**: 1955–1964.

Törnroth-Horsefield S, Wang Y, Hedfalk K, Johanson U, Karlsson M, Tajkhorshid E, Neutze R, Kjellbom P. 2006. Structural mechanisms of aquaporin gating. *Nature* **439**, 688-94.

Tournaire-Roux C, Sutka M, Javot H, Gout E, Gerbeau P, Luu D, Bligny R and Maurel C. 2003. Cytosolic pH regulates root water transport during anoxic stress through gating of aquaporins. *Nature* **425**, 393–397.

Tyerman SD, Niemietz CM and Bramley H. 2002. Plant aquaporins: multifunctional water and solute channels with expanding roles. *Plant, Cell & Environment* **25**, 173–194.

Uehlein N, Lovisolo C, Siefritz F and Kaldenhoff R. 2003. The tobacco aquaporin NtAQP1 is a membrane CO_2 pore with physiological functions. *Nature* **425**, 734–737.

Uehlein N, Otto B, Hanson TD, Fischer M, MacDowell N and Kaldenhoff R. 2008. Function of Nicotiana tabacum aquaporins as chloroplast gas pores challenges the concept of membrane CO_2 permeability. *The Plant Cell* **20**, 648–657.

Van der Goot FG, Podevin RA, Corman BJ. 1989. Water permeabilities and salt reflection coefficients of luminal, basolateral and intracellular membrane vesicles isolated from rabbit kidney proximal tubule. *Biochimica et Biophysica Acta - Biomembranes* **986**, 332–340.

Wallace IS and Roberts DM. 2004. Homology modeling of representative subfamilies of Arabidopsis major intrinsic proteins. Classification based on the aromatic/arginine selectivity filter. *Plant Physiology* **135**, 1059–1068.

Wudick MM, Luu DT and Maurel C. 2009. A look inside: localization patterns and functions of intracellular plant aquaporins. *New Phytologist* **184**, 289–302.

Wuestehube LJ and Schekman RW. 1992. Reconstitution of transport from endoplasmic reticulum to Golgi complex using endoplasmic reticulum-enriched membrane fraction from yeast. *Methods in Enzymology* **219**, 124–136.

Yakata K, Hiroaki Y, Ishibashi K, Sohara E, Sasaki S, Mitsuoka K and Fujiyoshi Y. 2007. Aquaporin-11 containing a divergent NPA motif has normal water channel activity. *Biochimica et Biophysica Acta - Biomembranes* **1768**, 688–693.

Zeidel ML, Ambudkar SV, Smith BL and Agre P. 1992. Reconstitution of functional water channels in liposomes containing purified red cell CHIP28 protein. *Biochemistry* **31**, 7436–7440.

Zhang Y. 2008. I-TASSER server for protein 3D structure prediction. *BMC Bioinformatics* **9**, doi:10.1186/1471-2105-9-40.

Chapter 4

The uncharacterized intrinsic protein from grapevine VvXIP1 shows unusual substrate specificity

A manuscript including this work is being prepared:

Noronha H*, Araújo D*, Conde C, Martins AP, Soveral G, Chaumont F, Gerós H. The uncharacterized intrinsic protein from grapevine VvXIP1 shows unusual substrate specificity.
**Both authors contributed equally to the experimental work.*

Authors´ contributions: HN and HG raised the hypothesis underlying this work. HN, DA, CC, GS, FC, SD and HG design the experiments. DA, HN, CC and APM performed the experiments. HN and DA analyzed the data. HN, DA and HG wrote the paper. CC, SD and HG directed the study.

Abstract

A MIP (Major Intrinsic Protein) subfamily called Uncharacterized Intrinsic Proteins (XIP) was recently described in several fungi and eudicot plants. In the present study, the localization, expression and functional characterization of the grapevine VvXIP1 were performed. Co-localization studies with ZmTIP2;1-YFP and VvXIP1-RFP fusion proteins in transiently transformed Nicotiana bethamiana leaves revealed that VvXIP1 is located in the tonoplast. Sopped-flow spectrometry in microsomal vesicles from yeast transformed with pVV214-VvXIP1 showed that VvXIP1 is unable to transport water but transports glycerol, copper, boron and H_2O_2. Trancriptional analysis showed a much higher steady-state expression of *VvXIP1* in leaves than in berries, canes or flowers from field grown grapevines (cv. Vinhão). Furthermore, *VvXIP1* transcripts were downregulated in plants treated with the copper-based fungicide Bordeaux mixture. Leaves from potted grapevines (cv. Aragonez) under severe water deficit showed lower number of *VvXIP1* transcripts than leaves from fully irrigated grapevines. In agreement, *VvXIP1* was downregulated by ABA and salt stress in *in vitro* cultured grape cells.

4.1 Introduction

Plants display a much larger diversity of MIPs than other organisms with 35 isoforms in *Arabidopsis thaliana*, 55 in poplar, 71 in cotton and at least 36 in maize (Chaumont *et al*., 2001). Twenty three different isoforms were found in the genome of the evolutionarily early land plant *Physcomitrella patens* (Bienert *et al*., 2011). The MIP superfamily in plants was initially divided into four subfamilies: the Plasma Membrane Intrinsic Proteins (PIPs), Tonoplast Intrinsic Proteins (TIPs), Nodulin 26-like Intrinsic Proteins (NIPs) and the Small Basic Intrinsic Proteins (SIPs). More recently, three new subfamilies were identified, the GlypF-like Intrinsic Proteins (GIPs) and the Hybrid Intrinsic Proteins (HIPs) in P. patens, and the Uncharacterized Intrinsic Proteins (XIPs) in a number of dicotyledonous plants, including tomato and grapevine (Danielson and Johanson, 2008; Chaumont and Tyerman, 2014).

XIPs are present in a wide variety of eudicot plant species, but not in *Brassicaceae* (e.g. *Arabidopsis*) and remain undetected in monocots (Gupta and Sankararamakrishnan, 2009). The most conserved feature of XIP protein sequences, which could be used as a signature for this subfamily, is the NPARC motif, with a cysteine residue located after the second NPA motif (Danielson and Johanson, 2008; Shelden *et al*., 2009; Vandeleur *et al*., 2009; Gupta and Sankararamakrishnan, 2009; Noronha *et al*., 2014). In addition, XIPs show considerable amino acid variation at both the first NPA motif and the ar/R filter. Based on the four amino acids defining the ar/R filters, XIPs from eudicots can be divided into four subclasses, two of which have an ar/R signature similar to that found in some plant NIPs, while the other two are even more hydrophobic (Bienert *et al*., 2011).

In grapevine, up until now, 23 MIPs were identified with genome sequence analysis in a single cultivar (Shelden *et al*., 2009; Tyerman *et al*., 2012). Several studies have linked AQP activity to the vine water status, but *Vitis vinifera* cultivars have different tolerance and responses to water stress, and these differences are particularly significant between isohydric and anisohydric grapevines. While Chardonnay (anisohydric) exhibited a significant increase in *VvPIP1;1* expression under water stress, Grenache (isohydric) did not show any alteration (Vandeleur *et al*., 2009). MIP expression also changes during maturation of grapes, and this phenomenon is correlated with the increase in hydraulic resistance observed in the post-veraison stages (Tyerman *et al*., 2012). In a recent study,

the endoplasmic reticulum (ER) grapevine small basic intrinsic protein VvSIP1 was purified to homogeneity and its incorporation in phosphatidylethanolamine liposomes confirmed its water channel activity (Noronha *et al*., 2014).

In the present study, we characterized the *VvXIP1* gene from grapevine and performed localization studies, expression analysis and functional characterization of VvXIP1.

4.2 Results

4.2.1 VvXIP1 protein sequence analysis

The tree depicted in Fig. 4.1 was constructed with different XIP members from plant and fungi. VvXIP1 is phylogenetically close to GhXIP1 from cotton and to PpXIP1 from peach. Fig. 4.2 shows the alignments of amino acid sequences from XIPs from *V. vinifera* (VvXIP1), *Populus trichocarpa* (PtXIP1), *Prunus persica* (PpXIP), *Gossypium hirsutum* (GhXIP1;1), *Ipomea nil* (InXIP1;1), *Nicotiana tabacum* (NtXIP1;1), *Lotus japonicus* (LjXIP1), *Ricinus communis* (RcXIP). All proteins share the highly conserved NPARC motif, despite the slight variations in the first NPA (NPV in most of the aligned species). Using TOPCONS (Bernsel *et al*., 2009) it was also possible to identify regions corresponding to the six transmembrane helixes.

4.2.2 Subcellular localization of VvXIP1

To study the subcellular localization of VvXIP1, the corresponding XIP1-RFP fusion proteins were transiently expressed in *N. benthamiana* epidermal cells. Fluorescent signal resulting from ZmPIP2;5-YFP expression was used as a plasma membrane reference. However, VvXIP1-RFP fluorescence did not co-localize with the YFP-ZmPIP2;5 signal, but labeled internal membranes and the signal appeared be more patchy. Furthermore, when VvXIP1-RFP was co-expressed with the YFP-ZmTIP2;1, a tonoplast marker, a clear co-localization was observed, suggesting that VvXIP1 locates in this internal membrane.

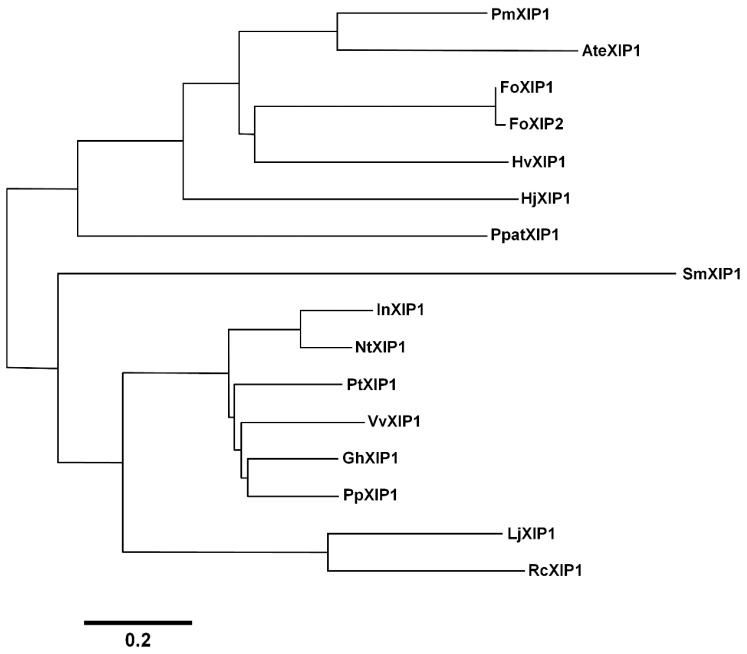

Figure 4.1 Phylogenetic tree comparing XIP proteins from plants and fungi. Amino acid sequences from *Vitis vinifera* (Vv), *Populus trichocarpa* (Pt), *Prunus persica* (Pp), *Gossypium hirsutum* (Gh), *Ipomoea nil* (In), *Nicotiana tabacum* (Nt), *Lotus japonicus* (Lj), *Ricinus communis* (Rc), *Physcomitrella patens* (Ppat), *Aspergillus terreus* (Ate), *Fusarium oxysporum* (Fo), *Penicillium marneffei* (Pm), *Hypocrea virens* (Hv), *Hypocrea jecorina* (Hj) and *Selaginella moellendorffii* (Sm).

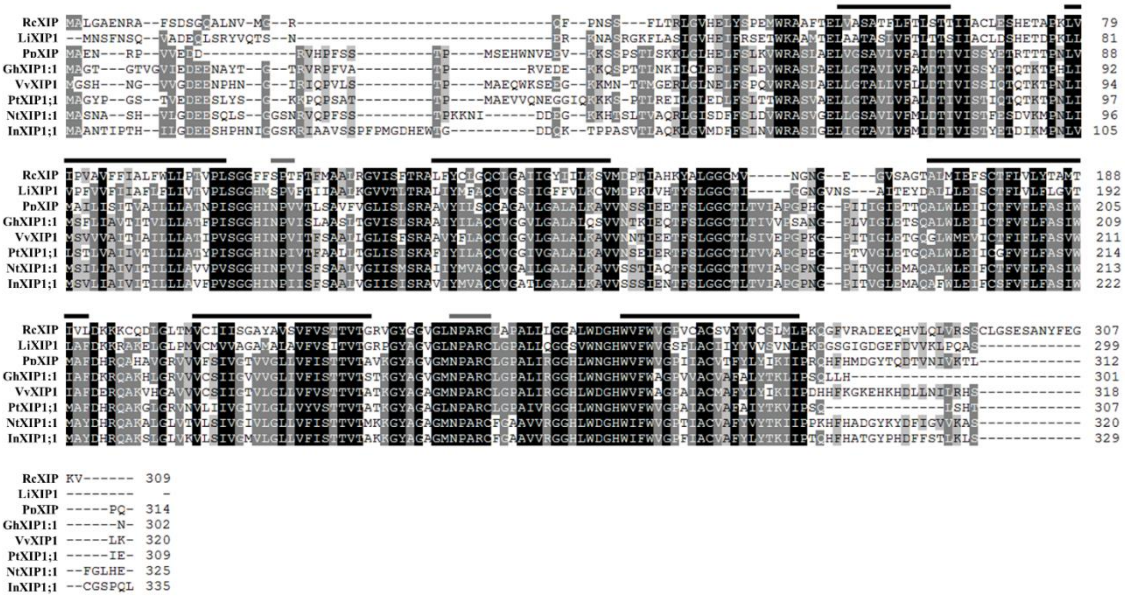

Figure 4.2 Alignment of eight plant XIPs (VvXIP1, PtXIP1, PpXIP, GhXIP1;1, InXIP1;1 NtXIP1;1, LjXIP1 and RcXIP) showing six transmembrane helix domains (black lines) and the conserved 'NPV' and 'NPARC' motifs (grey lines).

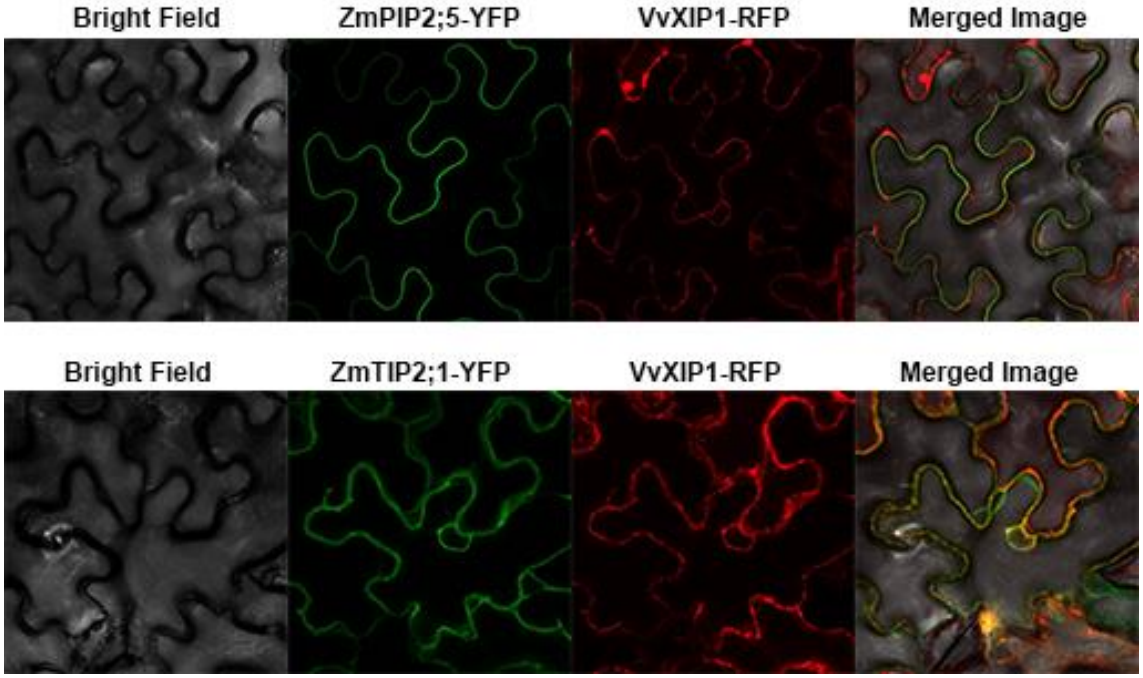

Figure 4.3 Subcellular localization of VvXIP1 in tobacco leaves. Plants were infiltrated with *Agrobacterium* transformed with *pH7RWG2-VvXIP1*, *pCambia2300-YFP-ZmPIP2;5* and *pCambia2300-YFP-ZmTIP2;1* plasmids. Images were acquired 2 days after infiltration in a confocal microscope.

4.2.3 VvXIP1 transports glycerol but not water

To functionally characterize VvXIP1, the protein was overexpressed in the yeast strain YSK1172 (AQy-null). VvXIP1-GFP fluorescence signal was distributed through most of the cell, including the ER and the vacuole (not shown). To study membrane permeability by stopped flow light-scattering spectrophotometry a total membrane fraction from yeast cells transformed with *pVV214-VvXIP1* was purified. Vesicle size, measured by QELS, was homogeneous in all batches with a mean hydrodynamic diameter of 375 ± 62 nm (n=8). The figure 4.4A showed no difference in the rate of water efflux when control and vesicles from yeasts expressing *VvXIP1* were challenged with a hypertonic mannitol solution, resulting in similar osmotic permeability coefficient (P_f; Table 4.1). Likewise, the activation energies (E_a) determined in both vesicle batches show similar values (Fig. 5A and Table 4.1).

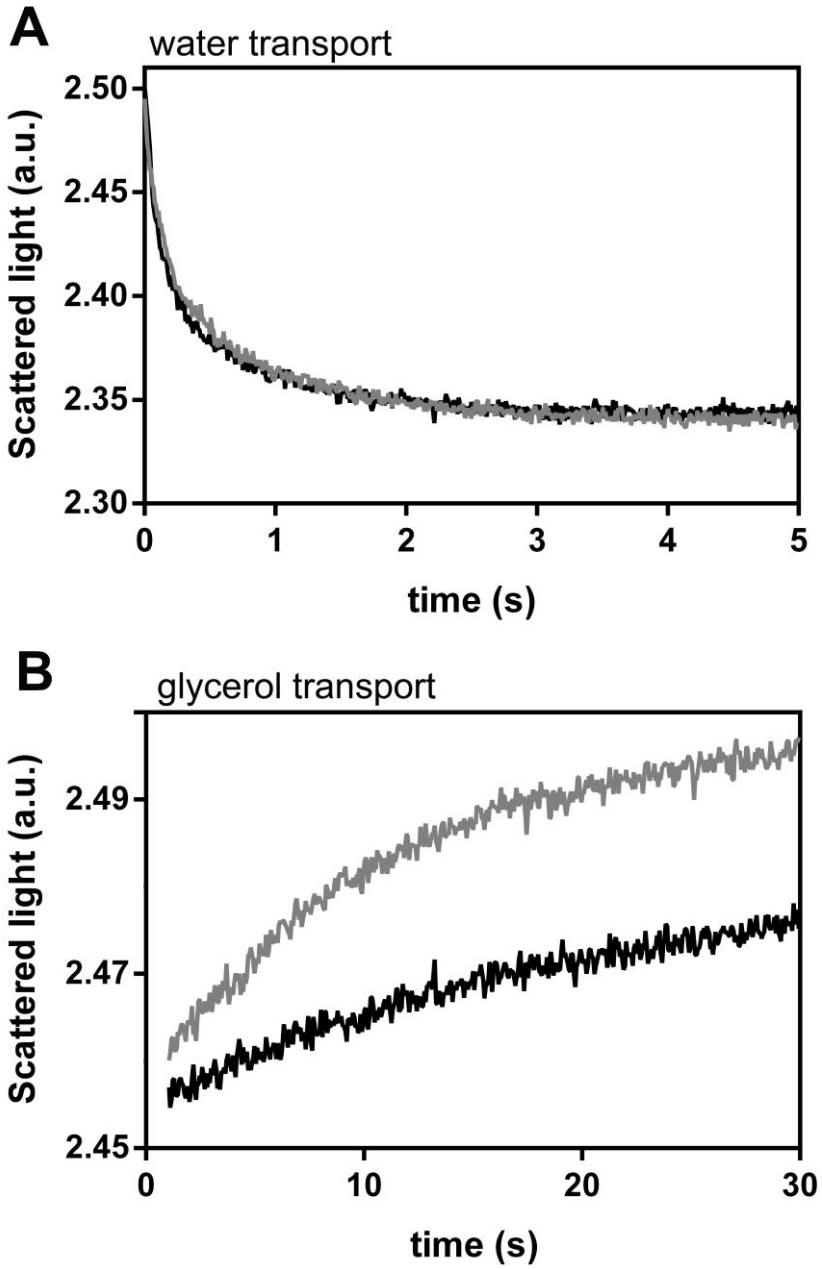

Figure 4 Stopped flow experiment for evaluation of the water and glycerol permeability in yeast membrane vesicles. Normalized scattered light intensity obtained from stopped-flow experiments with membrane vesicles collected from yeast cells transformed with *pVV214-VvXIP1* (grey) or the empty vector (black), suddenly exposed to an osmotic gradient of 240 mOsM with a mannitol solution (A) and with a glycerol solution (B).

		P_f (10^{-3} cm s^{-1})	E_a (kcal mol^{-1})
Water	*pVV214*	4.31 ± 0.0005	9.7 ± 0.95
	VvXIP1	3.70 ± 0.00007	9.1 ± 0.68
Glycerol	*pVV214*	9.62 ± 1 x 10^{-5}	26.0 ± 1.14
	VvXIP1	40.42 ± 2 x 10^{-5}*	11.8 ± 0.76*

Table 4.1 Permeability (P_f) and activation energy (E_a) for water and glycerol transport in yeast membranes obtained by stopped-flow spectroscopy (for details see Material and Methods). Asterisks denote significant differences compared to the control: * = P ≤ 0.01.

As shown in Fig. 4B, the swelling rate of the membrane vesicles from *VvXIP1*-expressing yeast cells when challenged with a hypertonic glycerol solution was much higher than in control vesicles. The corresponding permeability coefficients are shown in Table 4.1. As can be seen in Fig. 5B and Table 4.1, the E_a value associated with glycerol transport in vesicles from *VvXIP1*-expressing yeast cells (11.8 ± 0.76 kcal mol^{-1}) was much lower than in vesicles from the yeast transformed with the empty vector (26.0 ± 1.14 kcal mol^{-1}), indicating protein-mediated diffusion. Moreover, yeasts transformed with the *pVV214-VvXIP1* construct grew better than control cells (empty vector) in solid media supplemented with 1 and 2% ethanol and glycerol, confirming that glycerol can be transported byVvXIP1 (Fig. 4.6). Altogether, these results strongly suggested that VvXIP1 is unable to facilitate water diffusion but permeates glycerol.

4.2.4 VvXIP1 transports H_2O_2, copper and boron

H_2O_2 transport was tested through different approaches in the yeast strain YSH1172 (aqy-null) transformed with the construct *pVV214-VvXIP1*. When the probe CM-H_2DCFDA was used to measure H_2O_2 uptake by spectrofluorimetry, yeast cells expressing *VvXIP1* showed a much higher rate of fluorescence increase after H_2O_2 addition than control cells transformed with the empty vector (Fig. 4.7A). In agreement, when H_2O_2 was added to the incubation media, VvXIP1-transformed yeast showed a 3.5-fold higher rate of O_2 production than the control, as measured with a Clark electrode (Fig. 4.7B).

Furthermore, results suggested that 1 mM $HgCl_2$ completely inhibited H_2O_2 uptake. Moreover, the growth of the transformed yeast was severely inhibited when YNB media was supplemented with toxic levels of H_2O_2, 0.35 and 0.7 mM (Fig. 4.8).

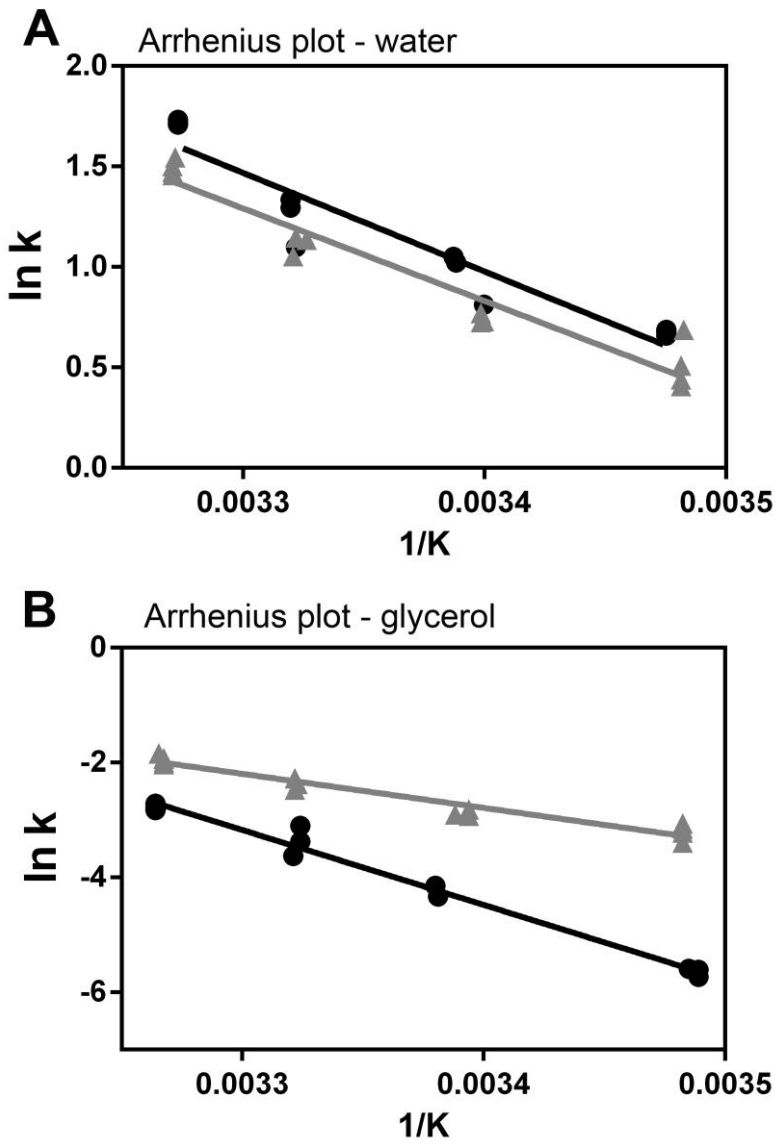

Figure 4.5 Stopped flow experiment to evaluate the activation energy (E_a) for water and glycerol transport in yeast vesicles. Normalized scattered light intensity was obtained from stopped-flow experiments performed according to a temperature gradient. Membrane vesicles purified from yeast cells transformed with *pVV214-VvXIP1* (grey) or the empty vector (black) were suddenly exposed to an osmotic gradient of 240 mOsM. The gradient was built with mannitol (A) to evaluate water transport and with glycerol (B) to evaluate glycerol transport.

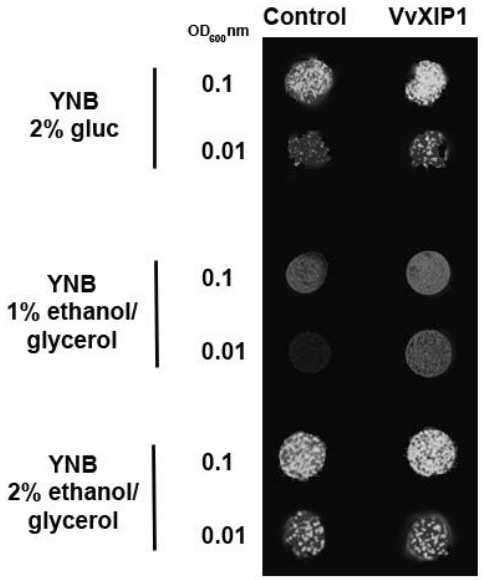

Figure 4.6 Yeast growth assays in glycerol rich media by cells expressing *VvXIP1*. Cultures of YSH1172 Aqy-null yeast cells transformed the empty vector or *pVV214-VvXIP1* were spotted at OD_{600} nm of 0.1 and 0.01 on medium containing the indicated concentrations of ethanol and glycerol and growth was recorded after 3 days at 30 ºC.

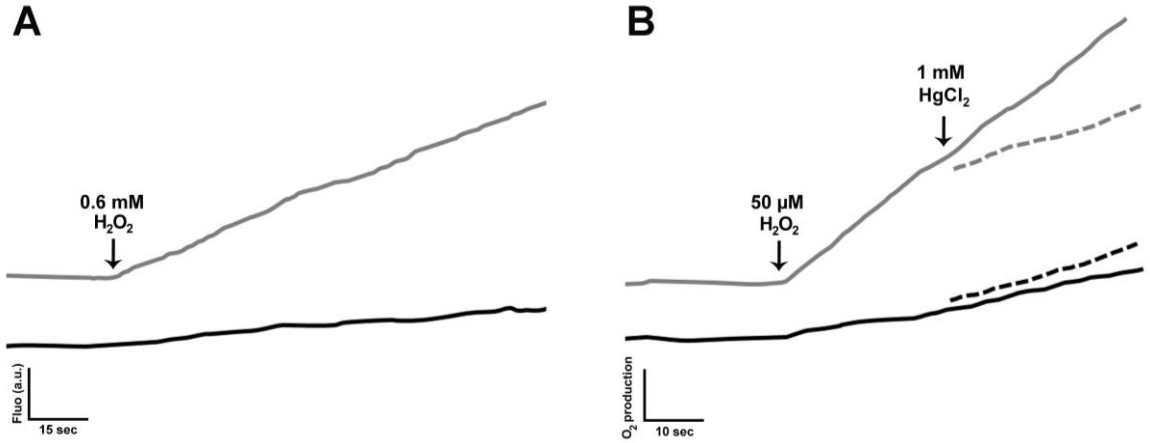

Figure 4.7 H_2O_2 transport by yeast cells expressing *VvXIP1*. Cultures of the yeast strain YSH1172 aqy-null transformed with the empty vector or *pVV214-VvXIP1* were incubated with CM-H_2DCFDA probe overnight and the fluorescence response after 600 µM H_2O_2 addition was monitored in a spectrofluorimeter (A). O_2 release monitored with a Clark electrode in response to 50 µM H_2O_2, which is inhibited by 1 mM $HgCl_2$ (B).

The yeast strains MPY2, MPY3 and YSH1172 were used to assess the VvXIP1 capacity to transport copper. MPY2 and MPY3 are, respectively, double and triple null-mutants in

copper transporters, and cannot survive when cultivated with respiratory substrates due to the lack of means to uptake high amounts of copper required for respiration.

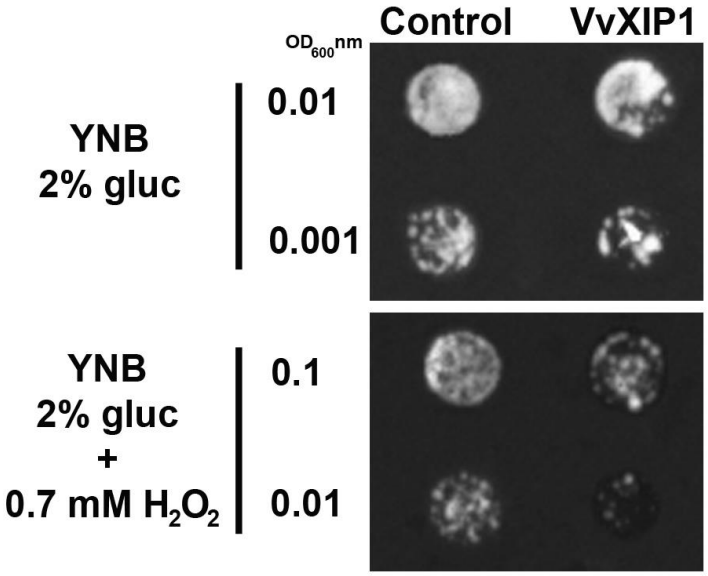

Figure 4.8 H_2O_2 sensitivity of yeast cells expressing *VvXIP1*. Cultures of YSH1172 aqy-null yeast cells transformed with the empty vector or *pVV214-VvXIP1*were spotted at an OD_{600} nm of 0.1 and 0.01 on medium containing the indicated concentrations of H_2O_2 and growth was recorded after 3 days at 30 ºC.

These yeast strains were transformed with *pVV214-VvXIP1* construct to evaluate if the capacity to grow in respiratory media was recovered. Furthermore, MPY strains were also transformed with *pVV214-VvCTR1*, a copper transporter recently identified and characterized by our group (Martins *et al*., 2014a). Results showed that VvXIP1 and VvCTR1 were able to restore yeast growth when both mutant strains were plated onto 100 µM $CuSO_4$ (Fig. 4.9A). Also, the expression of *VvXIP1* in YSH1172 strain increased yeast sensitivity to the toxic effects of copper, and thus reduced the growth in YNB media supplemented with 5 mM $CuSO_4$ (Fig. 4.9B).

Yeast growth assays were also performed to infer VvXIP1 capacity to facilitate boric acid diffusion. Expression of VvXIP1 significantly increased the tolerance of YSH1172 yeast cells to externally supplied 30 mM boric acid. However, 60 mM boric acid was toxic for both the transformed and control yeast (Fig. 4.10).

4.2.5 Role of VvXIP1 in osmotic stress response

It has been reported that aquaporin expression in yeast may lead to an osmotic stress oversensitivity (Leitão *et al*., 2012). In the present study YSH1172 aqy-null yeast cells were transformed with pVV214-VvXIP1 and incubated in YNB media supplemented with 2.1 M sorbitol. As shown in Fig. 11, cells transformed with VvXIP1 grew less than control yeasts, suggesting that they are more sensitive to osmotic stress.

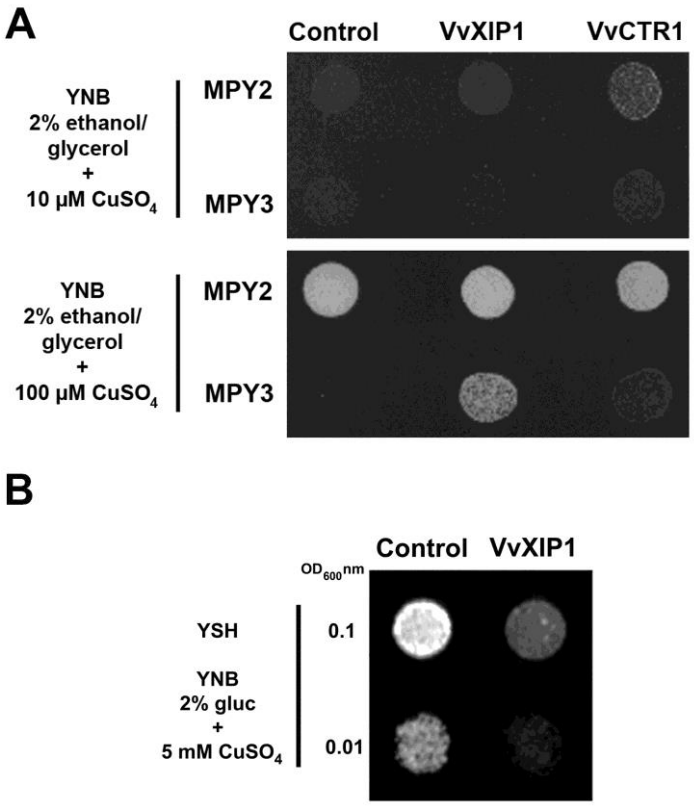

Figure 4.9 Copper effect on the growth of yeast cells expressing *VvXIP1*. Cultures of MPY2 (A), MPY3 (A) and YSH1172 (B) yeast cells transformed with empty vector, *pVV214-VvCTR1* (only used in MPY strains) and *pVV214-VvXIP1* were spotted at OD_{600} nm of 0.1 and 0.01 on medium containing the indicated concentrations of $CuSO_4$ and growth was recorded after 3 days at 30 ºC.

4.2.6 VvXIP1 transcriptional analysis

The expression of *VvXIP1* was studied in different organs of field grown cv. Vinhão grapevines. Total RNA was isolated from leaves, berries, canes and flowers. As shown in Fig. 4.12, steady-state transcript levels of *VvXIP1* were much higher in leaves than in the remaining organs.

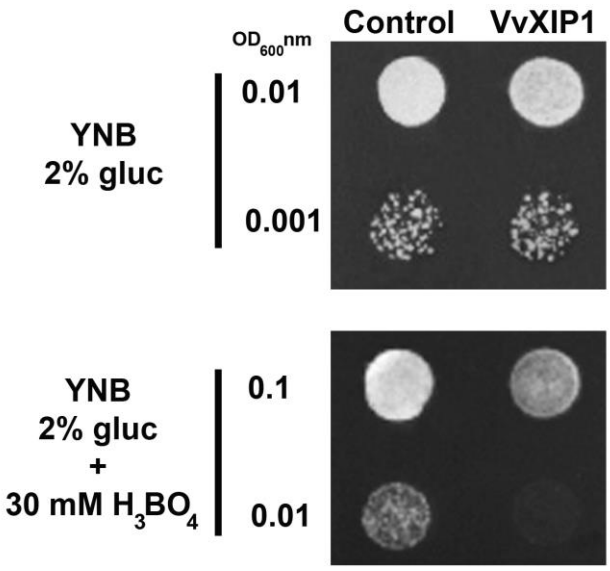

Figure 4.10 Boric acid effect on the growth of yeast cells expressing *VvXIP1*. Cultures of YSH1172 yeast cells transformed with empty vector and *pVV214-VvXIP1* were spotted at OD_{600} nm of 0.1 and 0.01 on medium containing the indicated concentrations of boric acid and growth was recorded after 3 days at 30 ºC.

To study the effect of water stress on the expression of *VvXIP1*, transcript levels were measured in leaves from potted cv. Aragonez grapevines cultivated in a greenhouse. As can be seen in Fig. 4.13A, *VvXIP1* steady-state transcript levels were lower in leaves from non-irrigated plants than in leaves from plants watered every two days, suggesting that water deficit downregulates the expression of *VvXIP1*.

Following the results from heterologous expression experiments, indicating that *VvXIP1* was able to mediate copper transport, we decided to study whether the application of Bordeaux mixture in field conditions could affect the expression of *VvXIP1*. This task took advantage of our previous work (Martins *et al*., 2014a,b). As shown in Fig. 4.13B, in leaves from cv. Vinhão vines treated with Bordeaux mixture (+ copper) a downregulation of *VvXIP1* expression was observed when compared to plants treated with a conventional triazole-based fungicide (- copper).

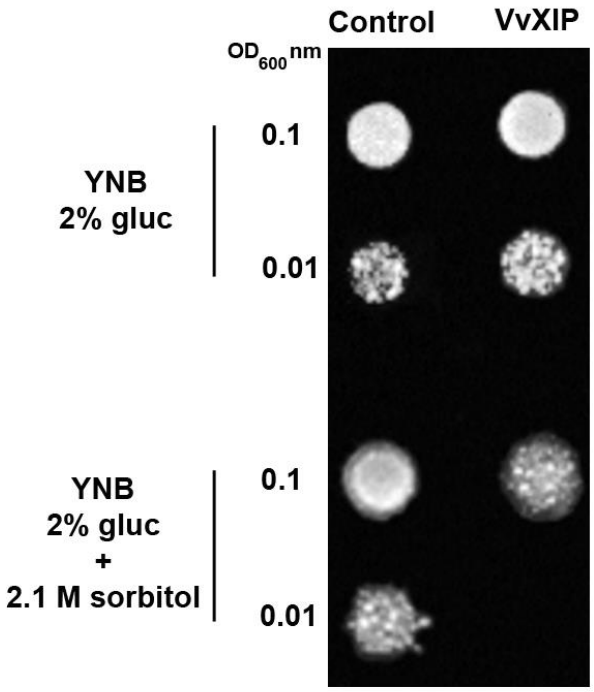

Figure 4.11 Sorbitol induced osmotic stress sensitivity of yeast cells expressing VvXIP1. Cultures of YSH1172 aqy-null yeast cells transformed with empty vector and *pVV214-VvXIP1* were spotted at OD_{600} nm of 0.1 0.01 on medium containing the indicated concentration of sorbitol and growth was recorded after 3 days at 30 ºC.

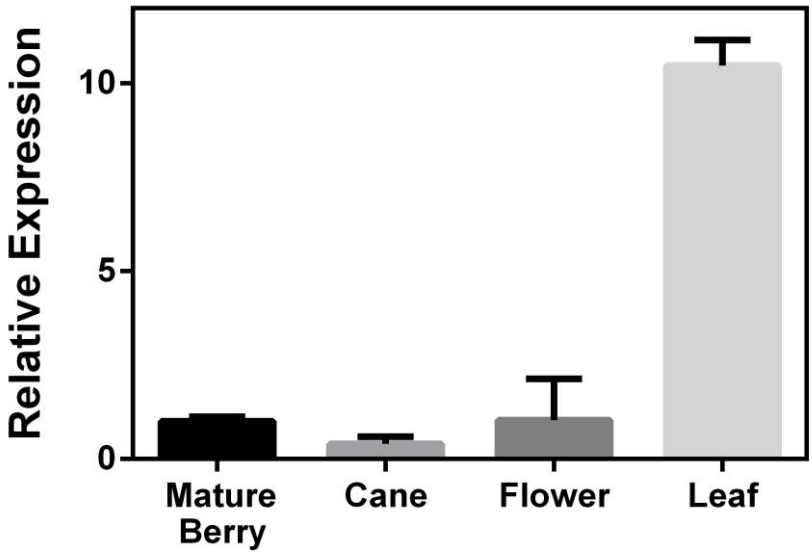

Figure 4.12 Study of *VvXIP1* expression in berries, canes, flowers and leaves from grapevine cv. Vinhão.

Despite the necessary cautions needed to extrapolate the results to a multicellular level, suspension-cultured cells have provided a convenient experimental system to study several important aspects of plant cell physiology, including gene expression and functional studies (Noronha *et al*., 2014; Conde *et al*., 2015). Additionally, in cell suspensions, the plasma membrane is readily amenable for challenging with exogenous stressors/elicitors. In the present study, cultured CSB cells were used to evaluate *VvXIP1* expression after an overnight incubation with 100 mM NaCl, 150 µM ABA, 150 µM SA and 2% (w/v) PEG. *VvXIP1* transcript levels were downregulated by ABA and NaCl but not affected by SA and PEG (Fig. 4.13C).

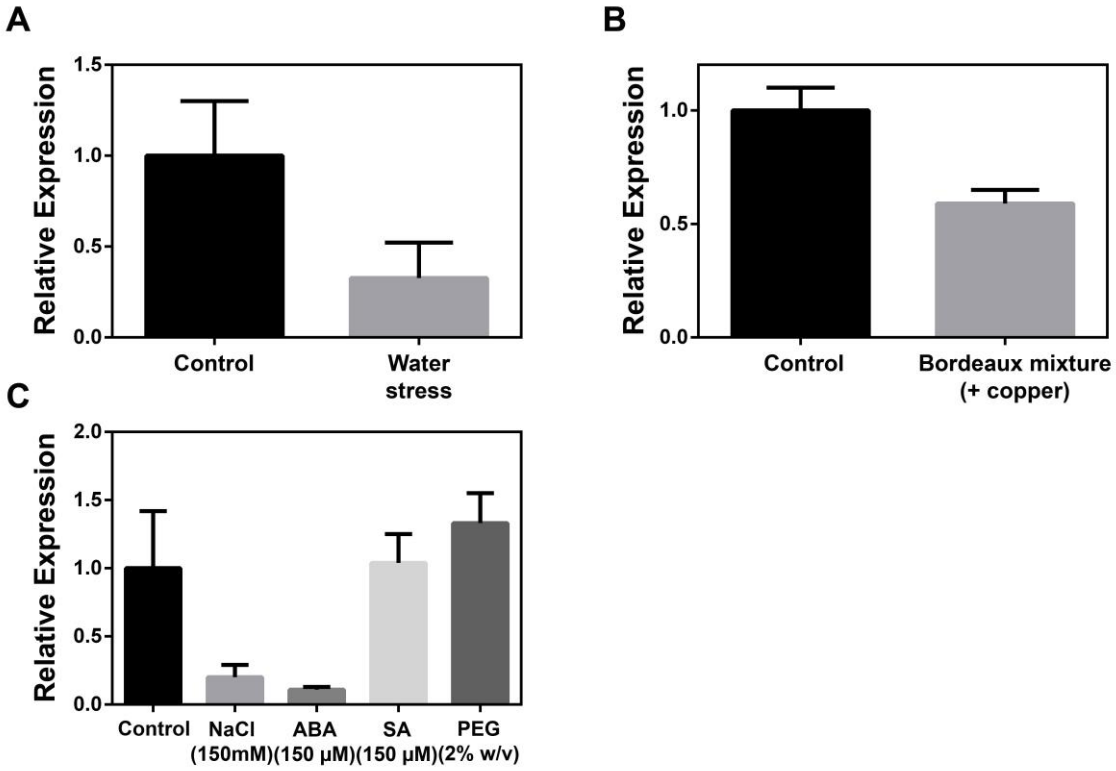

Figure 4.13 *VvXIP1* expression in response to potential stressors/elicitators determined by qPCR. *VvXIP1* steady-state transcript levels in leaves from field grown cv. Vinhão grapevines in response to copper treatments (Bordeaux mixture) (A), in potted grapevines (cv. Aragonez) under drought stress (B) and in CSB cell suspensions treated with salt, ABA, SA and PEG (C).

4.3 Discussion

4.3.1 VvXIP1 is a grapevine intracellular solute channel

So far the Uncharacterized Intrinsic Proteins (XIPs) were studied in few plant species and fungi, and much work remains to be done to fully understand its specificity and true physiological roles. The divergence in the composition of the NPA motives has been proposed to reflect differences in the substrate specificity, as previously observed in NIPs (Bienert *et al*., 2011). The alanine of the first NPA motif is replaced by valine in XIPs from *V. vinifera*, *P. persica*, *G. hirsutum* and *N. tabacum*, by isoleucine in *Ipomoea nil* and *P. trichocarpa*, and by threonine in *R. communis*. These changes could affect the specificity of XIPs that is rather unusual.

After their discovery at the plasma membrane of erythrocytes, researchers found that, similarly to other transporters and channels, aquaporins could also localize at intracellular membranes and transport other substrates than water (Maurel *et al*., 2009). Actually, it is known that TIPs have a key role in water transport at the tonoplast level and are tightly regulated by water deficit conditions (Tyerman *et al*., 2012). In addition, several aquaporins can be located to the membrane of other organelles, including the ER. This is the case of VvSIP1 that specifically transports water across the ER of grapevine cells (Noronha *et al*., 2014). In a previous work it was shown that the XIP aquaporin from tobacco NtXIP1;1 is located at the plasma membrane (Bienert *et al*., 2011), but our co-localization studies strongly suggest that VvXIP1 is not a plasma membrane channel but rather localizes at the tonoplast.

4.3.2 VvXIP1 specificity is unusual

H_2O_2 is an important molecule with dual functions, because it is an oxidative stress inducer but also a signaling molecule in plants (Foyer *et al*., 1997; Bolwell, 1999; Neill *et al*., 2002). In the present study we demonstrated with several approaches that VvXIP1 transports H_2O_2. Intriguingly, despite the fact that H_2O and H_2O_2 display high structural and electrostatic similarity VvXIP1 was unable to mediate water transport, which is in line with previous results in *Solaneaceae* XIPs (Bienert *et al*., 2011).

H_2O transport capacity of VvXIP1 was studied by stopped flow scattered-light spectrophotometry in yeast membrane vesicles, a technique recently used in our group to confirm water transport capacity of the intracellular aquaporin VvSIP1 (Noronha *et al*., 2014). Results showed that the permeability to water of membrane vesicles isolated from the yeast strain YSH1172 overexpressing *VvXIP1* was similar to control. Also, no changes were observed in E_a of water transport across the membrane of the vesicles. PtXIP2;1 and PtXIP3;3 from *P. trichocarpa* are water channels, although their water permeability is low when compared to members of the PIP subfamily (Lopez *et al*., 2012). Stopped-flow experiments also showed that glycerol permeates VvXIP1. Glycerol is a common substrate for non-water conducting MIPs, particularly from the NIP and XIP subfamilies (Bienert *et al*., 2011). The function of glycerol in plants is not yet fully established, but may have a role in fatty acids biosynthesis and as a carbon source (Auberts *et al*., 1994; Tisserat and Stuff, 2011).

Boron in plants is particularly important in leaves due to its role in the organization of cell wall pectic polysaccharides (Matsunaga *et al*., 2004; Miwa and Fujiwara, 2010). In the present study, growth assays of the transformed yeast with externally supplied boric acid suggested that VvXIP1 is able mediate the transport of boric acid, because the expression of *VvXIP1* significantly increased the tolerance of YSH1172 yeast cells to externally supplied boric acid, as reported previously by (Bienert *et al*., 2011; Sabir *et al*., 2014). However, at higher concentrations (60 mM) the toxicity of boric acid became evident, as reported in the literature (Takano *et al*., 2007; Sabir *et al*., 2014). These results can be related with the higher expression of *VvXIP1* in leaf tissues, suggesting that this aquaporin might have an important role in boron mobility in leaves.

The role of VvXIP1 in copper transport was also demonstrated in transformed yeasts. Copper is an important plant micronutrient, but highly toxic at high concentrations, leading to a reduction in photosynthetic activity, damage to lipids, proteins and DNA and, eventually, cell death. Recent results obtained in our group showed that the treatment of the grapevine with the copper-based fungicide Bordeaux mixture caused a transcriptional reprogramming of the expression of the *VvCTrs* (*V. vinifera* copper transporters) and a significant shift in grape berry composition and wine quality (Martins *et al*., 2012, 2014a,b). Following the observation that VvXIP1 may transport copper, we found that *VvXIP1* transcript levels in leaves are downregulated after Bordeaux mixture application in

the vineyard. These results open a new avenue of research on how VvXIP1 might cooperate with the copper transporters VvCTrs in the regulation of copper compartmentation/detoxification in grape cells.

4.3.3 VvXIP1 is expressed in leaves and downregulated by water-deficit stress

Results suggested that *VvXIP1* could play an important role in grapevine leaves because *VvXIP1* steady-state transcript levels where very high in leaf tissues. Also, *VvXIP1* is likely regulated by drought stress, because the levels of mRNAs were reduced by water deficit in leaves from cv. Aragonez. In agreement, in CSB cultured cells, *VvXIP1* transcript levels were reduced by ABA and salt. The role of ABA on plant response to abiotic stresses, including water deficit and salt stress is well-known (Tyerman *et al*., 2012). Thus, the treatment of maize roots with ABA results over 1–2 h in a transient increase in hydraulic conductivity of the whole organ and of cortical cells and also rapidly enhances the expression of some PIP isoforms (Maurel *et al*., 2008). In the present study, we also showed that VvXIP1 greatly increased yeast cell sensitivity to water-deficit stress imposed by sorbitol, clearly confirming that VvXIP1 has an important role in osmotic regulation. Considering that this protein was proven to be unable to transport water, this effect could be due to its role on the homeostasis of osmotically active solutes. The involvement of aquaporins in osmotic stress has been extensively studied (Tyerman *et al*., 2012), but the specific role of VvXIP1 deserves further investigation.

In summary, the functional analysis of VvXIP1 revealed an aquaporin with atypical features, being inactive for water transport but facilitating the transport of heavy metals like copper. What would be the physiological role of an intracellular aquaporin that mediates the incorporation H_2O_2, boron, copper, glycerol, but not water? Why substrates structurally and functionally so different could share the same channel? The addressing of these key questions in future work will expand our knowledge on the role of intracellular aquaporins and will shed light into their structure-function relationships.

4.4. Materials and Methods

4.4.1 In silico studies

Phylogenetic analysis was performed *in silico* using amino acid sequences from *Vitis vinifera* (F6I152), *Gossypium hirsutum* (D9DBX6), *Populus trichocarpa* (EEE86940), *Prunus persica* (M5VMI6), *Nicotiana tabacum* (ADO66667), *Lotus japonicus* (CCI69207), *Ricinus communis* (B9T717), *Physcomitrella patens* (XP_001758094), *Aspergillus terreus* (Q0CWK8), *Fusarium oxysporum* (N4U8H1), *Penicillium marneffei* (B6QIR3), *Hypocrea virens* (G9N6L5), *Hypocrea jecorina* (G9N6L5) and *Selaginella moellendorffii* (XP_002971714) obtained from the National Center of Biotechnology (NCBI), Uniprot and PlantGDB using the BLAST tool. The alignment of sequences was performed with PRANKSTER (Löytynoja and Goldman, 2005) and Genedoc (Nicholas *et al*., 1997). The phylogenetic tree was created using these alignments with PROTDIST, NEIGHBOR and RETREE from the PHYLIP software package (Felsenstein, 1989) and Mega 4 (Tamura *et al*., 2007). An alignment with VvXIP1 and several plant XIPs was performed and TOPCONS (Bernsel *et al*., 2009) was used to identify the transmembrane helix domains.

4.4.2 Plant material

Cv. Vinhão berries, canes, flowers and leaves were collected form a commercial vineyard near Guimarães, Portugal. Potted cv. Aragonez plants were grown in a greenhouse and subjected to different watering regimes during 4 weeks: full irrigation (FI – control), with plant watering every two days; and non-irrigation (NI), no watering. Leaves were collected when NI plants water potential was $-1.3 < \Psi pd < -0.9$ MPa (Conde *et al*., 2015).

Cell suspensions of *V. vinifera* L. (Cabernet Sauvignon Berry - CSB) were freshly established from somatic callus that had been previously initiated from Cabernet Sauvignon berry pulp. They were maintained on modified Murashige and Skoog (MS) medium, supplemented with 2% (w/v) sucrose in 250 mL flasks on a rotary shaker at 100 rpm in the dark, at 23 ºC (Decendit *et al*., 1996). Cells were subcultured weekly by transferring 10 ml aliquots into 40 mL of fresh medium. To study the effect of different treatments on *VvXIP1* expression, 5 mL aliquots were incubated overnight with 200 mM NaCl, 2% (w/v)

polyethylene glycol (PEG), 150 µM abscisic acid (ABA), or 150 µM salicylic acid (SA) at 23 ºC. After each treatment, cells were immediately frozen in liquid nitrogen and stored at -80.

4.4.3 Yeast strains and growth assays

The following yeast strains were used: YSH1172, MPY2 and MPY3. YSH1172 is a deletion mutant for AQY aquaporins and MPY2 and MPY3 are double and triple mutants (MPY17 strain with ctr1Δctr3Δ or ctr1Δctr3Δctr2Δ), respectively, in copper transporters, thus unable to grow with respiratory substrates such as glycerol and ethanol, which requires high amounts of copper. AQY-null strain was transformed with *pVV214-VvXIP* and *pVV214-Empty Vector*. MPY2 and MPY3 strains were transformed with *pVV214-VvXIP*, *pVV214-Empty Vector* and with *pVV214-VvCTR1*. VvCTR1 is a copper transporter recently identified and functionally characterized (Martins *et al*., 2014a). The *pVV214-VvXIP1* construct was prepared by Gateway (Qiagen) and the primers can be found in Table 4.2.

YSH yeast cells were grown in synthetic medium with 7 g/L YNB, 1.3 g/L SC, 2% agar powder, 2% glucose, 300 mg/100 mL leucine and 250 mg/100 mL tryptophan, washed and resuspended in sterile water to a final $OD_{600\ nm}$ = 1. Different dilutions (0.1, 0.01 and 0.001) were made and 10 µL of each suspension was spotted in solid medium with the following conditions/stressors: i) 2.1 M sorbitol, ii) 1% and 2% of ethanol and the same concentrations of glycerol, iii) 30 and 60 mM boric acid (adjusted to pH 5.5 with Tris), iv) 5 mM $CuSO_4$, v) 0.35 and 0.7 mM H_2O_2. Appropriate control plates inoculated with non-complemented mutants were prepared.

MPY yeast cells were grown in synthetic medium containing 7 g/L YNB, 1.3 g/L SC, 2% agar powder, 2% glucose, 25 mg/100 mL histidine, 30 mg/100 mL lysine and 25 mg/100 mL tryptophan, washed and resuspended in sterile water to a final $OD_{600\ nm}$ = 1; Different dilutions (0.1, 0.01 and 0.001) dilutions were made and 10 µL from each suspension were spotted in solid medium containing 10 and 100 µM $CuSO_4$. Yeast growth was observed during several days and images were collected with Chemidoc XRS (Bio-Rad).

	Primer forward (5' – 3')	Primer reverse (5'- 3')
qGAPDH	CACGGTCAGTGGAAGCATCATGA	CCTTGTCAGTGAACACACCAGTTGACTC
qVvXIP1	ATCATGTCGGTTGTTGTTGC	CAGCGCGTGAGAAAGAGATA
GATEWAY *VvXIP1*	GGGGACAAGTTTGTACAAAAAA GCAGGCTTCCAAATGGGTTCA CACAATGGGGTTG	GGGGACCACTTTGTACAAG AAAGCTGGGTCTATCAATG AATGCCTCAATATATTC

Table 4.2 Primer sequences used to perform quantitative real-time PCR and to insert VvXIP1 in expression vectors

4.4.4 Fluorescence assays

The YSH1172 aqy-null yeast strain was transformed with *pVV214-VvXIP1* and empty *pVV214* vector constructs and pre-cultured in YNB+SC solid medium. Liquid cultures were grown in the dark overnight in the presence of 1 μM 5-(and-6)-chloromethyl-2',7'-dichlorodihydrofluorescein diacetate acetyl ester (CM-H_2DCFDA, Molecular Probes), a fluorophore sensitive to reactive oxygen species (ROS) (Bienert *et al*., 2007). In its acetylated form, the dye can freely diffuse into yeast cells but, once inside, the fluorochrome is deacetylated and unable to cross the membrane making the cells susceptible to oxidation by ROS. After incubation, cells were washed three times with MOPS buffer (pH 7.0) and resuspended in the same buffer to a final $OD_{600\ nm}$ = 1.4. After the addition of H_2O_2, the fluorescence of 2 ml yeast suspension was followed over time at 20°C in a spectrofluorometer at an excitation/emission of 492/527 nm (Perkin Elmer Luminescence Spectrometer LS 50).

4.4.5 Clark electrode assays

The YSH1172 aqy-null yeast strain was transformed with *pVV214-VvXIP1* and empty *pVV214* vector constructs and pre-cultured in YNB+SC solid medium. Liquid cultures were then grown overnight. Cells were then washed three times and resuspended in water to a final final $OD_{600\ nm}$ = 1.0. H_2O_2 was then added to the cell suspension to a final

concentration of 50 μM and the O_2 formation was followed with a Clark electrode coupled to an YSI 5300 Biological Oxygen Monitor.

4.4.6 RNA isolation from grapevine berries and leaves

RNA from grape berries and leaves was isolated with a Qiagen RNeasy Plant Mini kit following the manufacturer's instructions. The extraction buffer was changed to 2% cetyltrimethyl ammonium bromide (CTAB), 2% soluble polyvinylpyrrolidone (PVP) K-30, 300 mM Tris-HCl (pH 8.0), 25 mM EDTA, 2.0 M NaCl, and 2% (v/v) β-mercaptoethanol. After an in-column DNase treatment, the RNA integrity was checked in a 1% agarose gel, and the first-strand cDNA synthesis was performed with the LongRange 2Step RT-PCR (Qiagen), following manufacturer's instructions.

4.4.7 Co-localization studies

The *pH7RWG2-VvXIP1-RFP* construct was prepared by Gateway (Qiagen) with the primers found in Table 4.2. Recombination sequences were introduced by PCR in the VvXIP1 cDNA without a stop codon and the fragment recombined into the entry vector *pDONR221* with the BP clonase enzyme. *VvXIP1* cDNA was then recombined into the *pH7RWG2* vector by the LR clonase enzyme. *pCambia2300-YFP-ZmPIP2;5* and *pCambia2300-YFP-ZmTIP2;1* were provided by F. Chaumont. The two constructs were separately introduced in *Agrobacterium tumefaciens* (GV3101) and transient transformation of *N. benthamiana* leaf epidermal cells was performed according to a previous report (Sparkes *et al*., 2006). Bacterial cells were cultivated overnight in liquid LB medium up to the exponential-stationary phase and then diluted to OD_{600nm} = 0.1 with infiltration buffer (50 mM MES pH 5.6, 2 mM Na_3PO_4, 0.5% glucose, and 100 μM acetosyringone). Diluted cells were cultivated again until the culture reached an OD_{600nm}=0.2. Four-week-old tobacco plants were infiltrated with the bacterial cultures and leaf discs were examined under the confocal microscope 2 days later in a Leica TCS SP5IIE scanning confocal microscope (Leica Microsystems). Data stacks were analyzed and projected using ImageJ 1.42m software (http://rsb.info.nih.gov/ij/). The yellow fluorescence signal from YFP was represented in green in all the acquisitions.

4.4.8 Real-time PCR studies

Quantitative Real-time PCRs were performed with a QuantiTect SYBR Green PCR Kit (Qiagen) and in a CFX96 Real-Time detection System (Bio-Rad), at an annealing temperature of 55ºC. RNA and cDNA samples were obtained as described above. Experiments were carried out in biological triplicates with the software Bio-Rad CFX Manager (Bio-Rad), using *VvGAPDH* as an internal control. To verify the absence of unspecific and primer-dimer amplification melting curves were performed after each run. The primers used to study the expression of *VvXIP1* and *VvGAPDH* can be found in Table 4.2.

4.4.9 Isolation of yeast membranes

YSH1172 yeast cells transformed with *pVV214-VvXIP1* were cultivated overnight in YNB medium with leucine and tryptophan. Cells were washed, resuspended in digestion buffer (1.35 M sorbitol, 10 mM citric acid, 30 mM Na_2HPO_4, 1 mM EGTA, pH 7.4) with 30 mM dithiothreitol (DTT), centrifuged and spheroplasts were obtained by digestion with zymolyase 20T (in digestion buffer). After complete digestion, monitored in phase contrast microscope, spheroplasts were pelleted and homogenized in a potter homogenizer after resuspension in HEPES-lysis buffer [20 mM HEPES, 50 mM potassium acetate, 100 mM sorbitol, 2 mM EDTA, 1 mM phenylmethylsulphonyl fluoride (PMSF), 1 mM DTT, pH 6.8]. The homogenate was centrifuged at 1000×g for 10 min and the supernatant saved. The membranes were then pelleted at 100 000×g for 30 min, resuspended (100 mM mannitol, 10 mM Tris-HEPES, pH 7.5), centrifuged again at 100.000 g for 30 min, flash frozen, and stored at -80 ºC. These procedures were performed according (Rodrigues *et al*., 2013; Noronha *et al*., 2014).

4.4.10 Stopped flow spectroscopy

Membrane permeability of the microsomal fraction from transformed yeasts was studied with the stopped flow technique (HI-TECH Scientific PQ/SF-53). Five runs were usually stored and analysed in each experimental condition, as described before (Soveral *et al*., 1997; Noronha *et al*., 2014). To assess water transport, vesicles resuspended in 100 mM mannitol, 10 mM Tris-HEPES (pH 7.5) (0.1 mL, 0.4 mg protein ml^{-1}) were mixed with

a 340 mM mannitol, 10 mM Tris-HEPES (pH 7.5) solution at 23 ºC to produce an inwardly directed gradient of impermeant solute (osmotic gradient 240 mOsM). The kinetics of vesicle shrinkage were measured from the time course of 90 º scattered light intensity at 400 nm until a stable light scatter signal was reached. Experiments were performed at 14-33 ºC to evaluate the activation energy of water transport (E_a).

To assess glycerol transport, vesicles resuspended in 100 mM mannitol, 10 mM Tris-HEPES (pH 7.5) (0.1 ml, 0.4 mg protein ml^{-1}) were mixed with a solution containing 100 mM mannitol, 240 mM glycerol and 10 mM Tris-HEPES (pH 7.5) at 23ºC to produce an inwardly directed gradient (osmotic gradient 240 mOsM). After a fast shrinkage due to water outflow, the kinetics of vesicle swelling due to glycerol influx (with consequent water influx) were measured from the time course of 90 º scattered light intensity at 400_{nm} until a stable light scatter signal was reached. The water permeability coefficient (P_f) and the glycerol permeability coefficient (P_{gly}) were estimated by fitting the light scatter signal to a single exponential curve with the equation $P_f = k(V_0/A)\ [1/V_w/(osm_{out})_\infty]$ (Soveral *et al*., 1997), where V_w is the molar volume of water, V_0/A is the initial volume to area ratio of the vesicle population and $(osm_{out})_\infty$ is the final medium osmolarity after the application of the osmotic gradient. The osmolarity of each solution was determined from freezing point depression by a semi-micro-osmometer (Knauer GmbH, Germany). The activation energies (E_a) were obtained from the slope of an Arrhenius plot ($\ln P_f$ or $\ln P_{gly}$ as a function of 1/T) multiplied by the gas constant R. Vesicle size (initial volume) was determined by quasi-elastic light scattering (QELS) by a particle sizer (BI-90 Brookhaven Instruments) as described by Soveral *et al*. (1997).

4.4.11 Statistical analysis

The results obtained were statistically verified by analysis of variances tests (one-way and two-way ANOVA using Prism v. 6 (GraphPad Software, Inc.) Post-hoc multiple comparisons were performed using the HSD Tukey test.

4.5 Acknowledgments

This work was supported by European Union Funds (FEDER/COMPETE Operational Competitiveness Programme) and Portuguese national Funds (FCT-Portuguese Foundation for Science and Technology): KBBE-2012-6-3117 "Inovinne", FCOMP-01-0124-FEDER-022692 and PTDC/AGR-ALI/100636/2008. HN was supported by a PhD grant from FCT (SFRH/BD/74257/2010). APM received a Ph.D. fellowship from Fundação para a Ciência e Tecnologia (FCT), Portugal (SFRH/BD/65046/2009). The Interuniversity Attraction Poles Programme-Belgian Science Policy (IAP7/29) and the Belgian French community ARC11/16-036 project. This work also benefited from the networking activities within the European funded COST ACTION FA1106 "QualityFruit".

4.6 References

Auberts S, Gout E, Blignyl R, Doucen R. 1994. Multiple effects of glycerol on plant cell metabolism. *The Journal of Biological Chemistry* **269**, 21420–21427.

Bernsel A, Viklund H, Hennerdal A, Elofsson A. 2009. TOPCONS: Consensus prediction of membrane protein topology. *Nucleic Acids Research* **37**, 465–468.

Bienert GP, Bienert MD, Jahn TP, Boutry M, Chaumont F. 2011. *Solanaceae* XIPs are plasma membrane aquaporins that facilitate the transport of many uncharged substrates. *The Plant Journal* **66**, 306–317.

Bienert GP, Møller ALB, Kristiansen KA, Schulz A, Møller IM, Schjoerring JK, Jahn TP. 2007. Specific aquaporins facilitate the diffusion of hydrogen peroxide across membranes. *The Journal of Biological Chemistry* **282**, 1183–92.

Bolwell GP. 1999. Role of active oxygen species and NO in plant defence responses. *Current Opinion in Plant Biology* **2**, 287–294.

Chaumont F, Barrieu F, Wojcik E, Chrispeels MJ, Jung R. 2001. Aquaporins constitute a large and highly divergent protein family in maize. *Plant Physiology* **125**, 1206–15.

Chaumont F, Tyerman SD. 2014. Aquaporins: Highly regulated channels controlling plant water relations. *Plant Physiology* **164**, 1600–1618.

Conde A, Regalado A, Rodrigues D, Costa JM, Blumwald E, Chaves MM, Gerós H. 2015. Polyols in grape berry: transport and metabolic adjustments as a physiological strategy for water stress tolerance in grapevine. *Journal of Experimental Botany* **66**, 889–906.

Danielson J, Johanson U. 2008. Unexpected complexity of the aquaporin gene family in the moss Physcomitrella patens. *BMC Plant Biology* **8**, doi:10.1186/1471-2229-8-45.

Decendit A, Ramawat K, Waffo P, Deffieux G, Badoc A, Mérrillon J. 1996. Anthocyanins, cathechins, condensed tannis and piceid production in Vitis Vinifera cell bioreactor cultures. *Biotechnology Letters* **18**, 659–662.

Felsenstein J. 1989. PHYLIP - Phylogeny Inference Package (Version 3.2). *Cladistics* **5**, 164–166.

Foyer CH, LopezDelgado H, Dat JF, Scott IM. 1997. Hydrogen peroxide- and glutathione-associated mechanisms of acclimatory stress tolerance and signalling. *Physiologia Plantarum* **100**, 241–254.

Gupta AB, Sankararamakrishnan R. 2009. Genome-wide analysis of major intrinsic proteins in the tree plant Populus trichocarpa: characterization of XIP subfamily of aquaporins from evolutionary perspective. *BMC Plant Biology* **9**, doi:10.1186/1471-2229-9-134.

Leitão L, Prista C, Moura TF, Loureiro-Dias MC, Soveral G. 2012. Grapevine aquaporins: Gating of a tonoplast intrinsic protein (TIP2;1) by cytosolic pH. *PLoS ONE 7*, e33219.

Lopez D, Bronner G, Brunel N, *et al*. 2012. Insights into *Populus* XIP aquaporins: Evolutionary expansion, protein functionality, and environmental regulation. *Journal of Experimental Botany* **63**, 2217–2230.

Löytynoja A, Goldman N. 2005. An algorithm for progressive multiple alignment of sequences with insertions. *Proceedings of the National Academy of Sciences, USA* **102**, 10557–10562.

Martins V, Bassil E, Hanana M, Blumwald E, Gerós H. 2014a. Copper homeostasis in grapevine: Functional characterization of the *Vitis vinifera* copper transporter 1. *Planta* **240**, 91–101.

Martins V, Hanana M, Blumwald E, Gerós H. 2012. Copper transport and compartmentation in grape cells. *Plant and Cell Physiology* **53**, 1866–1880.

Martins V, Teixeira A, Bassil E, Blumwald E, Gerós H. 2014b. Metabolic changes of *Vitis vinifera* berries and leaves exposed to Bordeaux mixture. *Plant Physiology and Biochemistry* **82**, 270–278.

Matsunaga T, Ishii T, Matsumoto S, Higuchi M, Darvill A, Albersheim P, O'Neill M a. 2004. Occurrence of the primary cell wall polysaccharide rhamnogalacturonan II in pteridophytes, lycophytes, and bryophytes. Implications for the evolution of vascular plants. *Plant Physiology* **134**, 339–351.

Maurel C, Santoni V, Luu DT, Wudick MM, Verdoucq L. 2009. The cellular dynamics of plant aquaporin expression and functions. *Current Opinion in Plant Biology* **12**, 690–698.

Maurel C, Verdoucq L, Luu D-T, Santoni V. 2008. Plant aquaporins: membrane channels with multiple integrated functions. *Annual Review of Plant Biology* **59**, 595–624.

Miwa K, Fujiwara T. 2010. Boron transport in plants: Co-ordinated regulation of transporters. *Annals of Botany* **105**, 1103–1108.

Neill SJ, Desikan R, Clarke A, Hurst RD, Hancock JT. 2002. Hydrogen peroxide and nitric oxide as signalling molecules in plants. *Journal of Experimental Botany* **53**, 1237–1247.

Nicholas K, Nicholas Jr H, Deerfield II D. 1997. GeneDoc: Analysis and visualization of genetic variation. *EMBNEW.NEWS* **4**.

Noronha H, Agasse A, Martins AP, *et al*. 2014. The grape aquaporin VvSIP1 transports water across the ER membrane. *Journal of Experimental Botany* **65**, 981–993.

Rodrigues J, Silva RD, Noronha H, Pedras A, Gerós H, Côrte-Real M. 2013. Flow cytometry as a novel tool for structural and functional characterization of isolated yeast vacuoles. *Microbiology* **159**, 848–856.

Sabir F, Leandro MJ, Martins AP, Loureiro-Dias MC, Moura TF, Soveral G, Prista C. 2014. Exploring three PIPs and three TIPs of grapevine for transport of water and atypical substrates through heterologous expression in aqy-null yeast. *PLoS ONE* **9**, e102087.

Shelden MC, Howitt SM, Kaiser BN, Tyerman SD. 2009. Identification and functional characterisation of aquaporins in the grapevine, *Vitis vinifera*. *Functional Plant Biology* **36**, 1065–1078.

Soveral G, Macey R, Moura T. 1997. Water permeability of brush border membrane vesicles from kidney proximal tubule. *The Journal of Membrane Biology* **158**, 219–228.

Sparkes IA, Runions J, Kearns A, Hawes C. 2006. Rapid , transient expression of fluorescent fusion proteins in tobacco plants and generation of stably transformed plants. *Nature Protocols* **1**, 2019–2025.

Takano J, Kobayashi M, Noda Y, Fujiwara T. 2007. *Saccharomyces cerevisiae* Bor1p is a boron exporter and a key determinant of boron tolerance. *FEMS Microbiology Letters* **267**, 230–235.

Tamura K, Dudley J, Nei M, Kumar S. 2007. MEGA4: Molecular Evolutionary Genetics Analysis (MEGA) software version 4.0. *Molecular Biology and Evolution* **24**, 1596–1599.

Tisserat B, Stuff A. 2011. Stimulation of short-term plant growth by glycerol applied as foliar sprays and drenches under greenhouse conditions. *Horticultural Science* **46**, 1650–1654.

Tyerman SD, Chaves MM, Barrieu F. 2012. Water Relations of the Grape Berry and Aquaporins. In: Gerós H, Chaves MM, Delrot S, eds. The biochemistry of the grape berry. Bentham Books, 3–22.

Vandeleur RK, Mayo G, Shelden MC, Gilliham M, Kaiser BN, Tyerman SD. 2009. The role of plasma membrane intrinsic protein aquaporins in water transport through roots: diurnal and drought stress responses reveal different strategies between isohydric and anisohydric cultivars of grapevine. *Plant Physiology* **149**, 445–460.

Chapter 5

Conclusions and perspectives

5.1 Conclusions and perspectives

Grapevine is economically one of the most important fruit species in the world. The control and optimization of berry yield and quality are major concerns for viticulturists, to whom extreme climate events clearly represent additional undesired challenges. The biochemical and molecular mechanisms of grape berry ripening in response to the environment has been the main target of the studies developed in our group over recent years. Towards this objective, we have combined studies in *in vitro* cell cultures (Conde *et al*., 2006; Martins *et al*., 2012), fruiting cuttings and berry samples (Martins *et al*., 2014a; Noronha *et al*., 2014) with field experiments (Martins *et al*., 2014b; Teixeira *et al*., 2014; Conde *et al*., 2015) taking advantage of different molecular, biochemical, metabolomic, and transcriptomic approaches. So far, most of our research outcomes have been predominantly of an academic nature, but our work also captivates the wine sector due to the importance of berry composition on wine quality. In particular, understanding the mechanisms and regulation of sugar transport and compartmentation during grape berry maturation has both an important fundamental and applied relevance, because fruit sugar levels are a critical parameter for wine quality.

Sugars are predominantly produced in the plastids of mature leaves, but these organelles play additional important roles, including the synthesis and accumulation of starch, as well as the synthesis of several secondary compounds (Wise, 2007). The remobilization of leaf transient starch during the night sustains cellular metabolism and continuously feeds sink tissues with sugars, thus plastids from sink tissues are carbohydrate-importing organelles. As reported in the Introduction, many transport steps are involved in the exchange of sugars across the biological membrane of both green and non-green plastids, but their characterization in grapevine is still incipient, clearly contrasting with the importance of sugars in this crop. Following the work previously developed by our group that aimed to elucidate important sugar transport steps at the plasma membrane level (Conde *et al*., 2006, Conde *et al*., 2015), here, we wanted to further unravel the biochemical mechanisms behind sugar exchange at the plastidial membrane. The results presented and discussed in Chapter 2 led to the identification of grapevine *GPT* members, and two transcripts, *VvGPT1* and *VvGPT2*Ω, were cloned and characterized. These findings are particularly relevant, since, to our knowledge, it was the first time that grapevine plastidial transporters were characterized. We showed that VvGPT1 and

VvGPT2Ω are glucose-6-Pi/Pi translocators, with the first being abundant in heterotrophic tissues. VvGPT1 mediates glucose-6-Pi transport into sink plastids, and likely has a fundamental role in the synthesis and accumulation of starch, as well as in the secondary metabolism. The approach used to demonstrate the transport capacity of VvGPT1 took advantage of previous work developed by Niewiadomski *et al*., (2005) with the *Arabidopsis pgi1-1* mutant (Yu *et al*., 2000). As shown in Chapter 2, leaves from this mutant are unable to accumulate starch due to the lack of plastidial phosphoglucose isomerase activity and, as a result, have a pale yellow color when stained with iodine. However, when the *pgi1-1* mutant was complemented with *35S-VvGPT1-GFP* and *35S-VvGPT2*Ω*-GFP*, leaves recovered the typical strong iodine blue staining of the wild type, suggesting that their chloroplasts became able to incorporate glucose-6-Pi, bypassing the phosphoglucose isomerase step to produce starch. Thus, in plastids from green tissues, which do not express glucose-6-Pi translocators, we demonstrated the function of a transporter protein mostly expressed in sink tissues.

Future work will be undertaken to characterize VvGPT1 and VvGPT2Ω at the protein activity level in chloroplasts purified from leaves of *Arabidopsis* complemented with *35S-VvGPT1* and *35S-VvGPT2*Ω. The quantification of the radiolabeled glucose-6-Pi entrapped by the purified plastids will enable the precise characterization of the kinetic properties and specificity of these proteins and may open additional challenges for future research.

The expression of *VvGPT1* and *VvGPT2*Ω is responsive to environmental and endogenous stimuli, including light intensity, sugar levels and hormones. Indeed, field experiments clearly showed that *VvGPT1* expression in the berries is dependent on the degree of sun exposure of the cluster, which most likely interferes with the accumulation of sugars and secondary metabolites in the fruit. This is a fascinating research topic, with important practical applications, that deserves further investigation in the future. For instance, besides the clear effect of the grapevine orientation, other agricultural practices, including defoliation, could affect the expression of these sugar transporters in sink tissues, and thus modify the berry composition, particularly the amount of sugars, anthocyanins, and other secondary metabolites. In this regard, one particularly noteworthy aspect is the importance of our collaboration with ITQB (Prof. Manuela Chaves and co-workers), ISA (Prof. Sara Amâncio and Prof. Carlos Lopes) and UTAD (Prof. José Moutinho Pereira and

co-workers) in achieving our goals, particularly in what concerns the connection between basic science and field experiments. In particular, the possibilities opened in the context of the European project INNOVINE (http://www.innovine.eu/home.html) to precisely adjust and monitor important parameters like water availability, berry temperature and sun exposure, has enabled the establishment of precise correlations concerning the effect of a specific environmental factors on gene expression and metabolism.

The treatment of CSB cells with MeJA induced a strong increase in the expression of *VvGPT1* and *VvPAL1*, further supporting the involvement of *VvGPT1* in the synthesis of secondary compounds. In a research project recently submitted to FCT (Portuguese Foundation for Science and Tecnhology) our group proposed to mitigate drought stress symptoms in grapevine through exogenous treatments with polyols and plant hormones and/or hormone-like bioactive molecules, in particular abscisic acid. These easy-to-implement and cost-effective strategies will be tested at the field level (in cooperation with Symington) in combination with different irrigation treatments. In this context, the effect of the foliar application of MeJA on grape berry composition, particularly in what regards sugars and secondary metabolites, also appears of particular interest.

Another important research line opened by our results on plastidial transporters concerns the mechanisms of starch accumulation during the winter in the woody tissues and roots, and its remobilization to allow rapid shoot growth in the spring. It has been shown that the strength of the various sinks to which photoassimilates are allocated varies during seasonal vine development (Davies *et al*., 2012). Sink strength is also affected by nutrient availability and soil fertility, vine water status, additional stresses such as insects and disease, and crop load – the ratio of fruit to active leaf area (Davies *et al*., 2012). Early vine growth relies on carbohydrate and nitrogen reserves stored in woody tissues, canes and roots, and starch is mobilized from canes, cordons, trunk, and roots to the developing shoots until mature leaves become net exporters of photoassimilates (Zapata *et al*., 2004). Indeed, most studies developed until now focus on starch degradation in the cereal endosperm, but different mechanisms are expected to be involved in the roots and woody tissues of grapevine, because at the time of germination the cereal endosperm is a dead tissue (Zeeman *et al*., 2010). Currently, we are using mature grapevine canes to study the mechanisms behind starch accumulation and remobilization. The transcriptome of starch remobilization in grapevine canes is an interesting research project that we want to

undertake, for which the collaboration with the University of Bordeaux will be particularly important. In particular, we want to study how the adjustment of source/sink ratio through the manipulation of the number of leaves per cluster affects the berry sugar status and the total carbon reserves stored in the amyloplasts of woody tissues. The results obtained may have important practical applications because canopy defoliation is an agricultural practice whose application by the farmers is mostly empirical.

Besides sugar, water content is also an important parameter of berry quality, which is particularly intermingled with sugar status during berry development. Thus, the co-expression of several aquaporins at the same time as sugars transporters suggests a functional link between sugar and water fluxes during the processes of unloading and sugar accumulation in the flesh cells (Fontes *et al*., 2012). Water deficit generally leads to smaller berries, with higher surface/volume ratio, increasing the concentration of several compounds that accumulate in the skin, like anthocyanins and other phenolic metabolites (Chaves *et al*., 2010; Conde *et al*., 2015). However, water deficit may affect the primary and secondary metabolism of the berry through modifications in gene expression, as shown in the present work for sugar transporters and aquaporin genes. What should be the role of an intracellular aquaporin? This fascinating research topic was explored in Chapters 3 and 4 of the present study. It was discussed that intracellular AQPs may play important roles in organelle water transport and intracellular water homeostasis, and may also transport small solutes important for cellular signaling. Nonetheless, their physiological role in plants, particularly in grapevine, is still far from being fully understood. We wanted to explore in detail the localization and function of aquaporin members from SIP and XIP families – VvSIP1 and VvXIP1 – and how they are expressed in berry tissues and regulated by environmental conditions, in particular by water-deficit stress.

VvSIP1 is localized at the ER and is not particularly responsive to environmental stresses and hormonal treatments, with the exception of heat, which induced its expression in cultured cells. After the purification of ER membranes from yeasts overexpressing VvSIP1, its transport capacity was assessed by stopped-flow spectroscopy. This technique was performed at the laboratory of Prof. Graça Soveral (University of Lisbon) and revealed particularly powerful to demonstrate water transport through VvSIP1, because our previous results in Xenopus oocytes had been inconclusive. The purification of VvSIP1 was performed at Université catholique de Louvain (UCL) in the laboratory headed by Prof.

François Chaumont using a Ni-NTA affinity chromatography. After the purification of the ER membranes from yeasts overexpressing VvSIP1, the optimization of the conditions to extract the protein from the ER, including the detergent type and the appropriate detergent:protein ratio, was particularly challenging. The purified protein was incorporated into artificial liposomes in our laboratory at University of Minho and its transport activity measured again by stopped-flow at University of Lisbon following previous experiments in ER vesicles from yeasts overexpressing VvSIP1.

The work originated from the cooperation between University of Minho, University of Lisbon, Université catholique de Louvain and University of Bordeaux was published in an International Journal and presented in Chapter 3 (Noronha *et al*., 2014). Importantly, it opens good perspectives for future work that may include the characterization of VvSIP1 after site directed mutagenesis to elucidate which amino acid residues are crucial for protein activity, specificity and regulation.

Although few SIPs have been characterized at a molecular and biochemical levels, much work is still needed to pinpoint their specific physiological role in the ER membrane. In this regard, the study of *Arabidopsis* mutants could be particularly useful. However, the analysis of T-DNA insertion mutants of AtSIP1;1 and AtSIP2;1 showed no visible modifications in *Arabidopsis* growth, morphology and stress responses (Ishikawa *et al*., 2005; Maeshima and Ishikawa, 2008). Therefore, a thorough exploitation of phenotypes at the cellular level is needed, and the analysis of the ER ultrastructure may also provide relevant information on the physiological role of SIPs. Also, the overexpression of SIP members in *Arabidopsis*, tobacco or tomato, or even RNAi-mediated knockdown of SIPs in grape suspension-cultured cells may provide additional information on these intracellular water transporters in a near future.

As referred to before, XIPs were studied in few plant species and fungi so far, and much work remains to be done to fully understand their physiological role. For this reason, this protein family was named Uncharacterized (X) Intrinsic Proteins (Gupta and Sankararamakrishnan, 2009; Bienert *et al*., 2011). The results presented in Chapter 4 showed for the first time that a XIP protein can be targeted to the tonoplast. Also, stopped-flow spectroscopy studies with membranes from yeast over-expressing *VvXIP1*, demonstrated that this aquaporin is intriguingly unable to mediate the transport of water,

but transports glycerol. Plate growth assays showed that, besides glycerol, VvXIP1 can transport boron, H_2O_2 and copper. Interestingly, in vines treated with Bordeaux mixture, a common copper-based fungicide, the expression of *VvXIP1* in leaves was reduced. These results are particularly interesting, because they opened new possibilities to study the cooperation of VvXIP1 and VvCTrs in the regulation of copper compartmentation/detoxification in grape cells.

The capacity of VvXIP1 aquaporin to transport copper is likely to have a significant impact in the scientific community, because the transport charged molecules have not been described so far. Even in the case of boron uptake, it has been shown that the undissociated boric acid (H_3BO_3) is the form that crosses the water channel. In this regard, additional studies are in progress to characterize copper transport across VvXIP1 in transformed yeasts using copper-sensitive fluorescent probes and radiolabelled copper. In particular, the Cu-sensitive fluorophore Phen Green, revealed useful in our laboratory to characterize copper transport in cultured cells from grape (Martins *et al*., 2012). This topic is also particularly important for grapevine, since in many vineyards copper has accumulated to very high and toxic levels in the soils as a result of decades of treatment with copper sulfate (Bordeaux mixture).

Deciphering the physiological role of XIPs is particular difficult because no homologs can be found in the *Arabidopsis* genome (Bienert *et al*., 2011). Alternatively, the use of tomato, a fleshy fruit like grape berry, for over-expression studies may be an interesting approach that may allow the identification of the physiological role of VvXIP1 during fruit development.

As referred to before, understanding how sugars and water, along with other important solutes, including organic acids and secondary compounds, are transported and compartmented in grape cells, and how these processes are influenced by environmental stresses and endogenous signals are of extreme basic and applied importance. The continued work on achieving this goal will ultimately enable the improvement of grapevine productivity and grape berry quality in the context of the ongoing climatic changes, through the precise adjustment of the agricultural practices, like canopy management and irrigation, or through mitigation strategies, including the foliar spraying with exogenous substrates or hormones.

5.2 References

Bienert GP, Bienert MD, Jahn TP, Boutry M, Chaumont F. 2011. *Solanaceae* XIPs are plasma membrane aquaporins that facilitate the transport of many uncharged substrates. *The Plant Journal* **66**, 306–317.

Chaumont F, Tyerman SD. 2014. Aquaporins: Highly regulated channels controlling plant water relations. *Plant Physiology* **164**, 1600–1618.

Chaves MM, Zarrouk O, Francisco R, Costa JM, Santos T, Regalado a. P, Rodrigues ML, Lopes CM. 2010. Grapevine under deficit irrigation: hints from physiological and molecular data. *Annals of Botany* **105**, 661–676.

Conde C, Agasse A, Glissant D, Tavares R, Gualtar C De, Assimilats T, Physiologie L De, Gerós H, Delrot S. 2006. Pathways of glucose regulation of monosaccharide transport in grape cells. *Plant Physiology* **141**, 1563–1577.

Conde A, Regalado A, Rodrigues D, Costa JM, Blumwald E, Chaves MM, Gerós H. 2015. Polyols in grape berry: transport and metabolic adjustments as a physiological strategy for water stress tolerance in grapevine. *Journal of Experimental Botany* **66**, 889–906.

Davies C, Boss PK, Gerós H, Lecourieux F, Delrot S. 2012. Source/Sink Relationships and Molecular Biology of Sugar Accumulation in Grape Berries. In: Gerós H, Chaves MM, Delrot S, eds. The biochemistry of the grape berry. Bentham Books, 44–66.

Fontes N, Delrot S, Gerós H. 2012. Grape Cell Vacuoles: Structure-Function and Solute Transport Across the Tonoplast. In: Gerós H, Chaves M, Delrot S, eds. The biochemistry of the grape berry. Bentham Books, 160–171.

Gupta AB, Sankararamakrishnan R. 2009. Genome-wide analysis of major intrinsic proteins in the tree plant Populus trichocarpa: characterization of XIP subfamily of

aquaporins from evolutionary perspective. *BMC Plant Biology* **9**, doi:10.1186/1471-2229-9-134.

Ishikawa F, Suga S, Uemura T, Sato MH, Maeshima M. 2005. Novel type aquaporin SIPs are mainly localized to the ER membrane and show cell-specific expression in *Arabidopsis thaliana*. *FEBS Letters* **579**, 5814–20.

Maeshima M, Ishikawa F. 2008. ER membrane aquaporins in plants. *European Journal of Physiology* **456**, 709–16.

Martins V, Bassil E, Hanana M, Blumwald E, Gerós H. 2014a. Copper homeostasis in grapevine: Functional characterization of the Vitis vinifera copper transporter 1. *Planta* **240**, 91–101.

Martins V, Hanana M, Blumwald E, Gerós H. 2012. Copper transport and compartmentation in grape cells. *Plant and Cell Physiology* **53**, 1866–1880.

Martins V, Teixeira A, Bassil E, Blumwald E, Gerós H. 2014b. Metabolic changes of Vitis vinifera berries and leaves exposed to bordeaux mixture. *Plant Physiology and Biochemistry* **82**, 270–278.

Niewiadomski P, Knappe S, Geimer S, Fischer K, Schulz B, Unte US, Rosso MG, Ache P, Flügge U-I, Schneider A. 2005. The Arabidopsis plastidic glucose 6-phosphate/phosphate translocator GPT1 is essential for pollen maturation and embryo sac development. *The Plant Cell* **17**, 760–775.

Noronha H, Agasse A, Martins AP, *et al*. 2014. The grape aquaporin VvSIP1 transports water across the ER membrane. Journal of Experimental Botany **65**, 981–993.

Teixeira A, Martins V, Noronha H, Eiras-Dias J, Gerós H. 2014. The first insight into the metabolite profiling of grapes from three *Vitis vinifera* L. cultivars of two controlled appellation (DOC) regions. *International Journal of Molecular Sciences* **15**, 4237–4254.

Wise RR. 2007. The diversity of plastid form and function. In: Wise RR, Hoober JK, eds. The structure and function of plastids. Springer, 3–27.

Yu TS, Lue WL, Wang SM, Chen J. 2000. Mutation of Arabidopsis plastid phosphoglucose isomerase affects leaf starch synthesis and floral initiation. *Plant Physiology* **123**, 319–326.

Zapata C, Deléens E, Chaillou S, Magné C. 2004. Partitioning and mobilization of starch and N reserves in grapevine (*Vitis vinifera* L.). *Journal of Plant Physiology* **161**, 1031–1040.

Zeeman SC, Kossmann J, Smith AM. 2010. Starch: its metabolism, evolution, and biotechnological modification in plants. *Annual Review of Plant Biology* **61**, 209–234.